Geological Survey of Israel
Ministry of Energy

The nitrogen cycle in Lake Kinneret - Geochemical and isotopic perspectives

Tami Zilberman



Report GSI/03/2021

February 2021

©Published by the Geological Survey of Israel
32 Yeshayahu Leibowitz St. Jerusalem 9692100, Israel

Cover pictures:

Lake Kinneret photos, taken from the research boat.
Pictures taken by Tami Zilberman.

Cover design: Tirza Tzuberi

Geological Survey of Israel
Ministry of Energy

The nitrogen cycle in Lake Kinneret - Geochemical and isotopic perspectives

Tami Zilberman

Thesis for the degree of "Doctor of Philosophy"

submitted to the senate of the Hebrew University of Jerusalem.

The study was carried out under the supervision of:

Dr. Ittai Gavrieli, Geological Survey of Israel.

Prof. Boaz Lazar, Hebrew University of Jerusalem.

Dr. Ami Nishri, Israel Oceanographic and Limnological Research, Kinneret Laboratory

Report GSI/03/2021 February 2021

To my dear family

Ido

Yaara

Rotem

Eytan

ACKNOWLEDGEMENTS

I would like to extend my warm thanks to all those who assisted me to bring this work to a successful completion.

I express my special thanks and gratitude to my advisors, Boaz Lazar, Ittai Gavrieli, and Ami Nishri. The three of you, each in your own way, have given me the precious tools for scientific and especially geochemical thinking. This guidance always came together with support, encouragement, patience, and kindness. I have learned a lot from you and profoundly benefitted from your knowledge and experience.

My warmest thanks to Avner Ayalon for his continued support and his help in everything, especially in the stable isotope lab.

Special thanks to my friends and colleagues Mira Matthews, Yehudit Harlavan, Gal Yasur, Rotem Golan, Galit Sharabi, Nadya Teutch, Netta Shalev, Aya Schneider-Mor, Anton Vaks, and Yoav Bendor for their helpful ideas, fruitful discussions, companionship, moral and support.

I would like to thank Gal Yasur and Sergei Sladkevitz for being my “right-hand” in running the stable isotope lab, help with performing analyses and taking care of, and managing the lab during my maternity leaves.

Natalya Tapliakov is thanked for teaching me the laboratory work with patience and smile, for her generous advices, and her significant input in developing together the analytical procedures.

Many thanks to Galit Sharabi, Olga Berlin, Jonathan Keinan, Efrat Eliani, Dina Stiber for their great assistance with the chemical and isotopic analyses.

To Shlomo Ashkenazi, Yaacov Mizrahi, Rami Madmon, Guy Ariel, and Michael Kitin for their great help in the field work.

The Geological Survey of Israel (GSI) is thanked for providing me with the lab and fieldwork infrastructure for carrying out many aspects of this work.

I would like to thank the previous Directors of the GSI, Ittai Gavrieli and Rivka Amit, the present Director Yossi Yechieli, and the Deputy Director Yoram Biton for help and encouragement.

I deeply appreciate and am grateful to the Heads of the Geochemical Department Yehudit Harlavan, Naomi Porat and Nadya Teutch for their help and support during the course of this research.

Thanks to the staff of the Institute of Earth Science at the Hebrew University, Batya Moshe, Magiuy Perkin, and Sandra Kaplan for their kindness and help.

I would like to thank the skippers from Israel Oceanographic and Limnological Research, Kinneret Laboratory, Moti Diamant, Oz Tsabari-Da, and the lab staff, Edit Leibovici, Diti Viner-Mozzini, Miki Shlichter and Yossi Yacobi for their technical assistance.

Thanks to Tanya Rivlin from the Interuniversity Institute for Marine Sciences of Eilat for technical assistance in the lab work.

Thanks are due to my dissertation committee members Yeala Shake and Orit Sivan for valuable discussions and their helpful and important remarks.

I would like to thank Amitai Katz and Ilana Berman for reviewing my PhD lecture.

I wish to thank the two anonymous reviewers of this dissertation for their helpful remarks.

I wish to express my love and appreciation to my supporting family, in-laws and my close friends. You were always so understanding and loving, thank you for always being there for me, listening and advising. I could not make it without you.

To my parents, I wish to thank for standing by me, taking interest in my work and their pride in any achievement.

To my children, Yaara, Rotem and Eitan, who two of them were born during the course of this work, for making the challenge even more challenging but made my hart full.

And last but not least, to Ido, for his love, support and his belief in me.

ABSTRACT

The main objective of this thesis is to characterize and quantify the nitrogen cycle in Lake Kinneret (LK) using nitrogen (various N-species) mass-balances and isotopic ($\delta^{15}N$) compositions.

The research is described in 4 main chapters which deal with the following issues:

1. Development and verification of the methods for analyzing the isotopic compositions of dissolved inorganic nitrogen (DIN) species are outlined in Chapter 3 (other small modifications for the more commonly used methods are included under Methods, Chapter 2). The chapter describes refined methods and provides protocols for the determination of $\delta^{15}N$ in nitrate (NO_3^-) and nitrite (NO_2^-), and $\delta^{15}N$ in ammonium (TNH_3) in the presence of one or the other two species. The methodology described in the chapter was used in the study of LK.
2. Description of the seasonal water column dynamics of nitrogen species and dissolved oxygen (DO) in LK based on weekly depth profiles conducted during the period 2010-2016 at the center of the lake (Chapter 4). These profiles are used to formulate a nitrogen mass balance and to quantify the processes and rates controlling the nitrogen cycle in LK.
3. Description of the seasonal water column dynamics of the isotopic compositions of: nitrate, nitrite, ammonium and particulate organic matter (PNorg) in LK in depth profiles representing all seasons over several years (Chapter 5). These data are provided together with the nitrogen content and its isotopic composition in the main nitrogen sources to the lake (e.g. Jordan River water, Nahal Meshushim, etc.). The nitrogen isotope analyses in the lake and its sources were proved to be crucial for understanding and identifying the processes controlling the nitrogen system of LK. This chapter also discusses an incubation experiment that was conducted in order to follow the decomposition of POM in LK water column and to characterize the N-isotopic fractionation during ammonification of POM.
4. Summary and conclusions (Chapter 6) which includes a synthesis (Section 6.1), which provides a cartoon-like summary of my view on the nitrogen cycle of LK as described in chapters 4 and 5, depicting the lake during 3 important limnologic seasons: mixing, onset of stratification and stratification, and an overview of LK annual nitrogen fluxes.

Following is a brief summary of the results (all abbreviations and acronyms are explained in the glossary attached to this thesis):

LK is a monomictic lake (overturns once a year) that develops an anoxic hypolimnion during spring/summer stratification and fully mixes during winter. These physical characteristics of the lake cause marked fluctuations in its redox state, from reducing hypolimnion during spring/summer stratification to fully oxidizing water column during fall/winter mixing. The variations in the lake's nitrogen cycle, which are controlled by these dynamics, were studied by following the water column's vertical (5 m intervals) and temporal (weekly basis) variations in the nitrogen species and their isotopic composition for ~6 years. The elemental and isotopic mass balances of nitrogen that were constructed from these profiles were used to identify and quantify the major processes controlling the nitrogen system in LK. On annual scale, the NO_3^- and TNH_3 bulk inventories were found to be within the same order of magnitude but varied in opposite directions (when one increased the other decreased), while exhibiting different depth distributions, depicting the physical-chemical dynamics of the lake.

Seasonal variations in the hypolimnetic (below 15 m) inventories of nitrogen species and dissolved oxygen (DO) in the lake were used to quantify and define the annual N-species transformation and processes. Following the onset of stratification and during the transition period from oxic to sub-oxic conditions (March-April), DO decreased substantially with no significant change in the distribution of N-species. This observation contrasts with the expected negative correlation between oxygenic respiration (DO decrease) and re-mineralization of organic matter (to oxidized nitrogen species or reduced ammonium). Here I propose that this phenomenon is a result of the process I describe as an "oxygenic denitrification" and/or "oxygenic anammox". Such process may proceed provided *nitrate or nitrite produced by oxygenic remineralization of POM will be contemporaneously consumed anaerobically through denitrification or anammox pathways, respectively, to form dissolved N_2, under ambient oxidized conditions*. When *observed on a macro scale* (limnologic scale), this is an apparent paradox: Ambient aerobic conditions under which *on a micro scale* anaerobic bacterial processes operate in low-oxygen to anaerobic microenvironments. In this thesis I suggest that such a process is possible *within oxygen deficient POM microenvironments which are sinking through the water column, the so-called* "***marine (lacustrine) snow***". While oxygenic respiration consumes oxygen

at the outer shell of the lacustrine snow, the nitrate/nitrite produced is consumed by denitrification/anammox in the anoxic inner shell, forming N_2 that diffuses to the water column. Thus, the net observed process in the hypolimnion at this period is "oxygenic denitrification/anammox" i.e., oxidation of particulate organic nitrogen and formation of N_2 (that can escape to the atmosphere), acting as a nitrogen sink in the lake.

As the DO concentration in the water column decreases below ~150 $\mu mol \cdot L^{-1}$, a dramatic decrease in nitrate and DO and increase in TNH_3 are observed. The dominant process operating at this stage is denitrification of the nitrate and ammonification of organic-N. By late fall the hypolimnion attains anoxic conditions, and the ammonification proceeds via sulfate reduction.

Mass balance calculations show that altogether, $\sim 115 \cdot 10^6$ mol of nitrogen are consumed and released as N_2 by these two processes of nitrogen removal, "oxygenic denitrification" (and/or "oxygenic anammox") by "lacustrine snow" and direct denitrification. These processes demonstrate that the magnitude of nitrogen removal within the lake does not depend just on the annual nitrogen inflow into the lake, but also on the ability of the lake to consume and transform the organic nitrogen in the hypolimnion to N_2. Though yearly inflow to the lake is important, other variables, which are not necessarily associated with nitrogen inventories, e.g., DO, rate of POM decomposition and sinking to the bottom of the lake, have also a significant role.

The main processes controlling the nitrogen cycle during the mixing period are nitrification of hypolimnetic ammonium, phytoplankton photosynthesis (assimilation), and the external nitrogen supply by the Jordan River. Nitrification is accompanied by a considerable isotopic fractionation, whereby the NO_3^- product is isotopically ^{15}N-depleted relative to the ammonium reactant. Hence, as reaction progresses, the $\delta^{15}N_{TNH3}$ of the diminishing residual ammonium increases progressively (Rayleigh distillation).

The main processes controlling the nitrogen cycle during the stratification period are assimilation, denitrification and ammonification. By late spring, both processes, nitrate assimilation in the epilimnion and denitrification in the hypolimnion, are accompanied by isotopic fractionations, resulting in ^{15}N-enriched residual nitrate. Ammonification of PNorg in the hypolimnion of the lake produces ^{15}N-enriched ammonium relative to PNorg, suggesting that the fractionation factor of nitrogen isotopes during ammonification is rather large and positive, in contrast to the commonly accepted view that there is virtually no fractionation during ammonification. This finding was also corroborated by a plankton incubation experiment as described below.

The annual variability in $\delta^{15}N_{PNorg}$ is the highest in the lake's nitrogen system, reflecting the isotopic composition of the assimilated N-species. Thus, the high $\delta^{15}N_{PNorg}$ recorded in spring indicates assimilation of the highly ^{15}N-enriched residual TNH_3 from nitrification. Assimilation of nitrate with low $\delta^{15}N_{NO3^-}$ begins later, when TNH_3 is completely exhausted, as reflected by the gradual decrease of the $\delta^{15}N_{PNorg}$. $\delta^{15}N_{PNorg}$ may reach very low values in early winter, due to N_2 fixation.

To study the fractionation factor of nitrogen isotopes during ammonification, an incubation experiment was performed. The results prove that decomposition of POM leads to significant increase in the $\delta^{15}N_{TNH3}$ (the ammonium product), as observed in LK during stratification period (see above). Mass- and isotopic-balances of PNorg and TNH_3 indicate that ammonium is not the sole product of the decomposition, and isotopically light DNorg is also formed.

This work shows that careful examination of seasonal variations in the distribution of the nitrogen species in the water column, together with their isotopic compositions, which vary considerably along the annual cycle, enables better understanding of the nitrogen cycle in LK. One of the important discoveries of this study is the significant role of "oxygenic denitrification" and/or "oxygenic anammox" in the overall nitrogen budget of the lake. This process was overlooked in previous studies and was identified here by a careful analysis of the high temporal resolution data base of the thesis.

Glossary of variables and abbreviations **(alphabetical order)**

Anammox - Anaerobic ammonium oxidation

DIN - Dissolved inorganic nitrogen, $NO_3^- + NO_2^- + TNH_3$

DNorg - Dissolved organic nitrogen

DNRA - Dissimilatory nitrate reduction to ammonium

DO - Dissolved Oxygen

DOS - DO Saturation

EA - Elemental Analyzer

ILOR - Israel Oceanographic and Limnological Research

IRMS - Isotope ratio mass spectrometer

GF/F – Glass microfiber filter

GSI – Geological Survey of Israel

KLL - Yigal Allon Kinneret Limnological Laboratory

LK - Lake Kinneret

NH_3 - Ammonia

NH_4^+ - Ammonium

NO_2^- - Nitrite

NO_3^- - Nitrate

PNorg - Particulate organic nitrogen

POM - Particulate organic matter

SA - Sulfanilic acid

TN - Total Nitrogen, DIN + TNorg

TNH_3 – Total ammonia, $NH_3 + NH_4^+$ (mostly ammonium in LK)

TNorg - Total organic nitrogen, DNorg + PNorg

$\delta^{15}N_{DNorg}$ - $\delta^{15}N$ of DNorg

$\delta^{15}N_{NO2^-}$ - $\delta^{15}N$ of NO_2^-

$\delta^{15}N_{NO3^-}$ - $\delta^{15}N$ of NO_3^-

$\delta^{15}N_{PNorg}$ - $\delta^{15}N$ of PNorg

$\delta^{15}N_{TNH3}$ - $\delta^{15}N$ of TNH_3

Table of Contents

ABSTRACT 1

Glossary of variables and abbreviations (alphabetical order) 7

1. Introduction 13

1. 1 Nitrogen in aquatic systems 13

1.1.1 The nitrogen cycle in the aquatic environment 14

1.2 Lake Kinneret (Sea of Galilee) 17

1.3 Research Goals 21

2. Methods 23

2.1 Sampling and field measurements 23

2.3 Chemical Analyses 24

2.4 Nitrogen and oxygen isotopic determination of N-species 25

2.4.1 Historical Background 26

2.4.2 Measurements of a single nitrogen species in solution 27

2.4.3 PNorg 33

3. Determination of $\delta^{15}N$ and $\delta^{18}O$ in individual N-species in the presence of other N-species – A refined method 34

3.1 Determination of $\delta^{15}NNO_3^-$ and $\delta^{18}ONO_3^-$ in the presence of nitrite 35

3.2 Determination of $\delta^{15}N_{TNH3}$ in the presence of nitrite 38

3.3 Determination of $\delta^{15}N_{NO3}^-$ and $\delta^{18}O_{NO3}^-$ in the presence of ammonium 41

3.4 Determination of $\delta^{15}N_{NO2}^-$ and $\delta^{18}O_{NO2}^-$ in the presence of ammonium 43

3.5 Determination of $\delta^{15}N_{TNH3}$ in the presence of nitrate 47

3.6. Determination of $\delta^{15}N_{NO2}^-$ and $\delta^{18}O_{NO2}^-$ in the presence of nitrate 48

3.7. Conclusions and analytical recommendations 48

4. Temporal variations of nitrogen species in Lake Kinneret – Clues to the governing biogeochemical processes 50

4.1 Seasonal and annual variations of the nitrogen species in the lake 51

4.2 Seasonal variations of N-species inventories of the lake 55

4.3 Temporal variations of hypolimnetic inventories of nitrogen and DO between onset of stratification and beginning of anoxia 59

4.3.1 The transformation from oxic to mid-oxic hypolimnion – Oxygenic denitrification/anammox and the role of lacustrine (marine) snow 59
4.3.2 The transformation from sub-oxic to anoxic hypolimnion 66
4.3.3 Total amount of nitrogen consumed in the hypolimnion between the onset of stratification and beginning of the anoxic period (between line I and II, Fig. 4.7) 67
4.4 Primary productivity - A major source of hypolimnetic nitrogen inventory 68
4.5 Inter-annual variabilities in the mass-balance of nitrogen 69
4.6 Hypolimnetic nitrogen inventories of nitrogen during anoxia 72
4.7 "Oxygenic denitrification and/or oxygenic anammox" - an overlooked pathway in the nitrogen cycle for LK 72
4.8 Summary 73
5. The Nitrogen Cycle in Lake Kinneret – Evidence from Nitrogen Isotopes 75
5.1 Introduction 75
5.1.1 Nitrogen isotope fractionation- Rules of the game 75
5.2 The isotopic composition of nitrogen in inflows into Lake Kinneret 78
5.3 Temporal variations in $\delta^{15}N$ of TNH_3, PNorg, and NO_3^- in LK 79
5.3.1 Processes controlling the seasonal variations in lake's $\delta^{15}N$ values of the different nitrogen species 81
5.3.2. Field evidence for fractionation of nitrogen isotopes during ammonification 84
5.4 Fractionation of nitrogen isotopes during ammonification - An experimental study 85
5.4.1 Experimental setup 85
5.4.2 Results 86
5.4.3. Variations in nitrogen species concentrations 88
5.4.4. Evolution of nitrogen isotope compositions during the incubation experiment 88
5.4.5. Fractionation factor of stable nitrogen isotopes ($\boldsymbol{\alpha}$) during ammonification 89
5.5 Conclusions 91
6. Summary and Conclusions 92
6.1 Synthesis – The nitrogen cycle during different seasons 92
6.2 Conclusions 95
7. Bibliography 97

List of Figures

Fig. 1.1. Nitrogen cycle in aquatic systems …….. 14

Fig. 1.2. Seasonal variations in temperature, DO, NO_3^- and TNH_3 ……... 19

Fig. 2.1. Location map of Lake Kinneret and the sampling sites in its drainage basin …… 24

Fig. 3.1. Flow-chart of preparation process of each of the 3 inorganic N-species prior to its Introduction to the IRMS for isotopic measurement……... 35

Fig. 3.2. Measured $\delta^{15}N_{NO3^-}$ vs. $\delta^{18}O_{NO3^-}$ in the experiments for the removal of pre-existing NO_2^- from solution ……... 37

Fig. 3.3. The apparent isotopic composition of nitrite as a function of TNH_3/NO_2^- ratio ……. 44

Fig. 3.4. $\delta^{15}N$ versus $\delta^{18}O$ for various tests of measuring the isotopic composition of nitrite in the presence of ammonium ……... 47

Fig. 4.1. Annual variations of TNH_3 and NO_3^- concentrations and DO saturation in LK ……. 54

Fig. 4.2. Mass calculation of TNH_3 in LK water body …….. 57

Fig. 4.3. Annual variations in the inventories of various DIN species, DO, and mixed layer depth In LK ……... 58

Fig. 4.4. Annual inventory variations of TNH_3, NO_2^-, NO_3^-, and the accumulated amount of TN from runoff to LK ……... 58

Fig. 4.5. Seasonal variations of TN, DIN and TN_{org} inventories in LK water column during 2011 …. 59

Fig. 4.6. Water column variations in T, DO, TNH_3, and NO_3^- in LK during spring 2012 …… 60

Fig. 4.7. Secular variations of hypolimnetic inventories of NO_3^-, NO_2^-, TNH_3, DIN and DO for February-July, 2012 …… 62

Fig. 4.8. Summary of the measured and calculated changes in the **DO** and $\mathbf{NO_3^-}$ inventories in the hypolimnion from the onset of stratification to the time of DO=0 ……. 63

Fig. 4.9. Conceptual model for N_2 formation within lacustrine snow micro-environments sinking through an oxic hypolimnion …….. 66

Fig. 4.10. The integrated water column primary productivity converted to nitrogen ……. 69

Fig. 5.1. Typical ranges for $\delta^{15}N$ and $\delta^{18}O$ values of nitrate ……. 77

Fig. 5.2. A map of Lake Kinneret's watershed showing the location of the sampling sites, and $\delta^{15}N_{NO3^-}$ and $\delta^{15}N_{PNorg}$ plotted against nitrogen concentrations in the water sources ……. 79

Fig. 5.3. Variations in NO_3^- and TNH_3 concentrations, $\delta^{15}N_{NO3^-}$, $\delta^{15}N_{TNH3}$, and $\delta^{15}N_{PNorg}$ during 2010 – 2014 in LK ……. 83

Fig. 5.4. Chemical and isotopic compositions during incubation experiments …… 87

Fig. 5.5. Chemical variations in the N-system during the plankton incubation experiment ……. 88
Fig. 5.6. $\delta^{15}N_{PNorg}$ and calculated $\delta^{15}N_{TNH3}$ of the minerallized PNorg plotted against the fraction of residual N in POM ($f(N_{POM})$) …….. 89
Fig. 5.7. $\delta^{15}N$ plotted against ($f\ PN_{org}$) of the PN_{org} during the incubation Experiment ……... 89
Fig. 6.1. Conceptual cartoon of the nitrogen cycle in LK depicting the main nitrogen input and output fluxes, processes and inventories in different limnologic statuses …….. 94

List of Tables

Table 2.1. Regents and Cd-column effect on the $\delta^{15}N$ and $\delta^{18}O$ values of the nitrite ……..31
Table 2.2. Isotopic compositions of nitrate, ammonium, and PNorg standards …….. 33
Table 3.1. Experimental set-up to remove nitrite in the presence of nitrate and $\delta^{15}N_{NO3^-}$ and $\delta^{18}O_{NO3^-}$ results with different concentration of SA ……36
Table 3.2. Experimental set-up to remove nitrite in the presence of ammonium and $\delta^{15}N_{TNH3^-}$ results with different concentrations of SA ……39
Table 3.3. Experimental set-up to remove ammonium in the presence of nitrate and $\delta^{15}N_{NO3^-}$ and $\delta^{18}O_{NO3^-}$ results ……39
Table 3.4. Experimental set-up for the determination of $\delta^{15}N_{NO2^-}$ and $\delta^{18}O_{NO2^-}$ in the presence of ammonium ……43
Table 3.5. Experimental set-up to remove ammonium in the presence of nitrite and $\delta^{15}N_{NO2^-}$ and $\delta^{18}O_{NO2^-}$ results ……45
Table 3.6. Experimental set-up and $\delta^{15}N_{TNH3}$ results in the presence of nitrate ……...47
Table 3.7. Experimental set-up and $\delta^{15}N_{NO2^-}$ and $\delta^{18}O_{NO2^-}$ results in the presence of nitrate ……... 48
Table 3.8. Concentrations and isotopic compositions of various N-species in LK water during the different seasons ……49
Table 4.1. Calculated values for nitrogen removal from the hypolimnion during the different stages of the stratification period for 2012-2014 ……71
Table 5.1. Chemical and isotopic compositions during the incubation experiment …… 87

Supplementary Tables (in separate folder)

Table S1. Concentrations of N-species and DO in selected water layers of LK measured weekly during 2010 - 2016.

Table S2. Calculated integrals of N-species and DO in the entire water body of LK, sampled weekly during 2010 - 2016.

Table S3. Calculated integrals of N-species and DO in the hypolimnion of LK (defined here as deeper than 15m), measured weekly during 2012- 2014.

Table S4. Daily inflow volume of the Jordan River into LK, N-species concentrations, and the calculated total accumulated amounts during 2010 - 2016.

Table S5. Calculated total N productivity of LK at water depth of 0-15 m during 2010-2016.

Table S6. Oxygen degree of saturation (DOS) calculated for four selected water layers (1, 15, 25, and 35 m) of LK during 2010-2016.

Table S7. Nitrogen concentration and $\delta^{15}N$ values of N-species in selected water depth of LK measured during 2010 - 2014.

Table S8. Chemical and isotopic compositions as a function of time during incubation experiment E1-2 (sulfate addition).

1. Introduction

1. 1 Nitrogen in aquatic systems

Nitrogen is a major constituent in both terrestrial and aquatic ecosystems and is essential for all forms of life. It is present in the environment in a range of species and oxidation states, including ammonium (NH_4^+), nitrite (NO_2^-), nitrate (NO_3^-), nitrous oxide (N_2O), nitric oxide (NO), organic nitrogen, and inorganic nitrogen gas (N_2). However, elevated concentrations of nitrogen species, can be harmful to the aquatic environment. This is particularly true for nitrate, which, as has been observed in numerous fresh and marine coastal waters throughout the world, can lead to eutrophication and deterioration of water quality. As such, nitrogen pollution is a serious and well recognized problem in the sustainable management of groundwater and surface water in many river basins and lakes (e.g., Hill et al., 1973; Cuello et al., 1976; Rajagopal and Tobin, 1989; Kellogg et al., 1992; Vitousek et al., 1997; Weyer et al., 2001; Widory, 2013). Main nitrogen sources include: mineral fertilizers, animal manure, domestic or industrial wastewater, atmospheric deposition, or decomposition of soil organic matter. However, identifying the sources of N-species and understanding their biogeochemical cycling in aquatic systems is often challenging.

Nitrate has become one of the common contaminants found in groundwater (NATIONAL RESEARCH COUNCIL, COMMITTEE ON TOXICOLOGY, 1995; Nolan et al., 2002) and is one of the world's major pollutants of drinking water resources. Elevated concentrations of nitrate in drinking waters can induce adverse effects on human health such as the blue baby syndrome (FAO/WHO, 1996; Avery, 1999). Ammonium and nitrite are also toxic, because they are rapidly oxidized to NO_3^- in aerobic conditions. Accordingly, World Health Organization recommends a guideline value for nitrate of 50 mg/l in drinking water, ~3 mg/l nitrite whereas ammonium is not of direct importance for health in the concentrations to be expected in drinking-water (WHO, 1986).

1.1.1 The nitrogen cycle in the aquatic environment

The nitrogen cycle is the biogeochemical cycle by which nitrogen is transformed through multiple chemical forms as it circulates through the atmosphere and the terrestrial, and aquatic ecosystems. The conversion between the nitrogen species is carried out through both biochemical and chemical processes (e.g., Huang and Wozniak, 1981; Kendall, 1998; Peterson et al., 2001; Seitzinger et al., 2002; Arrigo et al., 2005; Francis et al., 2007). Fig. 1.1 presents the essential processes occurring in the nitrogen cycle in the aquatic environment, depicting the processes occurring under oxidized and reduced conditions within a stratified water body. Note that in addition to the transformation within the aquatic system, the major external sources of nitrogen are riverine particulate and dissolved nitrogen species, while sedimentation of organic matter is a major sink (along with discharge or pumping).

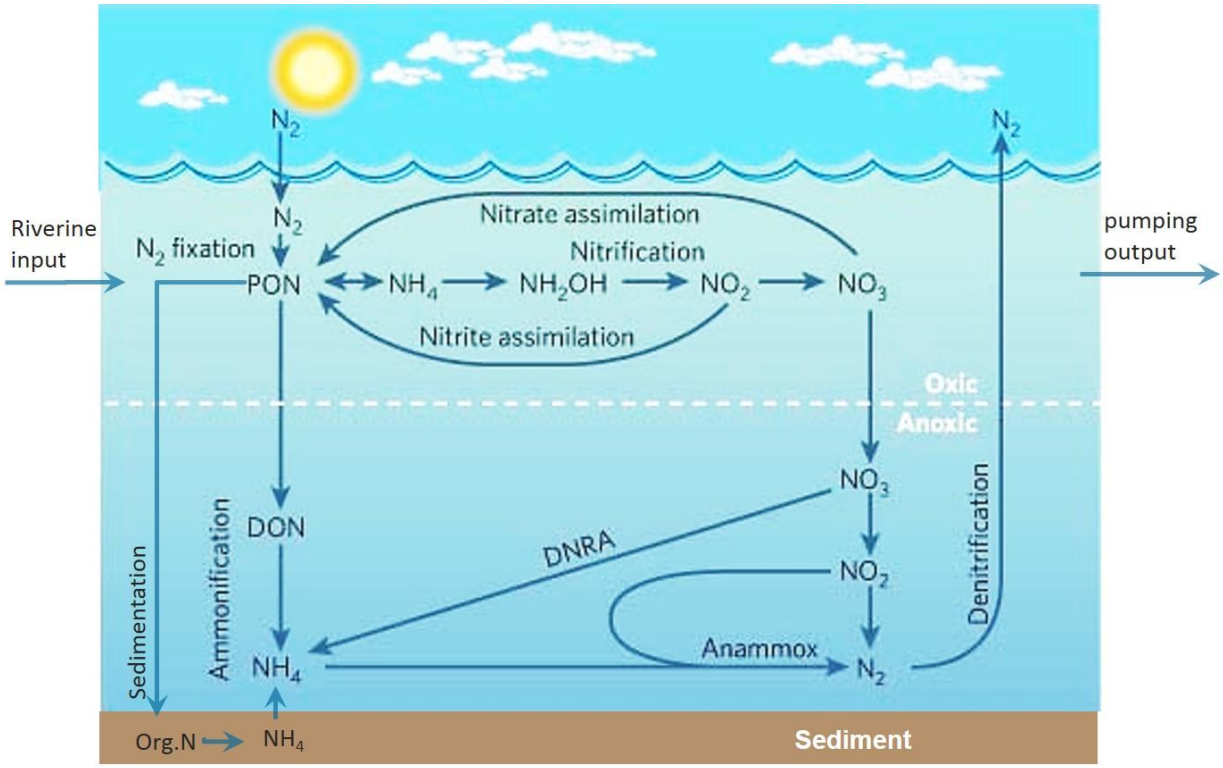


Fig. 1.1. Nitrogen cycle in aquatic systems (modified from Arrigo, 2005). Acronyms are defined below and in the glossary.

Nitrification: $NH_4^+ \rightarrow NO_2^- \rightarrow NO_3^-$

Nitrification is the oxidation of ammonium to nitrate. This process commonly occurs by at least two species of nitrifying bacteria under oxic conditions for the purpose of deriving metabolic

energy. Various byproducts may be produced during nitrification and released into the environment including both aqueous compounds (e.g., NH_2OH and NO_2^-) and gaseous compounds (e.g., NO and N_2O).

Assimilation (uptake): $NO_3^- \rightarrow$ POM; $NH_4^+ \rightarrow$ POM

Assimilation refers to the transformation of inorganic nitrogen compounds (e.g., nitrate and ammonia) into nitrogen compounds incorporated into POM (particulate organic matter, i.e. nitrogen in amino acids) via uptake by flora (Fig. 1.1). Generally, oxidized forms of N are initially reduced to NH_4^+ and then assimilated into organic matter (e.g., Hoch et al., 1992; Pennock et al., 1996; Waser et al., 1998; Altabet et al., 1999; Granger et al., 2004, Kendal et al., 2007).

Nitrogen fixation: $N_2 \rightarrow$ POM

Nitrogen fixation occurs by bacterial fixation of atmospheric N_2, converting it to organic nitrogen (Cleveland et al. 1999).

In addition, it occurs also due to human activities (industrial and agricultural) that produce reactive N (NOx, NHy, and organic N). Concern about the impact of anthropogenic fixation processes due to increased fossil-fuel combustion and fertilizer use lead to increased interest in uses of nitrogen isotopes in environmental studies (Galloway et al., 1995, 2004).

Denitrification: $NO_3^- \rightarrow N_2$

Denitrification is the microbial reduction of nitrate to nitrogen gas (N_2), followed usually by its degassing to the atmosphere. It occurs in sub-oxic to anoxic conditions, usually at O_2 concentrations that are less than 20 µM, when O_2 respiration is limited, and is responsible for the transformation of significant amounts of the originally fixed nitrogen back to the atmosphere (Arrigo, 2005; Fig. 1.1).

Dissimilatory nitrate reduction to ammonium (DNRA): $NO_3^- \rightarrow NO_2^- \rightarrow NH_4^+$

DNRA; Fig. 1.1, or nitrate/nitrite ammonification, is a microbial anaerobic two stage respiration process, whereby nitrate is reduced to nitrite, and then to ammonium (Lam and Kuypers, 2011; Marchant et al., 2014).

Ammonification: POM → NH_4^+

Ammonification (Mineralization) is defined as the production of ammonium (NH_4^+) from organic matter. This process occurs in both oxic and anoxic environments; in oxic environments the released ammonium is often quickly consumed by algal assimilation or undergoes nitrification whereas in anoxic environments it tends to accumulate and may reach high concentrations.

Anaerobic ammonium oxidation (Anammox): $NH_4^+ + NO_2^- \rightarrow N_2 + 2H_2O$

Anammox is an anaerobic respiration pathway in which anaerobic bacteria mediate the oxidation of ammonium (N oxidation state -3) by nitrite (N oxidation state +3), yielding molecular nitrogen gas $N_{2(g)}$ (oxidation state = zero) through a comproportionation reaction. When first identified (Thamdrup and Dalsgaard, 2002; Arrigo, 2005) this process was a surprising revelation because until then the biological uptake of ammonium in anoxic environments was virtually unknown. There is a substantial amount of energy released through this process.

In addition to the above processes, a major external source of particulate and dissolved nitrogen species to lakes is riverine.

Nitrogen loss from the system occurs due to denitrification, sedimentation of organic matter, and export through pumping of lake water.

Isotope techniques are a major tool in tracing sources of nitrogen in surface and groundwater bodies and may be used to assess qualitative and quantitative aspects of nitrogen cycling in aquatic systems. The combined measurements of nitrogen species' concentrations and isotope compositions have facilitated the ability to trace the sources of dissolved nitrate and ammonium to more conclusively identify pathways of nitrogen cycling in many–hydrological settings (e.g., Kohl et al., 1971; Mariotti, 1984; Mayer et al., 2013).

The nitrogen isotope fractionation associated with the major processes in the nitrogen cycle in aquatic systems is described in detail in Chapter 5.

1.2 Lake Kinneret (Sea of Galilee)

Lake Kinneret (LK) is located in the northern part of the Dead Sea Rift Valley. The lake surface is at about 210 meters below sea level (mbsl). Its area is 167 km^2, length 22 km, width 12 km, maximum depth 43m (average depth, 24 m; Serruya 1971) and its average volume is $4 \cdot 10^9$ m^3. During the last century, the lake and its watershed have been subject to both intensive anthropogenic activity and recent restoration efforts. The effects of these activities on the biogeochemical system in general and on the nitrogen content and isotopic composition in particular are still unclear (Serruya, 1971, 1978; Serruya et al., 1980; Berman et al. 1992; Zohary et al. 1994; Berman-Frank et al. 1998; Hambright et al. 2000; Dubowski et al., 2003; Zohary, 2004; Hambright et al., 2008; Hadas et al., 2009; Goodwin, 2010).

The hydrological regime of LK, particularly of it outflows, have been altered over the last 6 decades. Until the 1960's excess water discharged naturally through the so-called Southern Jordan River. In 1964 the National Water Carrier project commenced, enabling the pumping of large volumes of water (often about 440 x 10^6 m^3 $year^{-1}$) from the lake and its conveyance and distribution throughout large parts of Israel for domestic consumption (Serruya, 1978). However, over the past decade or more, pumping from the lake has decreased substantially, coinciding with decrease of inflow to the lake. The latter is attributed to changes in precipitation patterns over northern Israel as well as to damming of water in the drainage basin (Mekorot, Israel National Water Co., Home page). Since 1995, as part of the Israel-Jordan peace treaty some 50 million cubic meters of water are supplies annually to the Hashamite Kingdom of Jordan.

Since the beginning of the 2018-19 rainy season, LK water level has risen considerably in April 2020 to -208.8 m, the highest level it has been since 2004, just 16 cm below the upper red line - due to strong rains and a radical decrease in pumping. The rise is impacted by the amount of water pumped into the national water carrier system. Such pumping nearly stopped in recent years due to dropping water levels. The rising waters have also had some positive side effects, slowing the lake's salinization process which had been endangering the water quality.

Dinoflagellate Peridinium gatunense Nygaard is the most important phytoplankton species of Lake Kinneret (Zohary et al., 2014). It forms massive spring blooms, impacting the entire ecosystem.

Lake Kinneret is a warm monomictic lake that is stratified 10 months a year, between spring and fall, and is fully mixed during the 2-3 months of winter (Fig. 1.2). This seasonal pattern is

reflected in temperature and oxygen profiles. It is also expressed in the distribution of the various nitrogen species along the water column (Fig. 1.2). In the winter, when the lake is well mixed and oxidized, the nitrogen species are homogeneously distributed throughout the water column, with dominance of NO_3^-. Stratification, which limits vertical exchange of water between layers, begins during spring and within few weeks oxygen becomes depleted in the bottom layers. During the summer and fall seasons, the hypolimnion is anoxic, and NH_4^+ accumulates in the bottom layers due to POM decomposition (ammonification). In late autumn, the deepening of the thermocline due to cooling of the epilimnion results in mixing with the oxidized water and nitrification of the NH_4^+ from the hypolimnion.

Several studies have focused on the nitrogen cycle in the Lake Kinneret (e.g., Cavari and Phelps, 1977; Smith et al., 1989; Ostrovsky et al., 1997; Gophen et al., 1999; Nishri et al., 2011; Nishri, 2014, and Nishri, personal communication). Their present understanding of the nitrogen cycle in LK can be summarized as following:

1. The largest external source of nitrogen to Lake Kinneret is the Jordan River. Combined riverine sources supply annual loads of approximately ~ 1,100 t N as NO_3^- and ~ 200 t N as organic N (Nishri, 2014). An additional, though smaller, external source of nitrogen to the lake is through N_2(g) fixation.

2. The seasonal pattern of riverine nitrogen inflows resembles that of riverine water discharge, of which over 60% is in winter. The nitrogen fixation takes place during the summer and fall (Gophen et al. 1999).

3. Following the annual overturn of the water column in early winter, about 800-1200 ton of nitrogen, which accumulated as ammonium in the hypolimnion, are dispersed through the entire water column.

4. In winter, the nitrified ammonium, previously mixed along the water column, plus riverine nitrate constitute the nitrate reservoir of the lake. Concurrently, the dissolved inorganic nitrogen (DIN) is consumed by algae. The common wisdom is that due to energy constrains algae prefer to first assimilate N(NH_4^+) rather than N(NO_3^-). This, as well as the nitrification processes explain why peak winter NH_4^+ is quickly reduced to the limit of detection in the epilimnion whereas NO_3^- prevails.

5. Upon the onset of thermal stratification, in March-April, nitrate is “trapped” in the hypolimnion layer. Within few weeks its concentration decreases until complete removal, mainly

due to denitrification which takes place in the oxygen-depleted hypolimnion. Following nitrate disappearance, ammonium which is the product of mineralization of organic matter, deposited from the upper layer, starts to accumulate in the hypolimnion. This accumulation continues until the overturn of the water column takes place (Fig. 1.2).

6. In the epilimnion, including the photic layer, nitrate concentration reaches its maximum in spring. The decline in concentration is then gradual and lasts until the end of summer.

Even though the nitrogen cycle in Lake Kinneret has been qualitatively identified and described, detailed understanding of some of the key processes, particularly those related to their quantification, is still lacking. For example, the relative importance of the various nitrogen sources to the lake remains unknown. Increased water inflow to the lake from the drainage area lead to maximum nitrate concentrations during the winter, yet the processes that control the decrease in the nitrate during the spring are not clear. Thus, in order to fully understand and reconstruct the nitrogen cycle in Lake Kinneret all processes must be identified and quantified.

Most available data on the isotopic composition of nitrogen in Lake Kinneret was published by Hadas et al. (2009). They found that large temporal variations in the nitrogen isotopic composition ($\delta^{15}N$) of POM and dissolved inorganic (DIN) species in Lake Kinneret occurred in response to seasonal phasing of dominant nitrogen cycle processes. The lowest $\delta^{15}N$ POM values were observed in early winter, a consequence of isotopic fractionation during NH_4^+ assimilation and the onset of nitrification, which was producing ^{15}N-depleted NO_3^- and ^{15}N-enriched NH_4^+ in the water column.

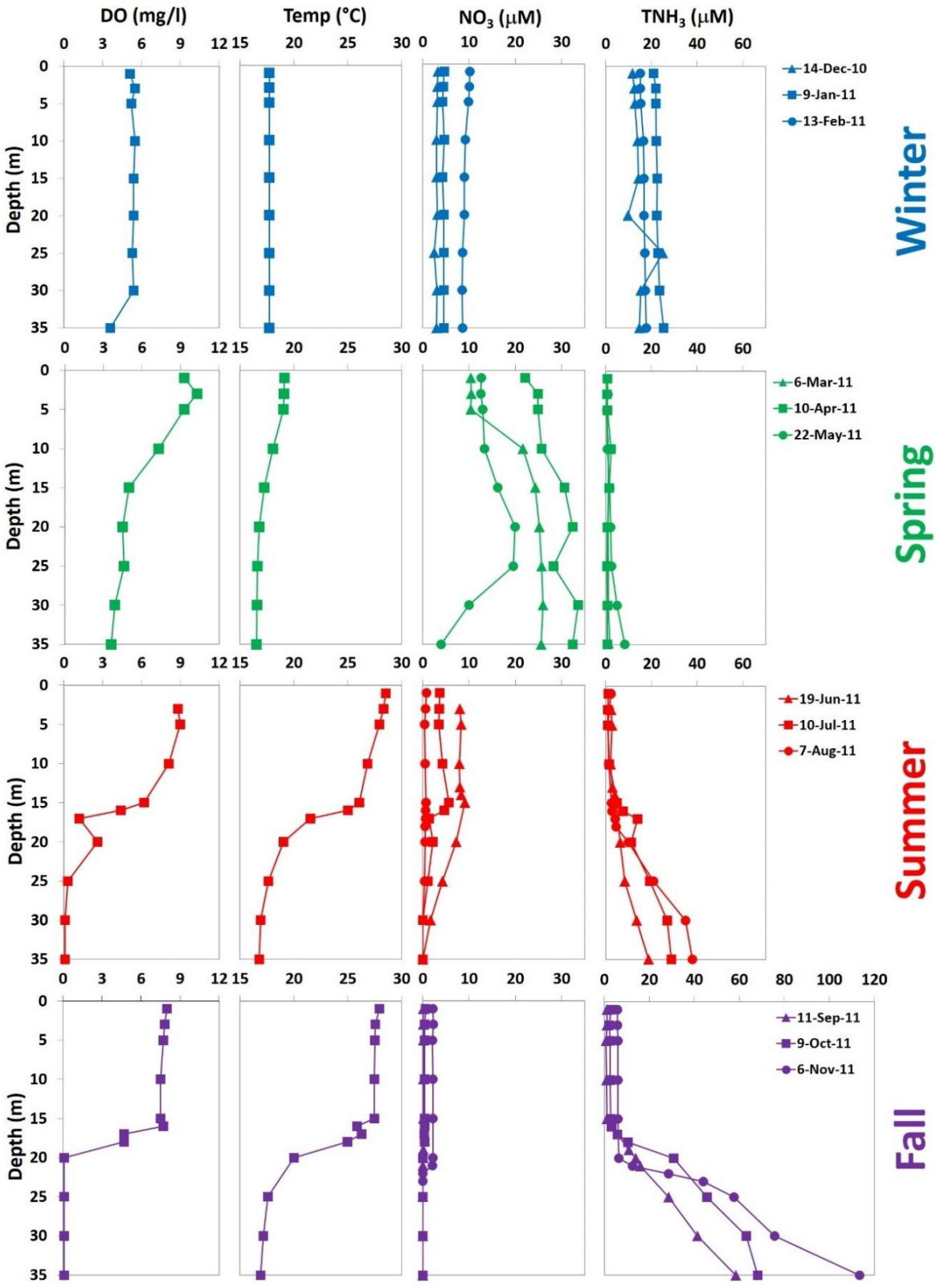


Fig 1.2. Seasonal variations in temperature, DO, nitrate and TNH_3 during winter (Dec-Feb), spring (March-May), summer (June-August), fall (Sep-Nov). Note that the TNH_3 scale is identical for all seasons and ends up at 120 μM in fall. The source of all the data presented, is the present study.

1.3 Research Goals

The annual cycling of nitrogen in aquatic systems that experience periods of anoxia and oxic conditions in the lower waters, such as the case in LK, is highly complicated (Fig 1.1). The species and reactions that need to be considered include several oxidation states and their transition, as well as particular and dissolved organic species.

The main goal of this thesis is to characterize and quantify the nitrogen cycle in Lake Kinneret using elemental mass-balance and isotopic compositions.

To achieve this goal, the study focused on the annual dynamics of the dissolved inorganic nitrogen species: nitrate (NO_3^-), nitrite (NO_2^-) and ammonium (NH_4^+) as well as the particular organic matter (POM) and their nitrogen isotopic composition in LK. Using insights gained from species concentration, isotope composition and changes in oxygen concentration in the hypolimnion, a mass balance for the nitrogen species was constructed and the processes involved in their transformation were quantified in relation to the seasonal and limnological cycle.

Specifically, the main goals of the study were:

1. To follow the seasonal variability of the concentrations and the isotopic compositions of the nitrogen species in the Lake Kinneret water column and determine their relation to a) the mixing/stratification regime and b) oxidizing/reducing conditions.
2. To identify, quantify and time the main processes responsible for the transformation of the nitrogen species in Lake Kinneret.
3. To identify and quantify the nitrogen sources and sinks in Lake Kinneret.

The study contains 4 chapters, each emphasizing a different aspect of the study. These include:

I. Development and verification of analytical methods for the determination of the isotopic compositions of dissolved inorganic nitrogen species and particulate organic matter at a range of concentrations and in the presence of other nitrogen species, and the application of these methods to LK (Chapters 2 and 3).

II. Description of the seasonal dynamics of nitrogen species and dissolved oxygen (DO) in LK based on weekly depth profiles conducted during the years 2010-2016 at the center of the lake. These profiles are used to formulate a nitrogen mass balance and to quantify the

processes and rates controlling the nitrogen cycle in LK (Chapter 4).

III. Dynamics of the isotopic compositions of the important nitrogen reservoirs in LK: NO_3^-, NH_4^+ and POM in depth profiles representing all seasons over several years. Data also include the nitrogen content and its isotopic composition in the main nitrogen sources to the lake (e.g. Jordan River water, Nahal Meshushim, etc.). This chapter also presents incubation experiment that was conducted in order to follow the decomposition of POM in LK water column and characterize the N-isotopic fractionation during POM ammonification. The detailed field and experimental study of the dynamics of nitrogen isotopic composition during ammonification of POM proved to be crucial in identifying and understanding the processes controlling the nitrogen system in LK (Chapter 5).

IV. Summary and conclusions (Chapter 6) which includes a synthesis (Section 6.1), which provides a cartoon-like summary of my view on the nitrogen cycle of LK as described in chapters 4 and 5, depicting the lake during 3 important limnologic seasons: mixing, onset of stratification and stratification.

2. Methods

2.1 Sampling and field measurements

Yigal Allon Kinneret Limnological Laboratory (KLL) of Israel Oceanographic and Limnological Research (IOLR) carries out weekly monitoring cruises to station A, which is at the center of LK (Fig. 2.1). Here, depth profiles are sampled at 5 m intervals using Niskin sampling bottles that are lowered to the desired depths. Prior to the lowering of the Niskin bottle a temperature profile is taken to identify the depth of the seasonal thermocline. Then, in addition to the 5m intervals, samples are taken 1m above, at the thermocline and 1m below it. The samples are then analyzed for various parameters at KLL.

For the benefit of my study, during the years 2010-2016 additional samples were collected during these cruises for particulate organic material (POM) and nitrogen isotopic measurements from depths of 1m, 15m, 25m, and 35m. These samples were immediately frozen and transferred to the GSI. In addition, as part of my study, cruises were also carried out seasonally during which I collected depth profile samples using a peristaltic pump (Masterflex L/S® Easy-Load Head). Prior or immediately after my cruises, potential nitrogen sources to the lake were sampled from riverine sources (Fig. 2.1B). The samples for the nitrogen isotopic analyses were frozen upon return to the GSI.

Prior to the isotope analyses, samples were filtered off-line in the field or in the lab through a GF/F filter by using a Millipore system attached to a pump. The filtered water samples were stored in 250 cc Nalgene bottles and kept frozen until analyses. The filter containing the accumulated organic matter was dried and kept for POM measurements.

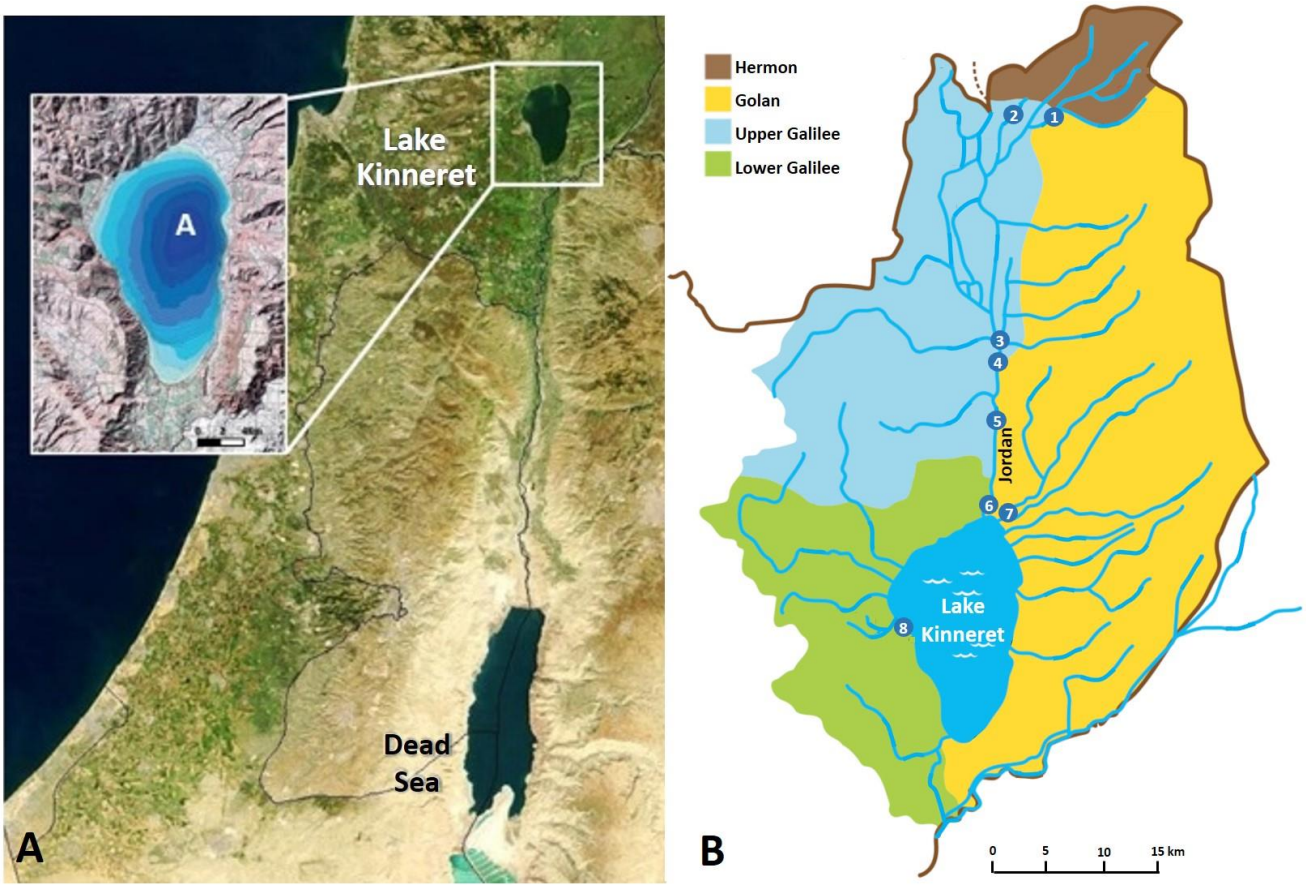


Fig. 2.1. Location map of Lake Kinneret and the sampling sites in its drainage basin. A. Site A marks the location from which LK water column was sampled. **B.** Map of Lake Kinneret's watershed showing the location of the sampling sites. The numbers denote" 1-Banias, 2-Dan, 3-Bnot Yaacov Bridge, 4-Pkak Bridge, 5- Huri Bridge, 6-Arik Bridge, 7- Meshushim, 8- Fuliya.

2.3 Chemical Analyses

The concentrations of dissolved oxygen (DO) and the dissolved inorganic nitrogen (DIN) species were measured at KLL as part of the laboratory's routine program. DO was analyzed using the Winkler titration method (American Public Health Association, 1992). For TNH_3, NO_2^-, NO_3^- (i.e. the DIN species) and dissolved organic nitrogen (DNorg) analyses, lake water samples were filtered through a 0.45 μm filter (Schleicher & Schuell). The DIN species were analyzed with a Flow Injection Analyzer (FIA, QuikChem 8000, Lachat Instruments). Nitrogen content was determined using the standard Kjeldahl method (Hadas et al., 2009), on filtered (0.45 μM) and non-filtered samples. In this procedure all forms of nitrogen are oxidized to nitrate and the difference between total nitrogen thus obtained to the various species that are measured

separately is attributed to organic forms of N (either particulate or dissolved). The samples were reacted with a mixture of potassium peroxodisulfate ($K_2S_2O_8$) and NaOH (1.5 N), and then measured with a spectrophotometer. The color reagent was prepared by mixing Diphenylamine-4-sulfonic acid sodium salt ($C_{12}H_{10}N\ NaO_3S$; 0.04 g) with 4,4'-Diaminodiphenyl sulfone (1.2 g) and Hydroxylamoniumchloride (1 g) with concentrated sulfuric and phosphoric acids (1:1). The reading was performed on a spectrophotometer at 570 nanometers wavelength.

With the Kjeldahl method, the unfiltered samples yield the total N (TN) and the difference between the filtered and unfiltered samples yield the organic nitrogen (PNorg). Dissolved organic nitrogen (DNorg) was calculated as the difference between the nitrogen content in the filtered samples and the DIN. The total organic nitrogen (TNorg = $PN_{org}+DN_{org}$) was calculated as **TN – (NO_3^-+NO_2^-+TNH_3).**

Primary production was determined by incubation with $NaH^{14}CO_3$ following Berman (1973). Water was sampled from the Niskin bottle via a narrow tube (avoiding air and gas exchange) into 60-ml glass bottles with glass stoppers (Wheaton). Prior to deployment back in the water column the samples were filtered to remove grazers. Each set consisted of light and dark bottles, with and without the addition of 3-(3,4-dichlorophenyl)-1,1-dimethylurea (DCMU; Sigma) ($5*10^{-6}$ M) to separate bacterial photosynthesis from eukaryotic one, respectively. Carbon fixation was measured by the addition of 200 µl of 25 µCi ml^{-1} $NaH^{14}CO_3$ (Amersham) to the bottles, which were then lowered to the original depth in the water column and incubated at in-situ depth, and therefore temperature and light, for 4 hours. Carbon fixation was terminated by filtering the samples on 0.45 µm nitrate cellulose membrane filters (Poretics). The filters were put in scintillation vials and exposed overnight to concentrated fuming HCl, to eliminate unfixed ^{14}C. A volume of 10 ml scintillation liquid (Ultima Gold, Packard) was added to each vial and the vials were counted in a Kontron liquid scintillation counter.

2.4 Nitrogen and oxygen isotopic determination of N-species

The methods I used for the determination of the isotopic composition of individual N-species are described below. Analyses were carried out on the IRMS in the Geological Survey of Israel. Also included is a short historical background on the development of the methods for the analyses of the isotope composition of the individual aqueous N-species**.** However, during my

thesis I found that the co-existence of several inorganic nitrogen species at non-negligible concentrations, which is often the case in LK and in other freshwater bodies worldwide, introduces substantial interferences to these methods. Chapter 3 of this thesis describes the method I developed for the determination of the isotopic composition of N-species in waters containing more than a single inorganic N-species.

2.4.1 Historical Background

The first nitrate–nitrogen isotope ratio measurements on water samples were reported in the 1950s by Hoering (1955, 1957). However, only in the early 1970's determinations of $\delta^{15}N$ values (see definition below) of dissolved ammonium and nitrate in water samples gained more widespread use in hydrological studies (e.g., Kohl, 1971; Edwards, 1973; Kreitler and Jones, 1975; Kreitler, 1979). Before the mid-1990's, the ***ammonium distillation*** method using Mg-oxide or Devarda's alloy (Cline and Kaplan, 1975) was widely used to measure nitrogen isotopes of NO_3^- in natural waters. This method involves the reduction of NO_3^- to NH_4^+, which is distilled and concentrated as ammonium sulfate salt and then combusted to produce N_2 gas for isotope measurement. Brooks et al. (1989) further developed the ***ammonium diffusion*** method for $\delta^{15}N$ measurements of NO_3^- and TNH_3. Sigman et al. (1997) modified the ammonium diffusion method for seawater NO_3^-, which is generally present only at very low concentrations. Silva et al. (2000) proposed a method using ***ion exchange*** resins for collection of NO_3^- and NH_4^+ followed by precipitation as silver salt. Bratkic et al. (2012) used the solid ***$AgNO_3$ method*** to determine the $\delta^{15}N$ of the nitrate according to the method of Silva et al. (2000) as modified by Fukada et al. (2003).

The development of automated continuous flow, purge and trap analyses, has made the rapid isolation of nitrous oxide (N_2O) and the analyses of its N and O isotope composition possible. Consequently, '***denitrification methods'*** were developed to measure the $\delta^{15}N$ and $\delta^{18}O$ values of NO_3^- simultaneously. Sigman et al. (2001) and Casciotti et al. (2002) used ***denitrifying bacteria*** whereas McIlvin and Altabet (2005) developed the ***Cd-reducing*** method to reduce dissolved NO_3^- to NO_2^- and then, (using azide), to N_2O. The latter method is now widely used in the analyses of both $\delta^{15}N_{NO3^-}$ and $\delta^{18}O_{NO3^-}$ compositions of nitrate in water (e.g., Bohlke et al., 2007; Flinn, 2012; Zeng and Wu, 2015; Mayer et al., 2013; Ohte et al., 2013). Zhang et al. (2007)

presented a quantitative method for the conversion of TNH_3 to NO_2^- which is then converted by azide to N_2O for the mass-spectrometric determination of $\delta^{15}N$.

During this study I adopted the method of McIlvin and Altabet (2005), Zhang et al. (2007), and Schilman et al (2007) for determining the isotopic composition of single inorganic N-species. I then further refined the method to enable the determining of the isotopic composition of N-species in the presence of other N-species (see Chapter 3). The methods used in this study for the determination of the isotopic composition of a single nitrogen species is described below.

2.4.2 Measurements of a single nitrogen species in solution

The isotopic composition of an element is usually presented as the ratio between the heavy and the light isotope, calibrated against an international standard. For nitrogen, the standard is atmospheric N_2, and the isotopic composition of nitrogen is defined as $\delta^{15}N_{air} = 0‰$ (equation 2.1):

$$\mathbf{2.1} \qquad \delta^{15}N = \left[\frac{(^{15}N/^{14}N)_{Sample} - (^{15}N/^{14}N)_{Air}}{(^{15}N/^{14}N)_{Air}}\right] \cdot 1000$$

In order to measure the isotopic compositions of nitrate, nitrite, and ammonium, each had to be transformed separately into $N_2O_{(g)}$. After chemical reduction to N_2O, the gas was stripped, collected and purified by a modified ThermoFinnigan Gas Bench II system connected to a ThermoFinnigan Delta V isotope ratio mass spectrometer (IRMS) where it was analyzed for the nitrogen and oxygen isotopic compositions as described in details by Schilman and Teplyakov (2007).

The precision of the isotope measurements is ± 0.5‰ for both $\delta^{15}N$ and $\delta^{18}O$.

2.4.2.1. Sample handling

Samples for isotope analyses of the nitrogen species were collected in 125 ml polyethylene bottle, filtered through 0.45μM filter and stored in a freezer until analysis. NO_3^-, NO_2^- and TNH_3 concentrations were measured beforehand by KLL on a different set of bottles, thereby allowing quality control on the chemical procedure described below.

2.4.2.2 Chemical preparation

In order to measure the isotopic compositions of nitrate and ammonium, each of these species of nitrogen was converted to NO_2^-, that subsequently was quantitatively converted to $N_2O_{(g)}$ to be analyzed on the IRMS.

Here I provide the protocol for the conversion of each nitrogen species to nitrite, emphasizing the modification and improvement introduced to each step. The instructions for the preparation of the different reagent used are given at the end of this section. The next Chapter (Chapter 3) describes the procedure that I developed in the framework of the present study to measure the N (and O) isotopic composition of a specific nitrogen species in the presence of another N-species, by removing the interfering species.

Nitrate

The method applied in the present study includes several modifications to McIlvin and Altabet (2005) protocol, as suggested by Schilman and Teplyakov (2005, 2006, 2007). The first step in transforming nitrate to $N_2O_{(g)}$ is its reduction to nitrite on a Cd column. The nitrite is then reduced to $N_2O_{(g)}$ using azide (N_3^-):

2.2 $$NO_3^- \xrightarrow{Cd-Col.} NO_2^- \xrightarrow{N_3^-} N_2O_{(g)}$$

Prior to the chemical procedure, the samples were diluted to NO_3^- concentration in the range of 2-20 µM (0.124-1.24 ppm) for a final solution volume of 40 ml, with 0.5 M NaCl and pH of 8.5 (see below). The presence of halides and the pH of 8.5 are the optimal conditions for the complete reaction between nitrite and azide to form nitrous oxide (Bunton and Stedman, 1959; Stedman, 1959a,b; McIlvin and Altabet, 2005) and to complete oxygen exchange between nitric acid and water (Stedman, 1952; Bunton et al., 1953, 1958, 1959; Bunton and Masui, 1960). The solution is then passed slowly through a column filled with granular cadmium, which ensures complete reduction of the nitrate to nitrite with no isotopic fractionation (Schilman and Teplyakov, 2005, 2006, 2007). This part of the procedure lasts only several minutes.

The first step of the procedure was setting the pH to 8.5 for all standards and samples. Instead of adding HCl to lower the pH to the desired value, I modified this procedure by first

adding 0.6 ml of 0.25 M EDTA solution, causing the pH to drop to a value between 2 and 4. The EDTA step also helped in processing samples that contained significant amount of metals which otherwise would hamper the efficiency of the column. The pH of the samples was then raised to ~7 by adding several drops of 1M NaOH, followed by dripping 1M imidasole solution until a pH of 8.5±0.1 was reached. In cases in which the pH overshot, several drops of 0.1M HCl were added, slowly decreasing the pH down to 8.5±0.1. pH was monitored with an electrode calibrated against pH standards of 4.0, 7.0 and 10.0.

The preparation of the Cd column for the reduction of NO_3^- to NO_2^- is a modified procedure based on Lachat Instruments' instructions (Lachat Cad Column Repack Instructions) for "copperizing and packing cadmium columns ". ***Note that the Cd is very toxic and should be treated carefully only under fume hoods, using gloves and safety glasses.*** The Cd granules have to be sieved to 0.25-0.50 mm size, ~5 g are needed to pack a column. The sieved Cd granules are washed with 15 ml of acetone in a 50 ml centrifuge vial, swirled and decanted. 10-15 ml of 1M HCl are added to the Cd granules and the vial again shaken, swirled and decanted. Next, the Cd granules are copperized with ~10 ml 0.2% $CuSO_4 \cdot 5H_2O$ solution, swirled for 10-20 sec, and decanted. At this stage, the color of the Cd granules should turn black. The latter process is repeated several times until a red/rust colloidal copper appears in the solution. At this point the copperizing process is stopped and the granules are washed several times with ammonia buffer and stored (in this solution) till use.

In preparation for the column treatment, tygon tubes, I.D. 3 mm, O.D. 5 mm, and 15 cm long, are connected to a peristaltic pump on one end, and set to 5 ml/min flow rate. Using the peristaltic pump, the tubes (including the column) are filled with the ammonia buffer. As the sample is transferred through the column system, the line is first flushed with ~15 ml of the sample (to waste) and the rest (~20 ml) is collected for further use.

In order to evaluate the yield of the reduction of NO_3^- to NO_2^-, 0.5 ml of Sulfanilamide solution and then 0.5 ml of NED solution are added to 2.5 ml of the sample after its passage in the column. The NO_2^- yield of the reduction is measured using a spectrophotometer, monitoring the absorption at a wavelength of 543 nm (e.g., Morris and Riley, 1963; Brewer and Riley, 1965; Wood et al., 1967). A yield of >85% is required to avoid isotopic fractionation during the nitrate reduction process in the Cd column (Schilman and Teplyakov, 2006).

The next step is the reduction of the nitrite to nitrous oxide. The samples are first diluted with 0.5M NaCl solution into a Gas Bench vials, to obtain NO_2^- concentrations in the range of 1-4 μM for the entire set (depending on the IRMS sensitivity). To start the reduction reaction, each vial is injected with 0.8 mL of sodium azide (NaN_3) reagent and placed in a 30°C shaking bath for 30 minutes. ***The sodium azide reagent is extremely toxic; thus, it must be handled very carefully***. The reduction reaction is stopped by injecting 0.3 mL of 6M NaOH to each vial. The samples are now ready for isotopic measurements. In cases that $Ca(OH)_2$ is formed within the sample solution, a white suspension will appear. Such samples should be centrifuged at 2000 RPM for 10 minutes to prevent capillary plugging of the Gas Bench by the suspension.

The optimal slope of the measured versus certified $\delta^{15}N$ values of nitrate standards that underwent the above reduction process is 2.0. This is because the product N_2O molecule comprises one N atom from the original nitrate and one N atom from the azide. Likewise, the optimal slope of the oxygen should be ~1.2. McIlvin and Altabet (2005) explain that this slope indicates an oxygen isotope exchange of ~20% between water and nitrite. These slopes are achieved at full transformation to N_2O and as such are good measures of the yield of the azide reduction.

Nitrite

Reduction of nitrite to $N_2O_{(g)}$ with azide follows directly the last step of Eq. 2.2. Since, as explained below (section 2.4.2.3), nitrate standards were used to measure the isotopic composition of the nitrite, I studied also the effect of the reagents and the Cd-column used in the nitrate preparation method (above) on the nitrite measurement. This was done by comparing the values measured on the laboratory's internal $NaNO_2$ standard with and without applying the procedure described above for nitrate (Table 2.1). The results show that with the reagents of the nitrate method (EDTA+Imidasol) and the Cd-column, the $\delta^{15}N$ values of nitrite measured in the liquid samples (0.9 and 1.2‰, Table 2.1), match the values measured directly on the same $NaNO_2$ salt by an EA ($\delta^{15}N$=0.95‰; Table 2.1) (Elemental Analyzer attached to a Delta V Thermo Finnigan IRMS). $\delta^{18}O$ values were not measured by the EA. Measuring a liquid sample without any pre-treatment (Samples 3.1. and 3.2 in Table 2.1), yielded significantly lower $\delta^{15}N$ and $\delta^{18}O$ values. The

addition of EDTA+Imidasol reagents to liquid samples without passing it through the Cd column resulted in $\delta^{15}N$ value that was somewhat lower than the value obtained by the direct EA measurement (difference of ~1‰; sample 2 in Table 2.1) This comparison indicates that the use of EDTA+Imidasol reagents in the preparation process of nitrite samples is essential, whereas using the Cd-column is optional. Therefore, in this study I used the EDTA+Imidasol method to measure the isotopic composition of nitrite, without passing the samples through a Cd column.

Table 2.1. Regents and Cd-column effect on the $\delta^{15}N$ and $\delta^{18}O$ values of the nitrite standard ($NaNO_2$).

Sample ID	EDTA+ Imidasol	Cd Column	$\delta^{15}N_{NO2^-}$ ‰	$\delta^{18}O_{NO2^-}$ ‰
$NaNO_2$ standard	-	-	0.95	-
1.1	+	+	0.9	3.1
1.2	+	+	1.2	2.7
2	+	-	0.0	0.9
3.1	-	-	-15.2	-2.6
3.2	-	-	-14.8	-2.6

Ammonium

The method used here for converting ammonium into $N_2O_{(g)}$ to measure its $\delta^{15}N$ value is a modified version of Zhang et al. (2007). According to this technique, the ammonium is oxidized to nitrite by hypobromide (BrO^-). Then, the nitrite is reduced to $N_2O_{(g)}$ with azide, as described above for nitrate (Eq. 1), including the pre-column treatment. The two steps of the procedure are:

$$\mathbf{2.3} \quad NH_4^+ \xrightarrow{BrO^-} NO_2^- \xrightarrow{N_3^-} N_2O_{(g)}$$

The sample is diluted to ammonium concentration ~5µM as compared to the wide concentrations range of 0.5-10.0 µM used by Zhang et al. (2007). This former concentration was found to be optimal, yielding recovery of 95-100%. Another modification to Zhang et al. (2007) is the introduction of an additional step after the addition of BrO^- and arsenite (used to eliminate the excess BrO^- after completing the first oxidation stage according to Zhang et al. (2007)). This step involves the lowering of the high pH that results from the addition of the hypobromide to pH of ~2 using 6M HCl. The verification of the methods also indicated that when analyzing freshwater (as in the case of LK), NaCl should be added to the sample to attain NaCl concentration of 0.5M, prior to the second (azide) reduction stage to increase the rate of nitrous oxide formation (McIlvin and Altabet, 2005).

Reagents

Ammonia buffer: To prepare a 1L volume of ammonia buffer, 76.5 g NH_4Cl, and 0.9 g EDTA are added, and the solution is brought to a 1L volume by adding DDW. The pH is adjusted to 8.5 by using 10M NaOH solution.

Sulfanilamide solution ($C_6H_8N_2O_2S$) is prepared by adding 0.5g sulfanilamide to mixture of 5 ml HCl conc. diluted with DDW to a volume of 50 ml.

NED solution, Naphthylenediamine Dihydrochloride ($C_{12}H_{16}Cl_2N_2 \cdot CH_3OH$) is prepared by dissolving 50 mg NED onto 50 ml DDW.

Sodium azide reagent solution: Is prepared by mixing a solution of 1:1 2M sodium azide and 20% acetic acid.

2.4.2.3 Standards

NO_3^-: The standards used for the nitrate isotope analyses are the international standard IAEA N-3 (Table 2.2), which is an internationally distributed solid KNO_3 reference material (Bohlke and Coplen, 1995; Gonfiantini et al., 1995; Revesz et al., 1997; Kornexl et al., 1999; Silva et al., 2000). Four internal standards were also used: $KNO_{3\ GSI.}$, US-1, US-2, and US-6. US-1, US-2, and US-6 are KNO_3, prepared at the GSI lab as mixtures of different proportions of the international standards USGS-32 ($\delta^{15}N$ = 180 ‰; $\delta^{18}O$ = 25.5 ‰) and USGS-34 ($\delta^{15}N$ = -1.8 ‰; $\delta^{18}O$ = -28 ‰).

TNH_3: Ammonium sulfate standards N1, and US-3, US-4, and US-5, prepared as mixtures of the international standards USGS-25 (-29.44‰), and USGS-26 (52.87‰), at concentrations of 5µM ammonium-sulphates (Table 2.2). Stock solutions of these standards (at pH ~2) were stored frozen to be used during the whole study.

NO_2^-: Since it is impossible to purchase international standard for $\delta^{15}N$ of nitrite, and the $\delta^{15}N$ values determined on several nitrite salts ($NaNO_2$) tested during this work spread on a relatively narrow range of 1±1‰, I used the nitrate standards (see above) as nitrite standards after their reduction to nitrite according to Eq. 2.2. Since the recovery of the procedure is very close to 100%, and the nitrate is fully converted to nitrite, it is assumed that the original isotopic

composition is preserved for the standards and the samples (Table 2.1). Hence, the nitrate standards were used to determine the $\delta^{15}N$ values of the nitrite.

2.4.3 PNorg

Water samples (250-2000 ml; depending on the POM load) were filtered through pre-weighed and pre-combusted GF/F filters at 450ºC, dried at 60ºC and re- weighed. Using the water volume and the POM weight, the POM concentration was calculated. A ~10% section of each filter was cut weighed and folded into tin capsules and the N amount (PNorg) and its isotopic composition ($\delta^{15}N_{PNorg}$) were measured by the elemental analyzer attached to IRMS (the EA specified in the nitrite method, above). The samples were calibrated against the international USGS-40, and low organic soil standards: B-2151 and B-2153, and the in-house acetanilide standard (Table 2.2).

Table 2.2. Isotopic compositions of nitrate, ammonium, and PNorg standards

	Standard	Source	Material	%N	$\delta^{15}N$ ‰	$\delta^{18}O$ ‰
Nitrate	**N-3**	IAEA	KNO_3	-	-4.7	-25.6
	$KNO_{3\ GSI}$	In-house	KNO_3	-	0.88	14.13
	US-1	USGS-32+USGS-34	KNO_3	-	11.0	-24.12
	US-2	USGS-32+USGS-34	KNO_3	-	14.98	-22.95
	US-6	USGS-32+USGS-34	KNO_3	-	60.73	-9.44
Ammonium	**N-1**	IAEA	$(NH4)_2SO_4$	-	0.49	-
	US-3	USGS-25+USGS-26	$(NH4)_2SO_4$	-	-10.41	-
	US-4	USGS-25+USGS-26	$(NH4)_2SO_4$	-	10.1	-
	US-5	USGS-25+USGS-26	$(NH4)_2SO_4$	-	21.0	-
PNorg	**Acetanilide**	In-house	Acetanilide	10.36	1.18	-
	USGS-40	USGS	L-glutamic acid	9.52	-4.52	-
	B-2151	Elemental Microanalysis Ltd., Okehampton, UK	soil	0.50	4.40	-
	B-2153	Elemental Microanalysis Ltd., Okehampton, UK	soil	0.13	6.70	-

3. Determination of $\delta^{15}N$ and $\delta^{18}O$ in individual N-species in the presence of other N-species – A refined method

In many aquatic systems several N-species may co-exist. This poses a challenge in the isotope analyses of the individual species because of interference problem. For example, the presence of significant amount of nitrite in the sample will interfere with the measurements of ammonium and/or nitrate, because during the procedure of the preparation of the latter for isotopic measurements, nitrite is an intermediate product. The methods described in Chapter 2 ignore such possible interspecies interferences. Specifically, it should be verified that the $N_2O_{(g)}$ evolved during the reaction with the azide (see Chapter 2) and measured on the IRMS is derived solely from the N-species of interest.

This chapter describes the methodologies that I developed during this research to measure the isotopic composition of a particular N-species present in solution with other N-species. In the following, I evaluate and test whether the presence of a specific N-species may interfere with the isotopic analyses of the N-species of interest. In case that those such interferences are identified, I test and suggest a procedure to remove the interfering species from solution.

The analytical methods developed here meet the following requirements: (1) Full removal of the interfering N-species from the analyzed solution; (2) No production of "new" N-species of the type to be measured during the removal process; (3) Efficient production of $N_2O_{(g)}$ (to be streamed by the Gas-Bench to the mass-spectrometer) from the analyzed species.

Experiments were carried out using artificial solutions that contained salts of the N-species of interest dissolved in distilled water at pre-determined concentrations.

A flow chart summarizing the preparation process adopted in this research for the analyses of nitrite, nitrate and ammonium, the 3 DIN species of interest in LK, prior to its introduction for isotopic measurement by the IRMS (Isotope Ratio Mass Spectrometer), is provided in Fig. 3.1.

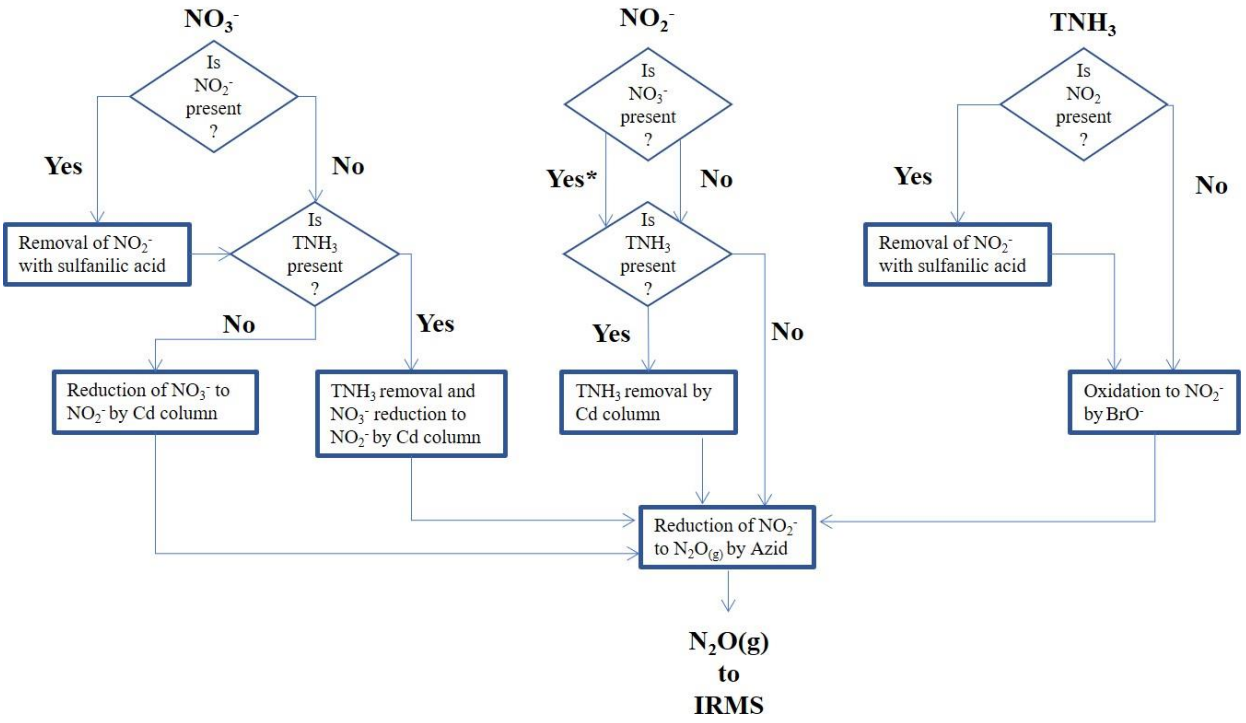


Fig. 3.1. Flow-chart of preparation process of each of the 3 inorganic N-species (the three main branches of the chart) prior to its introduction to the IRMS for isotopic measurement.
*In the rare case where the 3 species are present together, TNH_3 is removed by the Cd-column, and the measured $\delta^{15}N$ value is conducted on the remaining NO_2^- and NO_3^-; then, in a separate treatment of the same water sample, NO_2^- is removed from the NO_2^- + NO_3^- mixture according to the NO_3^- procedure (left branch of the chart), and $\delta^{15}N_{NO3}^-$ is determined; the $\delta^{15}N_{NO2}^-$ is calculated from the 2 separate measurements.

3.1 Determination of $\delta^{15}N_{NO_3^-}$ and $\delta^{18}O_{NO_3^-}$ in the presence of nitrite

Theoretically, it should be possible to determine the nitrogen isotopic composition of nitrate in samples containing significant concentrations of nitrite by measuring the isotopic composition of the mixture (nitrate+nitrite), and that of the NO_2^- alone (without Cd-column), and calculating back the isotopic composition of NO_3^-. However, as shown in Table 2.1, I found that passing a nitrite standard through the Cd-column, did not change its isotopic composition (samples 1.1 and 1.2 in Table 2.1), whereas skipping this step resulted in changes in the isotopic compositions of both the nitrogen and oxygen in the nitrite (decrease of ~1.0‰ in $\delta^{15}N_{NO2}^-$ and decrease of ~2‰ in $\delta^{18}O_{NO2}^-$, sample 2 in Table 2.1).

Thus, to ensure that the presence of nitrite will not interfere with the isotopic determination of nitrate, pre-existing nitrite must be removed prior to the Cd-column step (see flowchart in Fig. 3.1):

3.1 $$\boldsymbol{NO_3^-} + NO_2^- \xrightarrow{NO_2^- \, removal} \boldsymbol{NO_3^-} \xrightarrow{Cd-Col.} \boldsymbol{NO_2^-} \xrightarrow{N_3^-} \boldsymbol{N_2O}_{(g)}$$

The method used here for nitrite removal was boiling of the solution in the presence of sulfanilic acid (SA- $C_6H_7NO_3S$) (Yakushiji and Kanda, 1998; Zhang et al., 2007). A series of experiments using various concentrations of nitrate, nitrite and SA were conducted to examine the efficiency of the nitrite removal procedure and its effect on the quality of the isotopic determination. The results enabled to evaluate the optimal SA/nitrite ratio to be applied (E# 5-8 in Table 3.1; Zhang et al., 2007 suggested using SA/nitrite ratio of 1.5). The isotopic results of various experiments conducted on solutions having a nitrate to nitrite molar ratio of 1:1, with different concentration of SA (and without SA, E# 3 in Table 3.1) are summarized in Table 3.1 and Fig. 3.2. Note that $\delta^{15}N_{NO_3^-}$ and $\delta^{18}O_{NO_3^-}$ average values of the nitrate used in these experiments are 9.5±0.3‰ and -19.6±0.3‰, respectively (average of E# 1.1, 1.2 in Table 3.1; Fig. 3.2), and the isotopic compositions of nitrite are $\delta^{15}N_{NO_2^-}$ = 2.2‰, and $\delta^{18}O_{NO_2^-}$ = 6.9‰ (E# 2 in Table 3.1).

Table 3.1. Experimental set-up of nitrite removal in the presence of nitrate, and $\delta^{15}N_{NO_3^-}$ and $\delta^{18}O_{NO_3^-}$ values (nitrate to nitrite molar ratio of 1:1, both 20 µM), with different concentration of SA (E# 3 is without SA). Duplicates are represented by the digits after the decimal point in the left column. See Chapter 2 for details about the nitrate and nitrite standards. $\delta^{15}N_{NO_3^-}$ and $\delta^{18}O_{NO_3^-}$ average values of the nitrate target used in these experiments are 9.5±0.3‰ and -19.6±0.3‰, respectively, and the isotopic compositions of interfering nitrite are $\delta^{15}N_{NO_2^-}$ = 2.2‰, and $\delta^{18}O_{NO_2^-}$ = 6.9‰.

E# (experiment No.)	NO_3^- (µM)	NO_2^- (µM)	Sulfanilic acid (SA) (µM)	NO_2^- conc. following SA (µM)	NO_2^- conc. following SA and Cd-Col. (µM)	$\delta^{15}N$ (‰)	$\delta^{18}O$ (‰)
1.1	20	-	-	-	20	9.2	-19.9
1.2	20	-	-	-	21	9.8	-19.3
2	-	20	-	-	19	2.2	6.9
3	20	20	-	-	39	6.4	-7.8
4	20	20	- [1](boil)	20.2	35	5.9	-10.3
5.1	20	20	20	0.2	20	11.0	-19.2
5.2	20	20	20	0.2	18	11.9	-22.6
6.1	20	20	40	0.1	18	11.2	-25.3
6.2	20	20	40	0.0	18	11.5	-25.3
7.1	20	20	10	7.6	26	11.9	-14.6
7.2	20	20	10	7.3	25	11.7	-16.3
8.1	20	-	10	0.1	19	10.5	-24.8
8.2	20	-	20	0.1	19	10.7	-24.7
Bl.1	-	20	20	0.4	-	-	-
Bl.2	-	0	20	0.1	-	-	-

[1]Only boiling, without SA.

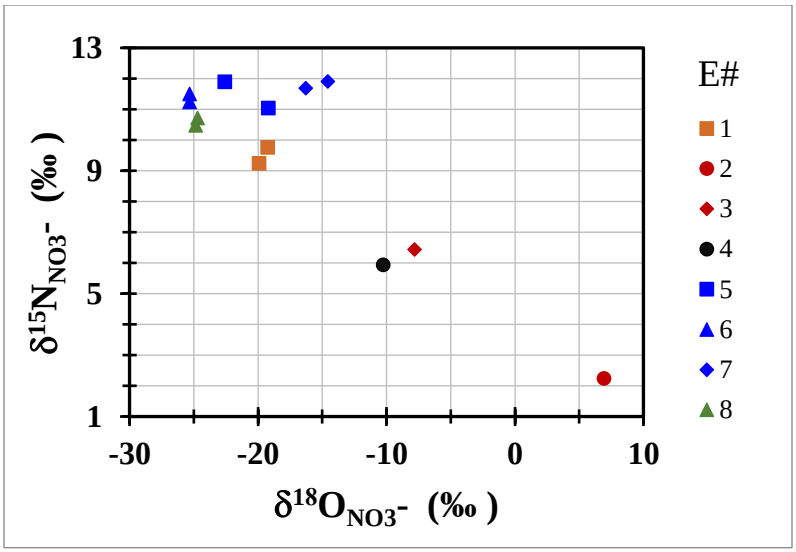


Fig. 3.2. Measured $\delta^{15}N_{NO3^-}$ vs. $\delta^{18}O_{NO3^-}$ in the experiments for the removal of pre-existing NO_2^- from solution (see Table 3.1 for details). E# 1 and 2 are the compositions of the pure standard solutions of nitrate and nitrite, respectively, the rest of the marks (E# 3-8) are explained in Table 3.1.

The experiments conducted to remove the nitrite using SA in different nitrate:nitrite:SA ratios (Table 3.1, Fig. 3.2) showed that:

1. The isotopic composition measured on mixture of NO_3^- - NO_2^- at a molar ratio of 1, without nitrite removal by SA (E# 3) or by just boiling the mixture for nitrite removal (E# 4), yielded intermediate values (between nitrate and nitrite end-members).

2. A mixture of 1:1:1 ratio for nitrate:nitrite:SA (E# 5) resulted in the complete removal of the nitrite, 100% recovery of the nitrate (see Chapter 2 for details on recovery), but showed a 1-2‰ increase in the $\delta^{15}N_{NO3^-}$ value. The reason for this increase is not clear, most likely related to the SA treatment.

3. A mixture ratio of 1:1:2, nitrate:nitrite:SA (E# 6), resulted in the complete removal of nitrite, $\delta^{15}N_{NO3^-}$ was similar to E# 5 (i.e. 1-2‰ higher than the standard), but $\delta^{18}O_{NO3^-}$ was lower by 5-6‰ than in E#5.

4. Lowering the SA in the mixture to 1:1:0.5, nitrate:nitrite:SA (E# 7), resulted in the removal of only ~2/3 of the nitrite (7 µM out of 20 µM were left, as indicated by 133% "recovery" of NO_3^-). In this case the apparent $\delta^{15}N_{NO3^-}$ increased by 1-2‰, as compared to E# 5 and E#6. This is rather puzzling, as one would expect to obtain an apparent $\delta^{15}N_{NO3^-}$ value that is lower than in E# 5 and E#6, somewhere between the initial $\delta^{15}N$ values of the nitrate and nitrite. This may indicate that isotopic fractionation takes place during partial removal of NO_2^- by SA. On the

other hand, the value of $\delta^{18}O_{NO3^-}$ (-15.4±1.2‰) represents an isotopic mixing, with excess of the nitrate over the nitrite, due to incomplete removal of the nitrite during its reaction with the SA.

5. Applying SA to a solution containing just 20 μM nitrate (no nitrite) with 10 or 20 μM SA (E# 8), shows that the SA present in the solution does not react with the NO_2^- product of the Cd-column. This is most likely due to the high pH of the NO_3^- containing solution introduced to the column (8.5; as oppose to the low pH in the NO_2^- removal process). However, the NO_3^- is partly affected by the SA, resulting in $\delta^{15}N$ increase by up to 1‰ (to 10.6±0.1‰), and $\delta^{18}O$ decrease by 3-4‰ (to -24.7‰). These results are in line with the result obtained from E#6 that contained the highest SA concentrations.

6. Applying SA and boiling the solution containing only the nitrite standard yielded very low blank value for nitrite (E# Bl.1), which was marginally higher than applying the SA on solution with no nitrite and nitrate (E# Bl.2).

Following the results of the set of experiments described above, the procedure adopted in this research was to pre-treat LK samples and remove their nitrite prior to measuring the isotopic composition of the nitrate. Such treatments were carried out whenever LK samples contained more than 10% nitrite relative to the nitrate content. Following the results of E# 5, the concentration of SA during such treatment was adjusted as to be similar to that of the nitrite present in the sample. This 1:1 SA/nitrite ration is not very different from the ratio of 1.5 recommended by Zhang et al., (2007). According to E#5 this treatment results in measured $\delta^{15}N_{NO3^-}$ value that is ~1.5‰ higher than the true $\delta^{15}N_{NO3^-}$ value, and with $\delta^{18}O_{NO3^-}$ value very similar to that of the nitrate (Table 3.1). Thus, in such pretreated LK samples, 1.5‰ was subtracted from the measured $\delta^{15}N_{NO3^-}$ value.

3.2 Determination of $\delta^{15}N_{TNH3}$ in the presence of nitrite

The methodology used to determine the impact of the presence of nitrite on the nitrogen isotopic composition of ammonium, was similar to that used for nitrate (Section 3.1). Different mixtures of TNH_3 + NO_2^- + SA were prepared and the efficiency of the removal of NO_2^- before oxidizing the ammonium to nitrite and its impact on the isotopic composition of the TNH_3, were tested.

The steps of the process for transforming TNH_3 into N_2O (g), from a mixture with nitrite are thus (see flow chart in Fig. 3.1):

$$\mathbf{3.2} \qquad \boldsymbol{TNH_3} + NO_2^- \xrightarrow{NO_2^- \ removal} \boldsymbol{TNH_3} \xrightarrow{BrO^-} \boldsymbol{NO_2^-} \xrightarrow{N_3^-} \boldsymbol{N_2O}_{(g)}$$

The optimal SA/nitrite ratio suitable to remove nitrite interference while preserving the original isotopic composition of TNH_3 was tested as described below (Table 3.2).

The isotopic compositions of the two end-members of $\delta^{15}N_{TNH3}$ and $\delta^{15}N_{NO2}^-$ (in-house standard) are given in Table 3.2 (E# 1 and E#2 respectively).

Table 3.2. Experimental set-up of nitrite removal in the presence of ammonium and $\delta^{15}N_{TNH3}$ results (ammonium to nitrite molar ratio of 5:6, concentrations in µM), with different concentrations of SA. Duplicates are represented by the digits after the decimal point in the left column (except of E# 7). See Chapter 2 for details of the ammonium and nitrite standards. $\delta^{15}N$ value of the target TNH_3 is 26.0‰, and $\delta^{15}N$ value of the interfering NO_2^- is 2.1‰ (E#1 and E#2, respectively).

E#	TNH_3 µM	NO_2^- µM	SA µM	NO_2^- µM following SA treatment	NO_2^- µM after TNH_3 Oxidation	$\delta^{15}N_{TNH3}$ ‰
1.1	5	-	-	-	5.4	25.9
1.2	5	-	-	-	5.5	26.0
2	-	6	-	[1]5.9	6.0	2.1
3	5	6	-	[1]5.7	11.0	12.4
4.1	5	6	6	0.0	4.2	27.6
4.2	5	6	6	0.0	3.9	26.5
5.1	5	6	12	0.0	3.6	-36.7
5.2	5	6	12	0.0	3.4	-29.4
6	5	-	6	0.0	4.5	-30.1
7.1	-	-	6	0.0	0.1	-36.4
7.2	-	6	6	0.0	0.1	-36.4
7.3	-	-	-	0.0	0.2	-32.9
8	5	-	3	0.0	4.4	24.9
9.1	5	6	3	1.2	5.7	24.1
9.2	5	6	3	1.2	5.5	22.1

[1] No attempt to remove nitrite, i.e., no SA and no boiling step.

The results (Table 3.2) suggest that:

1. Mixture of ammonium + nitrite at a ratio of 5:6 (5µM ammonium and 6µM nitrite) with no pre-nitrite removal (no SA) yielded $\delta^{15}N_{TNH3}$ = 12.4‰ (E# 3), as one would expect from such a mixture.
2. The same ammonium + nitrite mixture but pre-treated with 6µM SA (E# 4) resulted in complete removal of the nitrite, ~80% recovery of the ammonium with $\delta^{15}N_{TNH3}$ value which is higher by ~1‰ than that of the ammonium standard (E#1). This increase in $\delta^{15}N$ is very similar to the 1-2‰ increase in $\delta^{15}N_{NO3}^-$ in response to the addition and

pretreatment with SA at the same concentration as that of the interfering nitrite (E# 5 in Table 3.1).

3. The same ammonium + nitrite mixture with excess SA (12 μM), also resulted in complete removal of NO_2^- (E# 5). However, here, TNH_3 recovery was just ~70% and the $\delta^{15}N_{TNH3}$ value was dramatically offset to ~ -30‰, an obviously erroneous value.
4. Very similar erroneous $\delta^{15}N_{TNH3}$ (-30‰) value was obtained when SA (6 μM) was added to a solution containing TNH_3 with no nitrite (E# 6).

The results of E# 5 and E# 6 (points 3 and 4 above) may suggest that the excess SA (i.e. the fraction that has not reacted with the original nitrite) complexed with the nitrite produced from the oxidation of the ammonium (Eq. 3.2, Fig. 3.1) to yield in the azide step a highly depleted and erroneous isotopic composition for the ammonium.

It should be noted that the sulfanilic acid (SA) has similar color to that of the sulfanilamide, the reagent used for the spectrophotometric measurement of nitrite (Norwitz and Keliher, 1984). This means that if excess of SA remains in the solution after the ammonium oxidation step, it will be measured as nitrite by the spectrophotometer. However, during the next step of the procedure, the azide will produce only traces of N_2O that is characterized by very low $\delta^{15}N$ values (E# 5 and E# 6), similar to those of the blank (E# 7). Based on the above, I conclude that the nitrite concentration measured in E# 5 and E# 6 after the oxidation of the ammonium to nitrite, are erroneous and the high nitrite "recovery" is probably the result of the color of the complex formed by the excess SA.

It should be noted that the effect of the excess SA on the nitrite derived from oxidizing the ammonium is different from its effect on nitrite derived from nitrate (see section 3.1). The oxidation of ammonium is done at low pH which allows the SA to complex with nitrite, whereas the nitrate treatment is done at high pH, which prevents the formation of the complex.

5. E# 8 repeated E# 6 (ammonium with no nitrite) but with only 50% the SA concentration (3μM vs. 6μM in E #6). This experiment yielded $\delta^{15}N_{TNH3}$ = 24.9‰, a value that is just ~1.0‰ lower than the ammonium standard (compared to $\delta^{15}N_{TNH3}$ = -30‰ in E# 6). Based on the Rayleigh fractionation, this indicates that the isotopic fractionation coefficient between nitrite and the nitrite-SA complex is close, but slightly above 1: when ~40% of the nitrite produced from the oxidation of ammonium remained un-complexed with SA (E# 8

with initial SA/ammonium ratio of 0.6), the resulting $\delta^{15}N_{TNH3}$ was close to that of the TNH_3 standard. However, when the nitrite-SA complex contains almost all of the nitrogen from the original ammonium (E #6: initial SA/ammonium ratio of 1.2), leaving just traces of uncomplexed nitrite (very low remaining fraction, f, in the Rayleigh type function), the $\delta^{15}N_{TNH3}$ value decreased dramatically.

6. Experiment E# 4 repeated E# 9 but with SA/nitrite ratio of 0.5 (vs. 1 in E# 4). This experiment resulted in removal of ~80% of the original NO_2^- by SA (1.2μM out of 6 μM were left) and the $\delta^{15}N_{TNH3}$ value decreased by 2-4‰, due to mixing with the "light" residual nitrite, which has $\delta^{15}N$ value of 2.1‰ (E# 2).

Following these results, the method used in this thesis to determine $\delta^{15}N_{TNH3}$ in LK in the presence of nitrite as the interfering N-species was its removal by SA having a concentration equal or somewhat higher than the nitrite concentration in the sample (excess SA ≤ 50% of the TNH_3 concentration; E# 8).

3.3 Determination of $\delta^{15}N_{NO3^-}$ and $\delta^{18}O_{NO3^-}$ in the presence of ammonium

In order to determine if ammonium interferes with the measurement of the isotopic composition of nitrate and therefore needs first to be removed, I used a similar strategy to that described in Sections 3.1 and 3.2, measuring $\delta^{15}N_{NO3^-}$ in different mixtures of NO_3^-+TNH_3, with TNH_3/NO_3^- ratios varying between 0.5 and 4 (Table 3.3). The nitrogen isotopic composition of the ammonium standard used in the test ($\delta^{15}N_{TNH3}$ = -29.4‰) was very different from that of the nitrate standard ($\delta^{15}N_{NO3^-}$ = 1.2‰) (both are in-house standards). This large compositional difference allows easy identification of even small interference of ammonium on the isotopic determination of nitrate. Table 3.3 summarizes the isotopic compositions determined on the different test solutions.

A brief summary and conclusions of these tests is provided below (Table 3.3):

1. The results of all tests, with TNH_3/ NO_3^- ratios ranging between 0.5 and 4 (E# 2 to E# 5, Table 3.3) show that the presence of ammonium in the solution does not have significant

effect on the isotopic composition of the nitrate. The average $\delta^{15}N_{NO3}^-$ and $\delta^{18}O_{NO3}^-$ values in these tests are 0.9±0.3‰ and 15.2±0.7‰, respectively, i.e., within the expected compositions and with a reasonable scatter. Whereas no consistent trend was observed between $\delta^{15}N_{NO3}^-$ and TNH_3 concentrations, an increase in $\delta^{18}O_{NO3}^-$ value by ~1.0‰ to ~16.0‰ (n=2) was found in the solution most enriched with ammonium (TNH_3/NO_3^- ratio of 4).

2. Passing the solution through the Cd-column (nitrate reduction to nitrite) removes most of the ammonium, lowering its concentrations to 0-2.0 μM (column 6 in Table 3.3) and the TNH_3/NO_3^- ratio to 0.0-0.35 (column 7 in Table 3.3). As reflected in experiments E# 2 to E# 5, these low concentrations do not significantly interfere with the isotopic measurement of the nitrate.
3. The presence of ammonium does not interfere with the reduction efficiency of the Cd-column and the nitrite concentration after the reduction step (column 5 in Table 3.3) is similar, within error, to the nitrate concentration before the reduction step (column 2 in Table 3.3).

Table 3.3. Experimental set-up of ammonium removal in the presence of nitrate and $\delta^{15}N_{NO3}^-$ and $\delta^{18}O_{NO3}^-$ results. The isotopic composition of the nitrate target is: $\delta^{15}N_{NO3}^-$ = 1.2‰ and $\delta^{18}O_{NO3}^-$ = 14.8‰. $\delta^{15}N_{TNH3}$ of the interfering ammonium is -29.4‰

E#	NO_3^- μM	TNH_3 μM	TNH_3/NO_3^- Initial	NO_2^- μM (after Cd)	[1]TNH_3 μM (after Cd)	TNH_3/NO_3^- Final (after Cd)	$\delta^{15}N_{NO3}^-$ ‰	$\delta^{18}O_{NO3}^-$ ‰
1	5	-	-	5.8	-	-	1.2	14.8
2.1	5	2.5	0.5	5.3	0.7	0.14	0.7	15.1
2.2	5	2.5	0.5	5.5	2.0	0.37	0.9	14.8
3.1	5	5	1	5.2	0.1	0.02	0.9	14.0
3.2	5	5	1	5.2	0.0	0.00	1.2	14.9
4	5	10	2	4.4	0.8	0.19	0.7	15.5
5.1	5	20	4	4.6	1.0	0.22	0.9	15.5
5.2	5	20	4	5.0	0.7	0.15	1.3	16.4
Average of tests E# 2-E# 5							**0.9±0.3**	**15.2±0.7**

[1] measured as nitrite

These results indicate that ammonium does not interference with the determination of the isotopic composition of nitrate.

It should be noted that the tests were carried out on artificial mixtures of lab standards under aerobic solutions. However, in LK, as in most natural aquatic systems, high contents of ammonium are mostly found in anoxic waters. Our experience with other natural samples

containing mixtures of nitrate and ammonium (not LK water) is that the Cd-column quickly deteriorates, an observation that we attribute to the redox conditions of these waters. A careful inspection of the reduction yield of the Cd-column is therefore needed and the column should be re-packed with fresh copperized Cd when the reduction yield decreases below 85%. However, this did not pose a major obstacle in this study since when the LK's hypolimnion becomes anoxic, nitrate is no longer detectable in these waters. Thus, using the Cd-column to remove ammonium is applicable only in oxidized to sub-oxic natural water containing ammonium (e.g., few weeks after the onset of stratification in LK, see chapter 4).

3.4 Determination of $\delta^{15}N_{NO2^-}$ and $\delta^{18}O_{NO2^-}$ in the presence of ammonium

A priori, because the nitrite isotope analysis requires only the azide oxidation step (from nitrite to nitrous-oxide), without the Cd-column, ammonium is not expected to interfere with the determination of $\delta^{15}N_{NO2^-}$ and $\delta^{18}O_{NO2^-}$. To test this assumption a series of tests were carried out. The test solutions included mixtures with TNH_3/NO_2^- ratios from 0 to 4 (E# 1 to E# 3 in Table 3.4) ($\delta^{15}N_{NO2^-}$ = 0.7‰; $\delta^{15}N_{TNH3}$ = -14.4‰). Figs 3.3A & B show that the above assumption is not valid and that $\delta^{15}N_{NO2^-}$ values decrease linearly and $\delta^{18}O_{NO2^-}$ increase linearly with increasing TNH_3/NO_2^- ratio, respectively (note that the nitrite isotopic compositions are plotted at TNH_3/NO_2^- = 0). These results indicate that in the presence of ammonium, the determination of $\delta^{15}N_{NO2^-}$ and $\delta^{18}O_{NO2^-}$ should first include a step of ammonium removal. The reasons for the interference of ammonium in the nitrite isotopic analysis require further studies.

Table 3.4. Experimental set-up for the determination of $\delta^{15}N_{NO2^-}$ and $\delta^{18}O_{NO2^-}$ in the presence of ammonium**.** The isotopic composition of the target nitrite is $\delta^{15}N_{NO2^-}$ = 0.7‰, $\delta^{18}O_{NO2^-}$ = 4.3‰. $\delta^{15}N_{TNH3}$ of the interfering ammonium is -14.4‰

E#	NO_2^- µM	TNH_3 µM	$\delta^{15}N_{NO2^-}$ ‰	$\delta^{18}O_{NO2^-}$ ‰
1.1	1	-	0.7	4.1
1.2	1	-	0.6	4.5
2.1	1	0.5	0.1	4.6
2.2	1	0.5	0.3	4.8
3.1	1	2	-1.1	8.8
3.2	1	2	-0.7	7.7
4.1	1	4	-2.1	-
4.2	1	4	-2.0	10.1

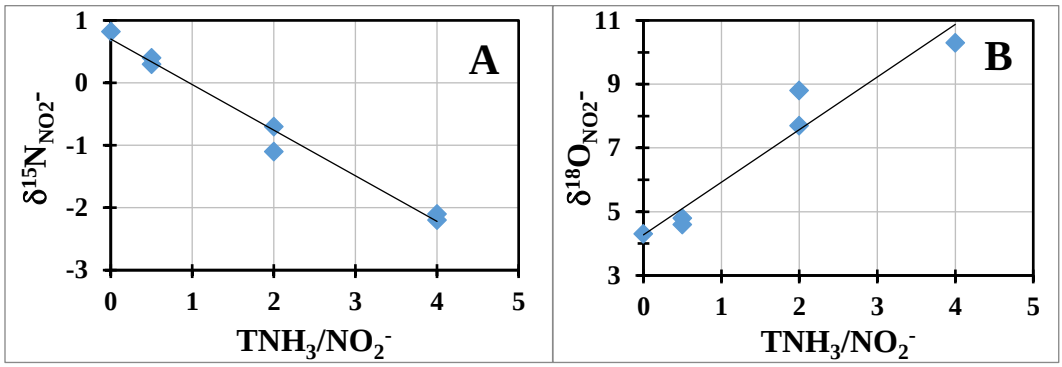


Fig. 3.3. The apparent isotopic composition of nitrite as a function of TNH_3/NO_2^- ratio: A- $\delta^{15}N_{NO2}^-$; B- $\delta^{18}O_{NO2}^-$. Note that the correct nitrite isotopic compositions are plotted at TNH_3/NO_2^- =0. The data are presented in Table 3.4.

In light of the above, several methods were examined to remove the ammonium: 1. Increasing the pH above 10 to convert all ammonium species to ammonia and allowing it to degas; 2. Purging the ammonia from the high pH solution by bubbling it with He gas; 3. Heating the high pH solution in order to enhance ammonia escape; and 4. Boiling the high pH solution in order to enhance ammonia escape. Each of the 4 methods was tested over several time windows lasting from few hours to few days. However, all were found to yield erroneous isotopic compositions and only partially succeeded in removing all of the ammonia. Extending the time windows to weeks does not make much sense and poses a risk of contamination.

On the other hand, based on the results described in Section 3.3 (measuring $\delta^{15}N_{NO3}^-$ and $\delta^{18}O_{NO3}^-$ in the presence of ammonium), passing an ammonium-containing solution through a Cd-column, removed most of it with no significant effect on the measured $\delta^{15}N_{NO3}^-$ and $\delta^{18}O_{NO3}^-$ (Table 3.3). Hence, the feasibility of using Cd-column for removing ammonium and its effect on the determination of $\delta^{15}N_{NO2}^-$ and $\delta^{18}O_{NO2}^-$ was tested by the experiments described below. The methodology is summarized as:

$$\mathbf{3.3} \qquad TNH_3 + \boldsymbol{NO_2^-} \xrightarrow{NH_4^+\ removal\ (Cd-Col.)} \boldsymbol{NO_2^-} \xrightarrow{N_3^-} \boldsymbol{N_2O}_{(g)}$$

As outlined in chapter 2 (section 2.4.2.2), the pretreatment of samples for the isotopic analyses of nitrite yields the best results when EDTA+Imidasol is reacted with the solution which is then passed through a Cd-column. Using the Cd-column is optional.

Thus the experimental procedure to remove ammonium prior to nitrite isotopic analyses included an initial step of adding EDTA+Imidasol to the test solution. The experiments were then conducted in two parts: First, the samples were passed through a Cd-column (Table 3.5a) and

second, they were subjected to an additional step of ammonia oxidation (Table 3.5b). In both parts, NO_2^- recovery and its isotopic composition were determined.

Table 3.5. Experimental set-up of ammonium removal in the presence of nitrite and $\delta^{15}N_{NO2}^-$ and $\delta^{18}O_{NO2}^-$ results. a) Results following reaction with EDTA+Imidalsol with and without Cd-Column. b) Results following an additional step of ammonia oxidation. The isotopic composition of the target nitrite is $\delta^{15}N_{NO2}^-$ = 0.0‰, $\delta^{18}O_{NO2}$- = 0.9‰. $\delta^{15}N_{TNH3}$ of the interfering ammonium is -14.4‰.

			a					b		
#E	**NO_2^- µM**	**TNH_3 µM**	**Cd-Col.**	**NO_2^- µM**	**$\delta^{15}N_{NO2}^-$ ‰**	**$\delta^{18}O_{NO2}^-$ ‰**	Ammonium Oxidation	**$^1NO_2^-$ µM**	**$\delta^{15}N$ ‰**	**$\delta^{18}O$ ‰**
1.1	-	20	used	0	-	-		0.0	-	-
1.2	-	20	used	0	-	-		0.0	-	-
2.1	20	20	used	18.1	2.4	8.9		16.5	-	-
2.2	20	20	used	18.3	2.1	8.6		17.5	-	-
3.1	20	-	used	18.8	0.9	3.1		17.9	-	-
3.2	20	-	used	18.8	1.2	2.7		17.9	-	-
4	5	5	-	5	-	-		9.4	-6.2	3.2
5	5	5	-	4.5	-2.0	8.8		-	-	-
6	5	-	-	5.0	0.0	0.9		4.3	-	-
7	-	5	-	0.5	-	-		4.8	[4]-14.4	5.4

A summary of the results of these experiments is given below:

1. Ammonium is efficiently removed by the Cd-column (E# 1.1.a, 1.2.a and E# 1.1.b, 1.2.b; Table 3.5).
2. Nearly a full recovery of the NO_2^- was achieved after the first part (Cd column E# 2.1.a and 2.2.a in Table 3.5a), and a very small change was observed after the second part (ammonium oxidation; E# 2.1b and 2.2.b in Table 3.5b). This corroborates the finding in Section 3.1 that nitrite is not impaired by the Cd-column (E# 2 in Table 3.1). The results further indicate that the Cd-column removes ammonium very efficiently.
3. $\delta^{15}N_{NO2}^-$ and $\delta^{18}O_{NO2}^-$ values increased after passing NO_2^- through Cd-column from ~0‰ to ~1‰ and from ~1‰ to ~3‰, respectively (from E#6a to E#3a in Table 3.5a and vector 1 in Fig. 3.4). This is similar to the ~1‰ increase in $\delta^{15}N_{NO2}^-$ and ~2‰ in $\delta^{18}O_{NO2}^-$ following passage of the nitrite through the Cd-column, as presented in Chapter 2 (Section 2.4.2.2).
4. The presence of ammonium results in an additional increase in the isotopic composition, to ~2.2‰ in $\delta^{15}N_{NO2}^-$ and ~8.7‰ in $\delta^{18}O_{NO2}^-$ (from E# 3a to E# 2a in Table 3.5 and vector 2 in Fig. 3.4). It should be noted that the trend observed for $\delta^{15}N_{NO2}^-$ (vectors 1 and 2 in Fig. 3.4) was not formed by simple mixing between the isotopic compositions of

pure ammonium (selected standard with very low $\delta^{15}N_{TNH3}$ value of -14.4‰, E# 7b and Fig. 3.4) and pure nitrite (line 3 in Fig. 3.4).

5. When the Cd-column step was not applied to remove the interfering ammonium prior to the mass-spectrometric measurement, the $\delta^{15}N_{NO2^-}$ decreased to a value of -2‰ and $\delta^{18}O_{NO2^-}$ did not changed (E# 5a as compared to E#2 in Table 3.5a and Fig. 3.4). This indicates that the very "light" ammonium used in this test did interfere in the measurement of the isotopic composition of nitrite.
6. Oxidation of the ammonium in a 1:1 mixture of NO_2^--TNH_3 (E# 4b in Table 3.5) resulted in ~100% yield of nitrite (the sum of NO_2^-+TNH_3) and $\delta^{15}N_{NO2^-}$ of -6.2‰ and $\delta^{18}O_{NO2^-}$ of 3.2‰; E# 4b), which lies on the simple isotopes mixing line (line 3 in Fig. 3.4) between nitrite (E# 6a in Table 3.5A) and ammonium (E# 7b in Table 3.5B).

The results of the above experiments indicate that ammonium is completely removed after passing the solution through the Cd-column. The method causes a slight increase of the $\delta^{15}N_{NO2^-}$ value (in the order of ~1‰) whereas the $\delta^{18}O_{NO2^-}$ value is significantly affected, increasing its value by ~5-6‰. Hence, just $\delta^{15}N_{NO2^-}$ (without $\delta^{18}O_{NO2^-}$) values should be considered in the presence of ammonium.

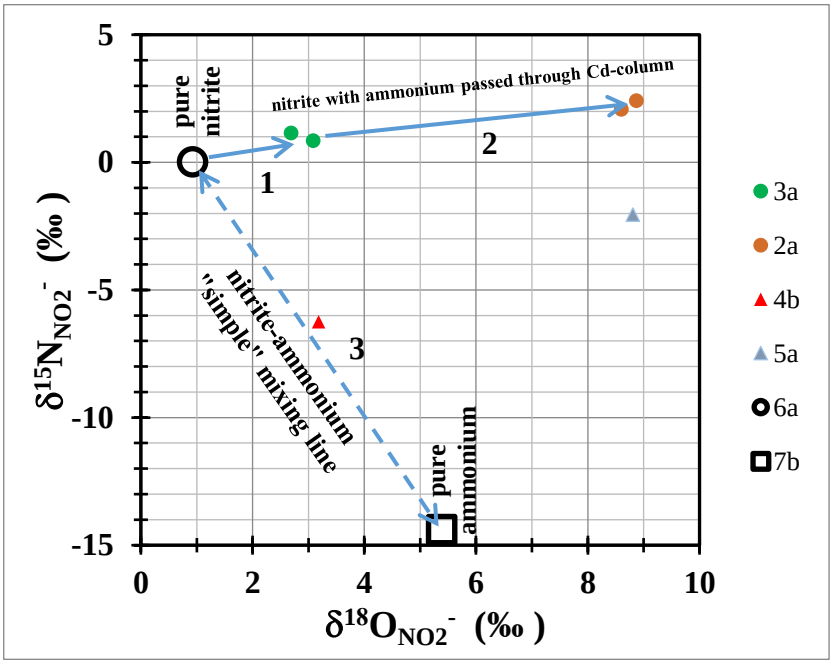


Fig. 3.4. $\delta^{15}N$ versus $\delta^{18}O$ for various tests of measuring the isotopic composition of nitrite in the presence of ammonium. Data in Table 3.5. Vectors 1, 2 and 3 are explained in items #3, #4 and #6, above.

3.5 Determination of $\delta^{15}N_{TNH3}$ in the presence of nitrate

A wide range of nitrate concentrations in which the NO_3^-/TNH_3 ratios varied between 0.5 and 4.0 (Table 3.6) was tested to evaluate the effect of nitrate on the isotopic measurement of ammonium. $\delta^{15}N_{TNH3}$ value used for the tests was 26.3‰ and $\delta^{15}N_{NO3}^-$ was 0.9‰. The isotopic analyses of the mixtures showed clearly that nitrate does not interfere with the isotopic measurement of ammonium.

Thus, the analyses of $\delta^{15}N_{TNH3}$ in LK did not require the pre-removal of nitrate from the samples when this N-species was present.

Table 3.6. Experimental set-up and $\delta^{15}N_{TNH3}$ results in the presence of nitrate. $\delta^{15}N_{TNH3}$ value of the target ammonium is 26.3‰, $\delta^{15}N_{NO3}^-$ of the interfering nitrate is 0.9‰.

TNH_3 µM	NO_3^- µM	$\delta^{15}N_{TNH3}$ ‰
5	-	26.3
5	-	26.4
5	2.5	26.5
5	2.5	26.0
5	5	26.3
5	5	26.2
5	10	25.8
5	20	26.5
5	20	26.8

3.6. Determination of $\delta^{15}N_{NO2^-}$ and $\delta^{18}O_{NO2^-}$ in the presence of nitrate

A wide range of nitrate concentrations in which the NO_3^-/ NO_2^- ratios varied between 0.5 and 4.0 (Table 3.7) was tested for evaluating the effect of nitrate on the isotopic measurement of nitrite. The nitrite and nitrate standard used for the tests had isotopic compositions of $\delta^{15}N_{NO2^-}$=0.6‰ and $\delta^{18}O_{NO2^-}$=4.3‰ and $\delta^{15}N_{NO3^-}$=9.6‰ and $\delta^{18}O_{NO3^-}$=-24.6‰, respectively. The results indicate that regardless of the NO_3^-/NO_2^- ratio, nitrate had no significant effect on the resulting $\delta^{15}N_{NO2^-}$ value while $\delta^{18}O_{NO2^-}$ value increased by ~1‰.

Thus, the determination of $\delta^{15}N_{NO2^-}$ and $\delta^{18}O_{NO2^-}$ in LK in the presence of nitrate did not require its removal prior to the isotopic analysis.

Table 3.7. Experimental set-up and $\delta^{15}N_{NO2^-}$ and $\delta^{18}O_{NO2^-}$ results in the presence of nitrate. The isotopic composition of the target nitrite is $\delta^{15}N_{NO2^-}$ = 0.6‰, $\delta^{18}O_{NO2^-}$ = 4.3‰. The isotopic composition of the interfering nitrate is $\delta^{15}N_{NO3^-}$ = 9.6‰, $\delta^{18}O_{NO3^-}$ = -24.6‰.

NO_2^- µM	NO_3^- µM	$\delta^{15}N_{NO2^-}$ ‰	$\delta^{18}O_{NO2^-}$ ‰
1	-	0.6	4.1
1	-	0.6	4.5
1	0.5	0.8	5.1
1	0.5	0.8	5.2
1	2	1.0	5.2
1	4	0.9	5.1
1	4	0.7	5.3

3.7. Conclusions and analytical recommendations

The interference in the isotopic analyses of one of the three major dissolved inorganic nitrogen species (nitrate, nitrite and ammonium) by the presence of another of the two DIN species was evaluated. If found to interfere, a range of reactions was tested to remove this interfering N-species from solution without impacting the isotopic analyses of the target species. The eventual end-product of all the methodologies is the transformation of the target N-species into N_2O gas. The gas is stripped from the solution, collected and purified by a modified ThermoFinnigan Gas Bench II system and transferred to a ThermoFinnigan Delta V isotope ratio mass spectrometer (IRMS) on which it is analyzed for its nitrogen and oxygen isotopic compositions. The instrumental precision of isotopic measurements is ±0.5‰ for both $\delta^{15}N$ and $\delta^{18}O$. $\delta^{15}N$ and N

content (% weight) of the solid standards were measured by elemental analyzer IRMS (EA-IRMS).

The isotopic measurements conducted using the methodology developed here was applied to determine the nitrogen isotopic composition of the DIN species in LK during several annual cycles. During each annual cycle the lake alternates between mixing (entire water column is under oxidizing conditions) stratification (reducing hypolimnion) and intermediate (e.g. onset of stratification) periods. These periods are accompanied by marked alternations in the abundance of the different N-species. Typical analyses of the concentrations and isotopic composition of N-species in the different seasons and depths is presented in Table 3.8. The isotopic compositions were determined following the respective procedures described above.

Table 3.8. Concentrations and isotopic compositions of various N-species in LK water during the different seasons.

Date	**Depth m**	**Lake's status mixed/ stratified (M/S)**	**TNH_3 µM**	**NO_3^- µM**	**NO_2^- µM**	**$\delta^{15}N_{TNH3}$ ‰**	**$\delta^{15}N_{NO3^-}$ ‰**	**$\delta^{18}O_{NO3^-}$ ‰**	**$\delta^{15}N_{NO2^-}$ ‰**
26.12.2010	1	M	26.3	3.9	0.3	23.1	6.5	13.3	-
9.1.2011	15	M	22.6	4.3	0.3	19.5	7.2	12.8	-
13.2.2011	1	M	15.1	10.2	1.1	22.3	5.8	8.6	-
3.7.2011	15	S	4.4	6.4	0.6	16.9	12.2	14.1	-
10.7.2011	15	S	4.9	5.6	0.6	16.2	9.7	16.3	-
11.5.2011	35	S	8.0	3.0	15.6	14.1	-	-	31.7
17.3.2013	1	M	0.9	36.7	1.4	-	6.8	3.8	-2.5
17.3.2013	35	M	1.0	39.1	1.7	-	6.2	3.2	5.0

Recommendations for determining isotopic composition of DIN species in freshwater lakes:

1. The determination of the isotopic composition of *either nitrate or ammonium in the presence of nitrite, requires first to remove the nitrite by sulfanilic acid (SA)*. The SA concentration should be as close as possible to the concentration of the nitrite. The nitrite removal process may increase the $\delta^{15}N_{NO3^-}$ by 1-2 ‰ and does not change the $\delta^{15}N_{TNH3}$.

2. The determination of the isotopic compositions of *either nitrate or nitrite in the presence of ammonium, requires first to remove the ammonium by passing the solution through a Cd-column*. The ammonium removal process may increase the $\delta^{15}N_{NO2^-}$ value by ~1‰. The presence of ammonium does not interfere with the determination of $\delta^{15}N_{NO3^-}$.

3. Nitrate has no significant effect on the determination of the isotopic composition of either nitrite or ammonium, hence *nitrate removal is not necessary.*

4. Temporal variations of nitrogen species in Lake Kinneret – Clues to the governing biogeochemical processes

This chapter focuses on quantifying the temporal variations of the different nitrogen species in LK, identifying the main biogeochemical mechanisms that control nitrogen transformations and attempting to estimate their magnitude and role in the lake's nitrogen budget. This task was achieved by quantitative processing the lake's water column profiles at high temporal resolution for the following parameters: the DIN (dissolved inorganic nitrogen = TNH_3 + NO_3^- + NO_2^-) species, nitrate (NO_3^-), nitrite (NO_2^-) and TNH_3 (total ammonia, TNH_3=NH_3+NH_4^+); the organic nitrogen species, PNorg (particular organic nitrogen) and DNorg (dissolved organic nitrogen), which make up the TNorg (total organic nitrogen); TN (total nitrogen), which is the sum of all nitrogen species (except of dissolved N_2) and DO (dissolved oxygen).
Note that the pK of $NH_4^+ \rightleftharpoons NH_{3(g)}$ is 9.2. Thus, given that the pH of the hypolimnion is around 7.5 implies that 99.9% of the TNH_3 is in the form of NH_4^+.

During the study period (2010-2016), samples of water and particulate organic matter were collected weekly at station A (located at the center of LK, Fig. 2.1) at a vertical resolution of 5 m which was increased to higher resolution of 1 m close to the seasonal thermocline (an example from year 2011 is provided in Fig. 1.2). N-species were determined also in the water of the Jordan River (JR), the main inflow to the lake.

All data are provided in Supplementary Tables S1 – S6 as follows: The concentrations (in mg/l units) of TNH_3, NO_2^-, NO_3^-, PNorg, DNorg, TN and DO in the various profiles and water depths are presented in Table S1. The temporal inventories (in mol·10^6 N units) of these variables in the lake are given in Table S2. The respective inventories in the hypolimnion (taken here to be below 15m depth), measured during 2012-2014 around the period of the onset of stratification are provided in Table S3. The relevant data for JR: its daily water inflow to LK (m^3/day units), the NO_3^-, PNorg, and TN concentrations (mg N/l units) and the annual accumulated inflow of nitrogen (10^6 mol N units) starting from the beginning of the hydrologic year (month of October), are presented in Table S4. The calculated nitrogen productivities (in daily 10^6 mol N/ epilimnion: see hereafter) at a monthly interval for LK's epilimnion are presented in Table S5.

Degrees of saturation of DO in the selected layers of LK's water column are presented in Table S6 (see hereafter).

4.1 Seasonal and annual variations of the nitrogen species in the lake

LK is a warm monomictic (mixes completely annually) lake. It is well-mixed in the winter, and thermally stratified from spring to late autumn, as reflected by the temperature and DO profiles (Fig. 1.2). Water column temperature during winter is homogenous at 16±2^{o}C. Upon the onset of stratification in spring the epilimnion gradually warms up reaching 28^{o}C at the end of summer whereas the deeper layer maintains its at pre-stratification temperature of ~18^{o}C. Stratification lasts throughout the fall as the surface water cools down until water column overturn takes place in November-December (Fig. 1.2). DO profiles show significant temporal and spatial variations, which are negatively correlated to TNH_3 and positively correlated with NO_3^-.

Seasonal variations of N-species in LK can be briefly summarized as follows (Fig. 1.2):

Winter: Water column is well mixed and oxidized. At the beginning of winter NH_4 is characterized by peak concentrations in the photic layer due the overturn event which mixes hypolimnetic water along the entire water column. Subsequently nitrate concentration increases due to nitrification (ammonium oxidation) and riverine supply.

Spring: Water column becomes stratified. In the hypolimnion DO declines followed by nitrate decline. In the epilimnion nitrate gradually declines due to assimilation by algae through photosynthesis.

Summer: The hypolimnion becomes anoxic while in the epilimnion nitrate continuous to decrease gradually due to assimilation. As the hypolimnion becomes fully anoxic and the system switches to SO_4 reduction, TNH_3 increases as a result of ammonification (bacterial mineralization of organic matter).

Fall: TNH_3 continues to accumulate in the hypolimnion because of ammonification. The beginning of mixing during late fall "injects" hypolimnetic TNH_3 into the oxidized epilimnion where it undergoes nitrification.

Temporal variations of TNH_3 and NO_3^- in four representative water depth layers (1 m, 15 m, 25 m, and 35 m) during the years 2010-2016, are shown in Fig. 4.1, depicting the following: 1) TNH_3 and NO_3^- are anti-correlated along the annual cycle. 2) TNH_3 concentrations are always the

highest in late autumn, and NO_3^- concentrations are the highest in spring. 3) The annual temporal pattern of TNH_3 and NO_3^- is similar during all years but vary in magnitude. 4) NO_3^- and TNH_3 variations were synchronized, i.e., NO_3^- concentration increase coincides with the dramatic TNH_3 decrease in the deep water. In three of the six years of the study (2013, 2014, 2016), NO_3^- started increasing when TNH_3 values dropped dramatically and nearly vanished. In the other three years of the study (2011, 2012, 2015) NO_3^- started increasing when TNH_3 was still present in the water column (~15-20 μM).

TNH_3: During the stratified season, TNH_3 is virtually zero in the oxidized epilimnion (1m and 15m) while in the hypolimnion its concentration increases with time and depth, reaching its maximum at the bottom (35m) in the late summer-early autumn (Figs. 1.2, 4.1). This indicates that the organic matter produced in the surface water layer (photic zone), undergoes ammonification in the hypolimnion, mainly at the bottom of the lake. As the epilimnion deepens towards full water column overturn in late fall-early winter, TNH_3 enriched water, previously contained within the hypolimnion, disperse and TNH_3 undergoes nitrification. In the photic part of the water column, part of it is also assimilated by flora. By the time the water column is fully mixed and aerated, TNH_3 concentrations are very low (~20 μM) and homogeneous throughout the water column. This residual TNH_3 is fully exhausted (either gradually or sharply) within several weeks (Fig. 4.1), by nitrification and assimilation, remaining almost zero throughout the rest of the mixed period. The decrease rates of TNH_3 during the onset of the mixed period are not constant; high decrease rates were observed during the years 2013, 2014 and 2016 and considerably lower decrease rates were observed during the years 2011, 2012 and 2015. The mechanisms (physical, microbiological, etc.) controlling the TNH_3 decrease rate during the fully mixed period in LK are currently not known.

NO_3^- is extremely low (0-3.5 μM) during late summer to early winter, reaching highest values during spring. Maximum annual NO_3^- concentrations vary considerably, from ~25 μM during 2014 to ~40 μM during 2013 (Fig. 4.1). During the mixed season, NO_3^- is homogeneous in the entire water column, reaching its maximum concentrations in spring. During the transition to summer and the formation of the thermocline, water column NO_3^- temporal evolution is different for the epilimnion and the hypolimnion: In the epilimnion (1 m and 15 m) NO_3^- starts to decrease early and gradually, due to assimilation (photosynthesis); In the hypolimnion (25 m and 35 m) NO_3^-

remains high for additional several weeks, before it decreases sharply due to denitrification. The denitrification processes and anoxic conditions evolve in the hypolimnion from bottom upwards, over a period of several weeks, as indicated by the decline in NO_3^- concentration which starts at the bottom and makes its way upwards.

A striking observation regarding the distribution of the N-species in LK's hypolimnion is that the annual TNH_3 maxima concentration is significantly higher than the respective NO_3^- maxima (Fig 4.1). This is counter-intuitive to the expected one-to-one changes in N-species distribution during the transformations from reduced nitrogen (ammonia) to oxidized nitrogen (nitrate). This apparent paradox is resolved when switching to plots of the temporal variations of the ***inventories*** of the different N-species as described hereafter in section 4.2.

DO: Dissolved oxygen degree of saturation (DOS: defined as the DO in the water sample divided by the calculated saturation value of DO (DOS=1) in this water at the same temperature, at 1 atm) vary significantly over an annual cycle at all depths (Fig. 4.1A). DOS>1 (Super-saturation) is observed at the lake surface during the spring bloom due to a faster rate of production (photosynthesis by phytoplankton blooms) than the rate of respiration plus oxygen gas exchange with the atmosphere. During the rest of the stratified period, after the decrease of phytoplankton blooms, surface water becomes very close to saturation with respect to DO (DOS~1) because the role of gas exchange increases relative to DO production by photosynthesis. DOS varies between years as a function of the rate of DO production. It is assumed that higher DOS super-saturation (Fig. 4.1A) reflects larger DO production during the blooming phase (e.g. years 2012, 2013, and 2014).

Annual variations of DO in the hypolimnion are controlled by oxidation of organic matter and water column mixing. Following the onset of stratification, hypolimnetic DO starts to decrease due to oxidation of organic matter at the onset of stratification (Fig. 4.1A). At mid depth (15 m), DO decreases to almost zero at the onset of stratification. However, later on, during the stratified period, DO starts to increase gradually. This gradual increase is a result of the deepening of the summer thermocline. At the onset of the mixing period, DO at mid depths (15-25 m) increases fast, reaching the surface water values as the mixed layer deepens. During that time, DO degree of saturation of surface water decreases due to mixing with DO-poor water from below. This small under-saturation remains also during complete water column mixing (DO degree of saturation constant at all depths) until the onset of stratification.

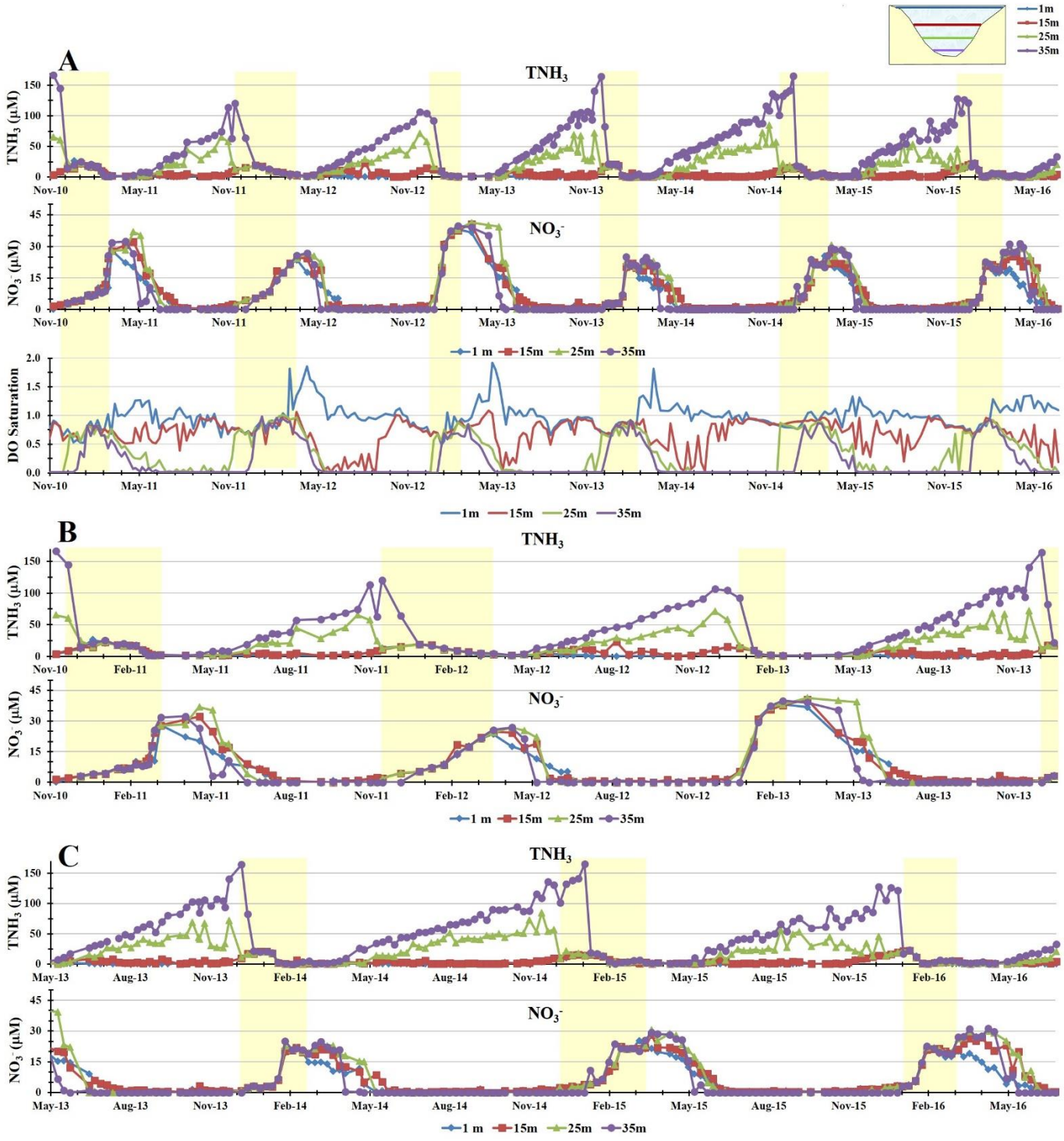


Fig. 4.1. Annual variations of TNH_3 and NO_3^- concentrations and DO saturation in four depths of LK (1 m, 15 m, 25 m, and 35 m). A- All study period (2010-2016). B- Zoom-in of TNH_3 and NO_3^- concentrations for the period 2010-2013; C- Zoom-in of TNH_3 and NO_3^- concentrations for the period 2013-2016. Mixing seasons (i.e., homogeneous water column) are highlighted by yellow rectangles.

4.2 Seasonal variations of N-species inventories of the lake

The inventories of each N-species in LK's water column were calculated by multiplying the interpolated species concentrations in every 1 m slice of the water column (e.g. Fig. 4.2A) by the water volume within this particular 1 m slice as obtained from the hypsometric curve of LK (Lake Kinneret Data Base) Fig. 4.2B) as demonstrated in Fig. 4.2C. The calculated species concentration was obtained by linear interpolation between the measured concentrations in 2 consecutive depths, above and below the depth for which the concentration was calculated. Note that, due to the hypsometry of LK (Fig. 4.2B), most of TNH_3 resides between 5 and 25 m (Fig. 4.2C), while its highest concentrations are below 30 m (Fig. 4.2A).

Integrating the quantitative curve yields the TNH_3 reservoir of the entire lake at each date. The sum of the masses of a species for all 1 m depth intervals (integral, e.g. Fig. 4.2C for TNH_3) is the species inventory (total mass) in the lake at that particular date. Plots of the secular variations in the inventories of DIN species and DO in LK during the years 2010-2016 are provided in Fig. 4.3.

The plot shows that the inventories of NO_3^- and TNH_3 are negatively correlated, similarly to the behavior of their concentrations (Fig. 4.1). The inventory of TNH_3 reaches its maximum during late summer-early autumn, towards the end of the stratified period, while NO_3^- reaches its maximum inventory in late winter- early spring, before the onset of stratification, and decreases gradually during summer down to practically zero at late summer.

The paradox of the large difference between the maxima of TNH_3 and NO_3^- concentrations (Fig. 4.1), mentioned in section 4.1 above, is solved by the species inventory plots, which show clearly that the maxima of both inventories have very similar values (Fig. 4.3). During years 2013-2016, the increase in NO_3^- inventory mirrored the decrease in TNH_3 inventory and NO_3^- maximum inventory was similar to the maximum of the preceding TNH_3 inventory. During these years, the load of nitrogen that reached LK through the Jordan River (JR), which is the main source of nitrogen to the lake, was relatively low (Fig 4.4). This suggests that most of the NO_3^- was produced by nitrification of the preceding internal TNH_3 inventory. On the other hand, during years 2010 and 2011 (and possibly 2012) when the load from JR was high, the maximum NO_3^- inventories were higher than those of the preceding TNH_3 maximum inventories suggesting input of an additional NO_3^- source (Fig. 4.4). This suggests that the magnitude of the seasonal variations of N-species inventories are controlled mostly by seasonal intra-lake physical-biogeochemical processes (e.g., oxic conditions during vertical mixing, hypolimnion anoxia during stratification, sediment

resuspension, etc.) whereas the TN input from Jordan River maintains the multi-annual (long-term) TN budget of the lake.

NO_2^- is an intermediate species in aquatic systems either during nitrification or during the opposite process of denitrification. In LK, one has to expect nitrification to occur at the beginning of winter as NH_4, previously contained in the hypolimnion, is mixed into the oxic part of the water column. Denitrification on the other hand will occur in the hypolimnion after stratification has developed and DO declined to sub-oxic levels, in late spring-early summer. The NO_2^- inventory appears as a very sharp and transient peak at the beginning of the mixing season (Fig. 4.3). It accumulates in the water for a short period when the nitrification rate is highest, as inferred from its appearance which coincides with the sharpest decline in TNH_3 inventory and increase in NO_3^- inventory (Fig. 4.3). In contrast, the period of NO_3^- decrease and TNH_3 increase is not accompanied by a NO_2^- peak (except of the year 2011 in which a very small NO_2^- was observed), indicating that at the onset of stratification, NO_3^- decreases due to denitrification, whereas TNH_3 increases as a result of ammonification of organic matter. This is the reason that any two consecutive maxima of TNH_3 and NO_3^- inventories, are not necessarily equal, e.g., in years 2010 and 2011, the NO_3^- inventory exceeds that of the preceding TNH_3 inventory.

The main flux of nitrogen out of the water column (N sink) is outgassing of dissolved N_2 to the atmosphere (Smith et al., 1989; Nishri, 2014). The dissolved N_2 is produced mainly in the sub-oxic lower water mass by denitrification and to some extent also by anammox. Nishri (2014) estimated that both processes account for the removal of approximately 70% of the annual riverine nitrogen inflow to the lake. Other fluxes that account for nitrogen removal are sedimentation and export of water through pumping. Based on the nitrogen inventories and seasonal variation in the N-species, and elaborated in section 4.3 hereafter, it is suggested here that denitrification and anammox were underestimated in previous studies (Smith et al., 1989; Nishri, 2014).

NO_3^- inventory decreases from its maximum value in the spring to zero during late summer (Fig. 4.3) due to a combination of assimilation, which produces PNorg, and denitrification, which produces dissolved N_2. Thus, not all the NO_3^- leaves the lake as N_2, as elaborated in section 4.3, below.

The onset of the mixing period and thermocline deepening is marked by a sharp TNH_3 decrease as a results of nitrification and N-assimilation, which consumes practically all the TNH_3 inventory

(between 70 and $140 \cdot 10^6$ mol N depending on the year) that was formed and stored in the hypolimnion in the preceding stratified period (Fig. 4.3).

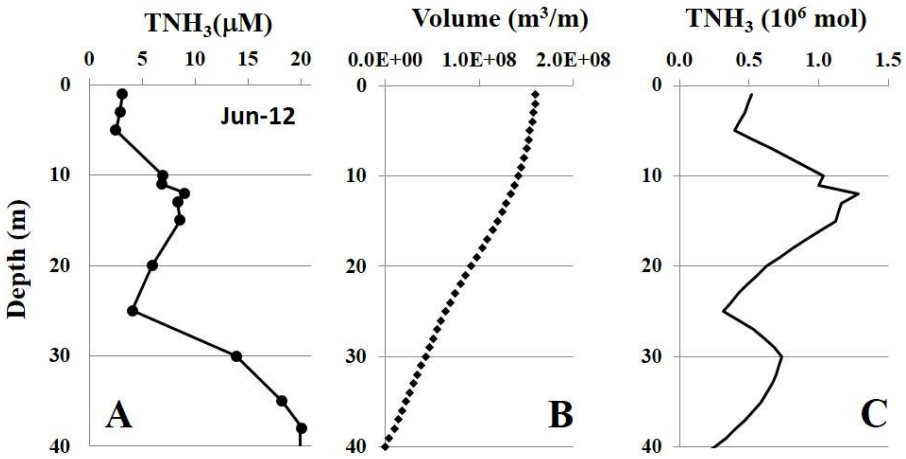


Fig. 4.2. Example of mass calculation of TNH_3 in LK water body. A-Depth profile of TNH_3 concentration (June 2012). B- Hypsometric volume curve of LK. C- Inventory of TNH_3 in horizontal 1m slices within LK water mass, the 1m intervals are calculated by interpolation of the available TNH_3 concentrations data to the 1 m intervals, multiplied by the corresponding volume. Bottom values were calculated by extrapolation down to 40 m.

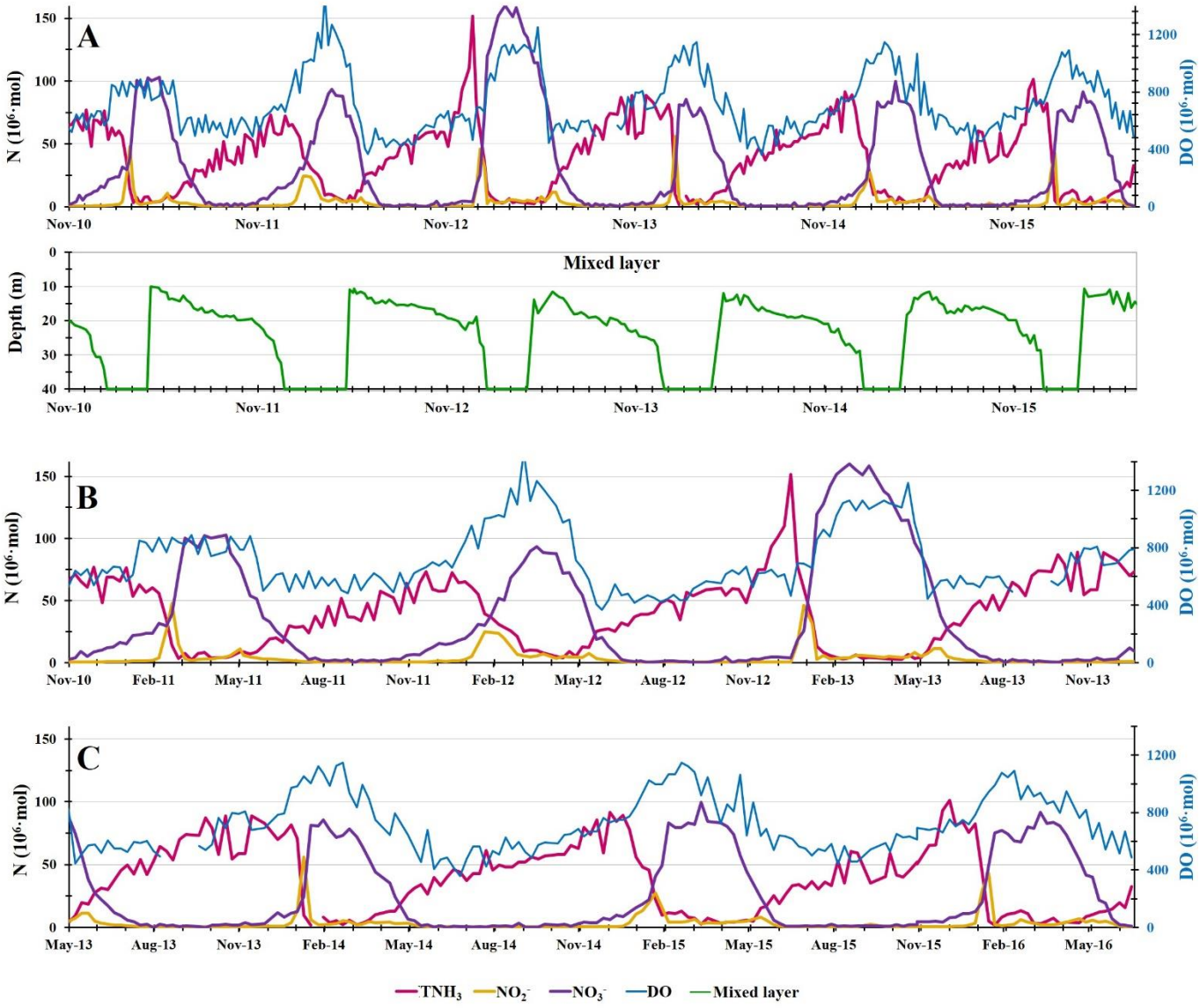


Fig 4.3. Annual variations in the inventories of various DIN species (TNH_3, NO_2^-, NO_3^-), DO, and mixed layer depth in LK. A- 2010-2016; and zoom in: B-2010-2013; C-2013-2016.

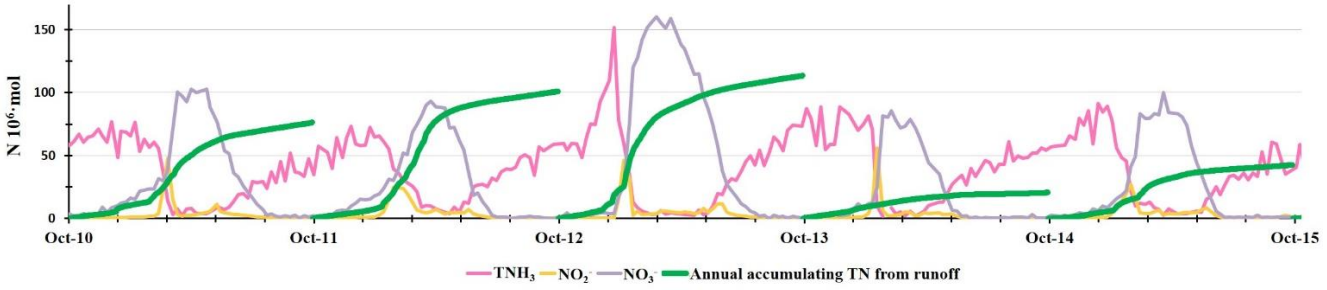


Fig 4.4. Annual inventory variations of TNH_3, NO_2^-, NO_3^-, and the annually accumulated amount of TN from runoff over every hydrological year (October to October; from the beginning of the rainy season).

DIN is not the sole nitrogen reservoir in LK and organic N-species are also significant nitrogen reservoirs (see definitions of the various organic N-species in the first paragraph of this chapter). However, the change in the inventory of the organic N-species (TNorg) during the year is rather small (See Fig. 4.5 for year 2011 as a representative example). In contrast, TN alternates seasonally by a factor of 2, between its maximum levels in March to its minimum in September mostly due to DIN variations. TNorg however is still an important and major reservoir in LK's nitrogen budget: it is formed as PNorg by assimilation (photosynthesis) in the photic zone and is disintegrated to TNH_3 in the deep water layers and to DNorg in the entire water column. As such, TNorg provides a basic substrate for transformations of nitrogen species in the different water layers in the lake.

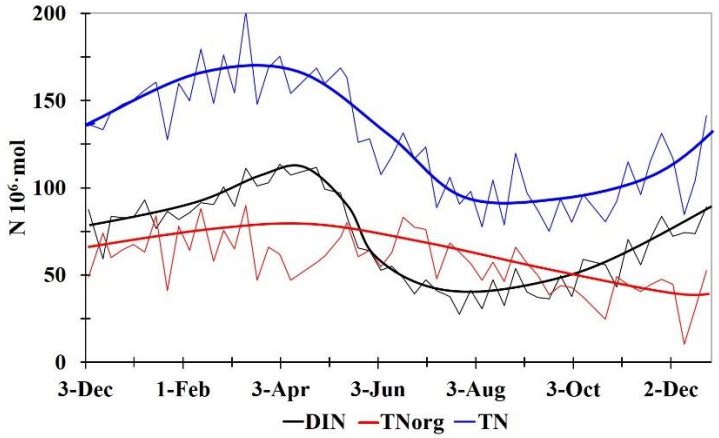


Fig. 4.5. Seasonal variations of TN, DIN and TNorg inventories in LK water column during the year 2011.

4.3 Temporal variations of hypolimnetic inventories of nitrogen and DO between onset of stratification and beginning of anoxia

4.3.1 The transformation from oxic to mid-oxic hypolimnion – Oxygenic denitrification/anammox and the role of lacustrine (marine) snow

The onset of stratification and the associated development of the thermocline, during early spring and its early stable phase are accompanied by major biogeochemical processes in the water column (Fig 4.6). Owing to the relatively closeness of the deeper layer within ~2-3 months, the

hypolimnion becomes anoxic, NO_3^- is removed from this layer and subsequently NH_4^+ starts to accumulate. For the sake of inventories calculations, the upper most part of the hypolimnion was selected as the 15m depth strata, which is typical depth of thermocline. On both sides of the thermocline lies the metalimnion, a strata of ca. 6 m depth which is characterized by a steep temperature gradient (Fig. 4.6). In reality during the summer the thermocline deepens slightly at a relatively slow rate. The biogeochemical dynamics during this period is best demonstrated in a plot of the inventories of the N-species and DO in the hypolimnion from start to end of stratification (Fig. 4.7). The species inventory calculations assume a fixed hypolimnion volume, which better represent the short-term changes in the inventories than using a varying hypolimnion volume for each individual temperature profile. Accordingly, in all of the following calculations the top of the hypolimnion was taken to be at 15 m depth, which is the depth of the steepest temperature gradient during early spring (Fig. 4.6).

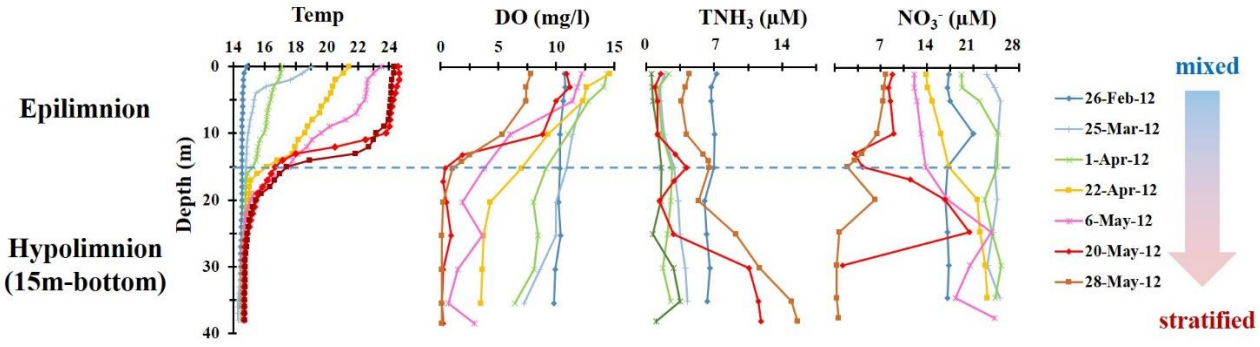


Fig 4.6. Water column variations in temperature, DO, TNH_3, and NO_3^- in LK's St. A during spring 2012 (from February 26 to May 28).

Several stages are recognized in the hypolimnion subsequent to the onset of stratification. Between Mar-25 to Apr 29 2012, hypolimnetic DO inventory drops by more than 50% of its pre-stratification inventory, suggesting an extensive aerobic respiration while both NO_3^- and TNH_3 inventories remain unchanged (Fig. 4.7). These latter observations are surprising since DO decreases due to aerobic bacterial respiration, a process that is commonly accompanied by mineralization of the organic-N. The potential rise in NO_3^- hypolimnetic inventory can be

estimated from the drop in DO using the Redfield relation stoichiometry, as represented by the following equation (Redfield et al. 1963):

4.1 $$[(CH_2O)_{106}(NH_3)_{16}(H_3PO_4)] + 138O_2 \rightarrow 106CO_2 + 122H_2O + 16HNO_3 + H_3PO_4$$

This equation is based on the average stoichiometry of the product of decomposition of organic matter in the presence of oxygen, as derived by Redfield et al (1963). The stoichiometry relations show that 106 mole of CH_2O, 16 mole of NH_3 and one mole of H_3PO_4 react with 138 mole of O_2, as presented in Eq. 4.1.

Between Mar-25 and Apr-29 (the time interval between the two vertical dashed lines I and II in Fig. 4.7), the change in hypolimnetic DO was $-276 \cdot 10^6$ mol ($\Delta DO = (202-478) \cdot 10^6$ mol); Fig. 4.7; Table S3), and the ratio of $\Delta NO_3^-/\Delta DO$ is: 16/-138=-0.116, which translates to an expected NO_3^- rise of **$32.0 \cdot 10^6$ mol** ($\Delta NO_3^- = (-276) \cdot (-0.116) \cdot 10^6$ mol). Thus, the inventory of NO_3^- in the hypolimnion during this period can be expected to increase from $39.1 \cdot 10^6$ mol to $71.1 \cdot 10^6$ mol (from state 1 to state 2 in Fig. 4.8). Such huge potential NO_3^- increase should have almost doubled the amount of NO_3^- trapped in the hypolimnion at the onset of stratification ($39.1 \cdot 10^6$ mol; dashed line I, Fig. 4.7). Yet, the observed ΔNO_3^- at that period was virtually zero (state 3 in Fig. 4.8), implying that the nitrogenous product of oxygenic mineralization is somehow removed from the water column. The obvious candidate for this removal mechanism is denitrification, which converts oxygenated-N, namely nitrate to N_2 (g). There are two known potential bacterially mediated pathways for denitrification: "ordinary denitrification" (the vector connecting between state 2 and state 3 in Fig. 4.8) and/or anammox (anaerobic ammonium oxidation). However, both processes operate only in ***sub-oxic to anaerobic environments***, while the hypolimnetic water column during that period is still highly ***aerobic*** (Fig. 4.7). Due to this apparent paradox, I termed these two alternative processes in LK's hypolimnion as "oxygenic denitrification" and/or "oxygenic anammox" and suggest below a scenario enabling these anaerobic processes to operate in aerobic water column.

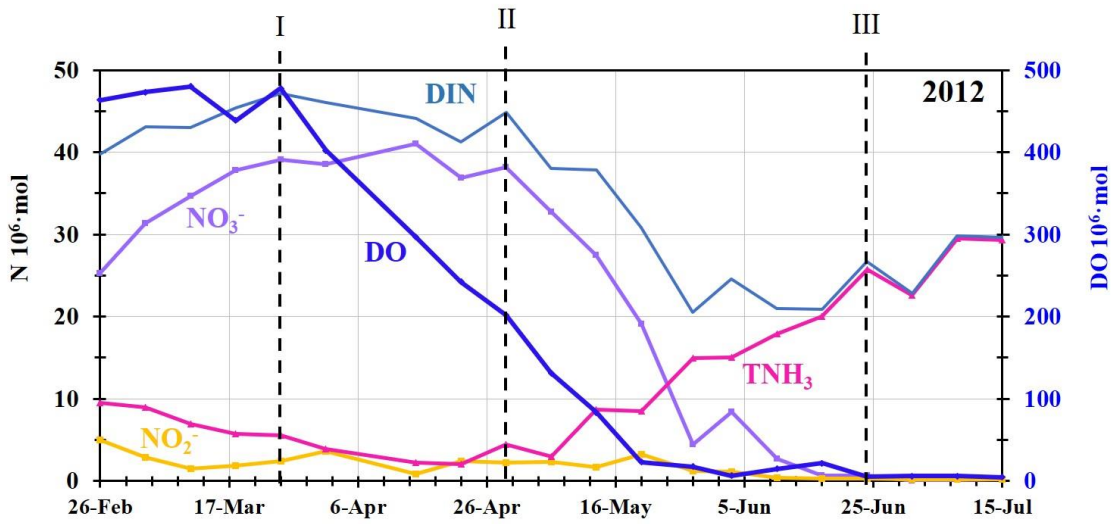


Fig. 4.7. Secular variations of hypolimnetic inventories of NO_3^-, NO_2^-, TNH_3, DIN and DO for the period February to July 2012. A <50% decrease in DO inventory is observed between Mar-25 and Apr-29 (the time interval between the two vertical dashed lines I and II) with virtually no change in DIN inventory. Between 29-Apr and 25-June (time interval between vertical dashed lines II and III), DO and NO_3^- inventories decrease to zero. Note that the scale of the DO axis (the right y-axis) is 10-fold the scale of the N-species (left y-axis).

Oxygenic Denitrification

Oxygenic denitrification requires the operation of 2 parallel processes: 1. Aerobic respiration to produce NO_3^-; and 2. Denitrification that consumes the produced NO_3^- and forms dissolved N_2. This final relative amount of N_2 product that is formed during the full denitrification of the 16 moles of NO_3^- produced by the aerobic respiration depicted in Eq. 4.1 is described by the following denitrification reaction:

4.2 $$0.1695[(CH_2O)_{106}(NH_3)_{16}(H_3PO_4)] + \mathbf{16}\boldsymbol{HNO_3} \rightarrow 17.97CO_2 + 30.03H_2O + \mathbf{9.355}\boldsymbol{N_2} + 0.1695H_3PO_4$$

Eq. 4.2 yields a denitrification mole ratio of $\Delta NO_3^-/\Delta N_2$ of (-16/9.355) = -1.71.

The stoichiometry for the respiration of organic matter respired by the combination of the two processes (equations 4.1 + 4.2), which summarizes the changes in PNorg, DO and N-species reservoirs, is as following:

4.3 $$[(CH_2O)_{106}(NH_3)_{16}(H_3PO_4)] + 118O_2 \rightarrow 106CO_2 + 130H_2O + 8N_2 + H_3PO_4$$

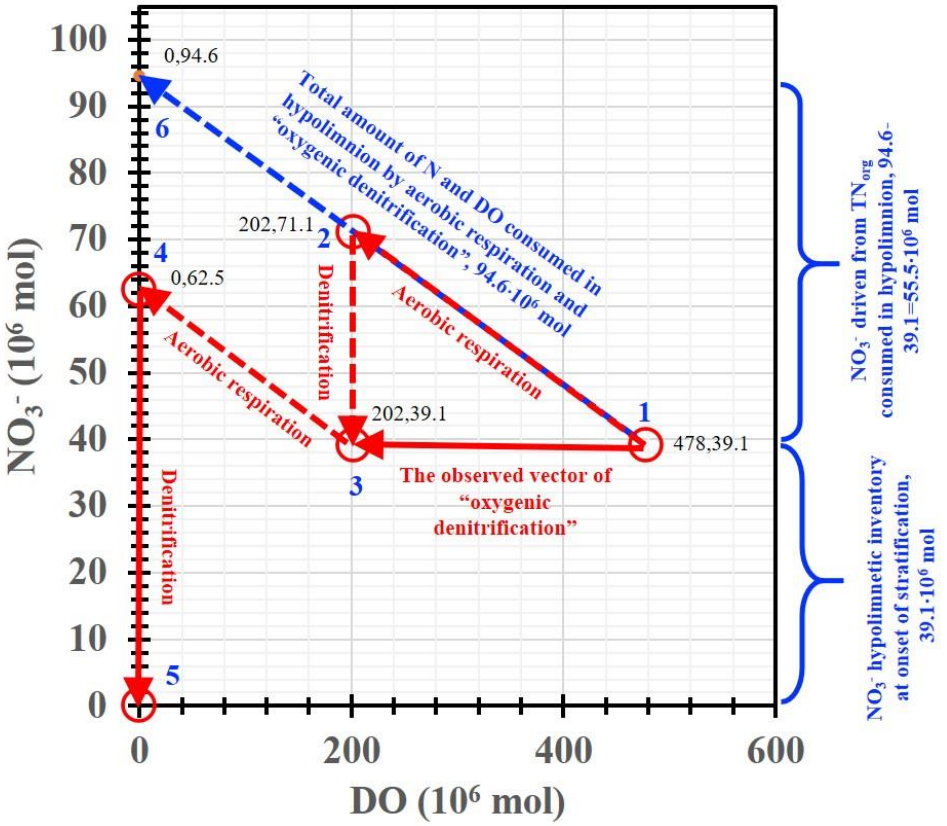


Fig. 4.8. Summary of the measured and calculated changes in the **DO** and **NO_3^-** inventories in the hypolimnion (presented as vectors) from the onset of stratification (March-26) to the time of DO=0 (June-25, 2012; Fig. 4.7). The different states in the hypolimnion during this period are marked by 1 to 6 (blue numbers close to each mark), starting from the onset of stratification (state 1, March 26) through state 3 (April 29), and ending when the hypolimnion is completely exhausted of DO and NO_3^- (state 5, June-25). The red arrows are the vectors of the different processes operating in the hypolimnion, moving it between its states. Solid arrows represent the observed inventories changes; dashed arrows are the vectors representing the suggested mechanisms that produced the observed changes (e.g. "oxygenic denitrification"). The blue dashed arrow is the vector representing the total amount of nitrogen consumed in the hypolimnion during this period. The biogeochemical processes represented by the different vectors are detailed in Sections 4.3.1 and 4.3.2.

As shown above, the calculated increase in hypolimnetic NO_3^- as a result of aerobic respiration of organic matter (Eq. 4.1) should have been $32.0 \cdot 10^6$ mol. This amount of NO_3^- was consumed by 'oxygenic denitrification', producing according to Eq. 4.2 a total of **$18.7 \cdot 10^6$ mol** of dissolved N_2 ($(-32.0/-1.71) \cdot 10^6$ mol; the change in nitrate divided by the denitrification ratio), which translates to the removal of **$37.4 \cdot 10^6$ mol** of N ($\Delta N_2 \cdot 2 = 18.7 \cdot 2 \cdot 10^6$) from the hypolimnion. This amount of nitrogen was ***removed during just ~1 month*** and is equivalent to more than 1/3 of the nitrogen supplied by runoff during year 2012, which was a year of relatively high nitrogen runoff input

(Fig. 4.4). It should be noted that the discussed nitrogen inventory is not included in the inventories presented in Fig. 4.7. It originated as particulate organic matter that was formed by photosynthesis in the photic zone, and was either trapped in the hypolimnion when the latter first formed, or sank to the hypolimnion after its formation.

The *oxygenic denitrification"* scenario that I suggest for resolving the paradox described implies that the denitrification processes operates within anaerobic (or very low oxygen) micro-particles, most likely within the so called "***marine [lacustrine] snow***", which slowly sinks through the water column of the lake (Figs. 4.9A, B). The lacustrine snow (sizes range 300-2,000 μm) is formed by aggregation of TEP (Transparent Exopolymer Particles, sizes range 2-200 μm), with average annual concentration in LK of $20 \cdot 10^6$ TEP/L. The bacteria populations inhabiting this lacustrine snow (and TEP) particles and fecal pellets produce nitrate by aerobic respiration, on the particles outside (Berman and Holenberg, 2005). The nitrate then diffuses into the inner suboxic or anoxic part of the particle (Alldredge and Cohen, 1987, Fig. 4.8A) where it is denitrified to dissolved N_2 (Fig. 4.9B). This suggestion is based on the microelectrodes study of Alldredge and Cohen (1987) on marine snow, who claim that "oxygen is partially, but continuously, depleted within and around marine snow in the dark and can be completely depleted within large fecal pellets. The existence of chemical microhabitats around macroscopic particles may permit processes requiring low oxygen, including denitrification". Thus, the overall process, termed here "oxygenic denitrification", or contemporaneous oxidation of particulate organic matter by DO and by NO_3^- (denitrification) in aerobic water column, would ideally operate on and within lacustrine (marine) snow particles that sink through an oxidized water column, as presented in Fig. 4.9B.

Oxygenic Anammox

Oxygenic anammox is an alternative process that may produce dissolve N_2 in aerobic environment as described in Fig. 4.9C. Anammox is a known alternative pathway for the production of $N_2(g)$ in water which does not necessarily involve the presence of nitrate. It is mediated by specific bacteria, whereby: $NH_4^+ + NO_2^- \rightarrow N_2(g) + 2H_2O$ in which N-species change from -3 & +3 to zero valence. A major issue of concern is in what type of oxidizing conditions can both NO_2^- and NH_4 form or co-exist. Anammox however, uses NO_2^- (whereas denitrification uses NO_3^-) as the oxidizing agent in anaerobic environment, to oxidize organic

matter and form N_2. Hence, as in the case of oxygenic denitrification, anammox also requires a first step of aerobic respiration of organic matter to produce nitrite (an intermediate N-species), according to the reaction:

4.4 $$[(CH_2O)_{106}(NH_3)_{16}(H_3PO_4)] + \mathbf{130}\boldsymbol{O_2} \rightarrow 106CO_2 + 122H_2O + \mathbf{16}\boldsymbol{HNO_2} + H_3PO_4$$

This NO_2^- is used by the anammox process with the stoichiometry described by the reaction:

4.5 $$0.1017[(CH_2O)_{106}(NH_3)_{16}(H_3PO_4)] + \mathbf{16}\boldsymbol{HNO_2} \rightarrow 10.78CO_2 + 21.22H_2O + \mathbf{8.807}\boldsymbol{N_2} + 0.1017H_3PO_4$$

As in the case of oxygenic denitrification, the sub-oxic microenvironment is provided by the lacustrine (marine) snow (Figs. 4.9A, C). According to Eq. 4.1 to Eq. 4.5, the N_2 production per one mole of DO consumed in both the denitrification and anammox scenarios are identical; i.e., the $\Delta N_2/\Delta DO$ ratio of denitrification (as inferred from Eq. 4.1 and Eq. 4.2) and anammox (as inferred from Eq. 4.2 and Eq. 4.5) are both $\Delta N_2/\Delta DO = 6.8 \cdot 10^{-2}$ (9.355/138 for denitrification and 8.807/130 for anammox). Thus, during the oxidized period of the hypolimnion, ~7 moles of N_2 are produced per 100 moles of DO used by aerobic respiration of particulate organic matter. It is impossible to distinguish between these two mechanisms using just redox mass balance and other proxies (e.g. gene expression) are required for that purpose.

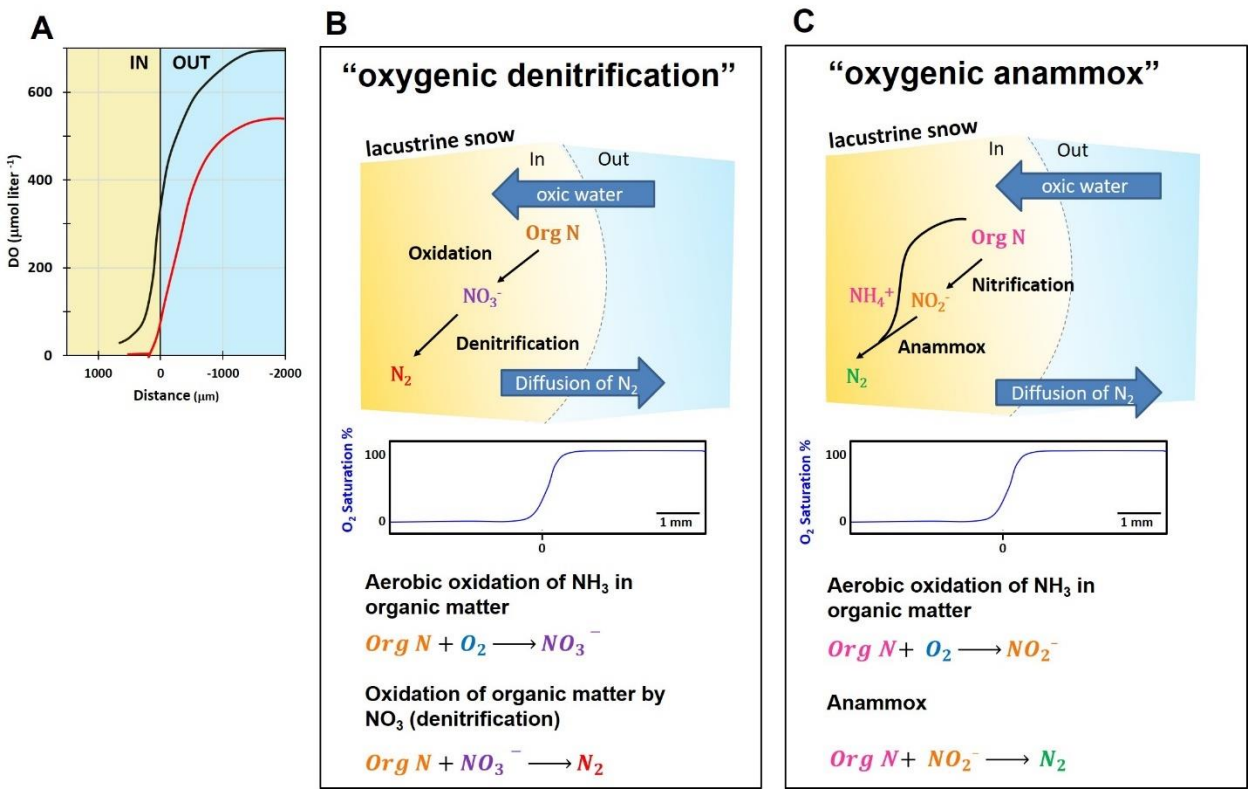


Fig. 4.9. Conceptual model for N_2 formation within lacustrine snow micro-environments sinking through an oxic hypolimnion. A. DO profiles across individual particles of ***marine snow*** showing almost complete DO depletion within 100 to 500 µm, "In" denotes inside the particle and "Out" denotes outside, in the bulk water (modified after Alldredge and Cohen, 1987). B. "Oxygenic denitrification" model. C. "Oxygenic anammox" model. The models depict a lacustrine snow particle (yellow) suspended in the water column (aqua) and show the fluxes across the particle/water interface. Schematic cross sections of DO from the water (100% saturation) into the particle (0% saturation) are shown under the particles.

4.3.2 The transformation from sub-oxic to anoxic hypolimnion

In late-April, when water column DO decreases below ~150 µM, denitrification is no longer limited to the micro-environment of the marine snow, and nitrate begins to decrease in the hypolimnion accompanied by TNH_3 increase (Fig. 4.6 and Fig. 4.7). Anoxic conditions are established by mid-May indicating that the denitrification phase is very fast, lasting only about 4 weeks (see the time interval between dashed lines II and III in Fig. 4.7).

The amount of DO in the hypolimnion when NO_3^- begins to drop is $202 \cdot 10^6$ mol (see section 4.3.1 and Fig. 4.7). By the time this DO has been completely consumed by aerobic respiration it has produced (according to the Redfield $\Delta NO_3^-/\Delta DO$ ratio, Eq. 4.1) $(138/16 \cdot 202) \cdot 10^6 = 23.4 \cdot 10^6$ mol of NO_3^-. During this period, the NO_3^- inventory is also completely exhausted, due to regular

nitrification process. If the denitrification process would not have accompanied this aerobic respiration the inventory of hypolimnetic nitrate would have risen to $62.5 \cdot 10^6$ mol (the vector connecting between state 3 and 4 in Fig. 4.8).

When DO levels become very low (sub-oxic), hypolimnetic NO_3^- inventory decreases by denitrification (Eq. 4.2) till its complete removal (as well as the DO inventory) in June (dashed line III in Fig. 4.7), as described by the vector connecting between state 4 and 5 in Fig. 4.8.

4.3.3 Total amount of nitrogen consumed in the hypolimnion between the onset of stratification and beginning of the anoxic period (between line I and II, Fig. 4.7)

The total amount of NO_3^- formed by oxic respiration (consumption of DO) in the hypolimnion, between the onset of stratification and beginning of the anoxic period (between line I and III, Fig. 4.7 as represented by the sum of vectors connecting states 1 and 2 and 3 and 4 in Fig. 4.8) is $55.4 \cdot 10^6$ mol. Adding this to the amount of NO_3^- that was present in the hypolimnion at the onset of stratification ($39.1 \cdot 10^6$ mol; dashed line I in Fig. 4.7 and state 1 in Fig. 4.8), yields a total of $94.5 \cdot 10^6$ mol of N (as NO_3^-) that were consumed by denitrification (the vector connecting state 6 with state 5 in Fig. 4.8) in the hypolimnion, producing dissolved N_2. From the above calculations, and given the denitrification ratio of 1.71 (eq. 4.2) I conclude that a minimum of ca. $(94.5/1.71) \cdot 10^6 = 55 \cdot 10^6$, moles of N_2 were produced in the hypolimnion during this period and have escaped to the atmosphere prior or following the overturn of the water column in winter 2012-2013. It should be noted that this total amount of nitrogen ($94.5 \cdot 10^6$ mol) is very close to the annual (2012) nitrogen inflow to the lake, $\sim 100 \cdot 10^6$ mol N (Fig. 4.4).

The total amount of organic nitrogen that was oxidized in the hypolimnion by aerobic respiration is $55.4 \cdot 10^6$ mol N (calculated from the difference between the y-axis values at state 6 and state 1; Fig. 4.8). This amount of nitrogen makes up ca. 60% of total amount of nitrogen that was consumed in the hypolimnion between the onset of stratification and beginning of the anoxic period (between state 6 and state 5, Fig. 4.8), the other 40% being the NO_3^- inventory that was trapped in the hypolimnion upon its formation. This large amount of nitrogen originated from PNorg produced by primary productivity (assimilation) in the photic zone and sank to the

hypolimnion. Because only a small fraction of the PNorg produced in the epilimnion, sinks to the hypolimnion (most of it is being re-mineralized very fast by aerobic respiration in the epilimnion and assimilated back), the measured PNorg produced by primary production at that period should be considerably larger than $55.4 \cdot 10^6$ mol N. In the section below, I evaluate this issue in detail.

4.4 Primary productivity - A major source of hypolimnetic nitrogen inventory

Out of the total $55.4 \cdot 10^6$ mol of PNorg that sank to hypolimnion from the onset of stratification to the beginning of hypolimnetic anoxia, $32.0 \cdot 10^6$ mol were re-mineralized during 34 d (from state 1 to state 2, Fig. 4.8) and while the rest, $23.4 \cdot 10^6$ mol (from state 3 to state 4, Fig. 4.8), were re-mineralized during 58 d (Fig. 4.7). Based on ^{14}C incubation measurements done by the Yigal Allon Kinneret Limnological Laboratory. The PNorg produced by photosynthesis in the epilimnion (depth of 0-15 m) during these 2 periods (between dashed line I and dashed line III in Fig. 4.10) were ~$400 \cdot 10^6$ mol and ~$350 \cdot 10^6$ mol, respectively (the aqua and purple areas in Fig. 4.10). The primary productivity curve was constructed using water column measurements of ^{14}C incubations at different depths (see section Methods) and multiplying them by the hypsometric curve of the lake. The results (carbon productivities) were divided by 6.6, the typical organic C/N (Redfield relation, Eq. 4.1) and the product is the integral of daily nitrogen productivity (mol/d of N). The total productivity for the 2 periods (between dashed line I and dashed line III in Fig. 4.10) is therefore ~$750 \cdot 10^6$ (~ $(400+350) \cdot 10^6$ mol), which is about 14 fold the amount of PNorg that was re-mineralized in the hypolimnion during that period.

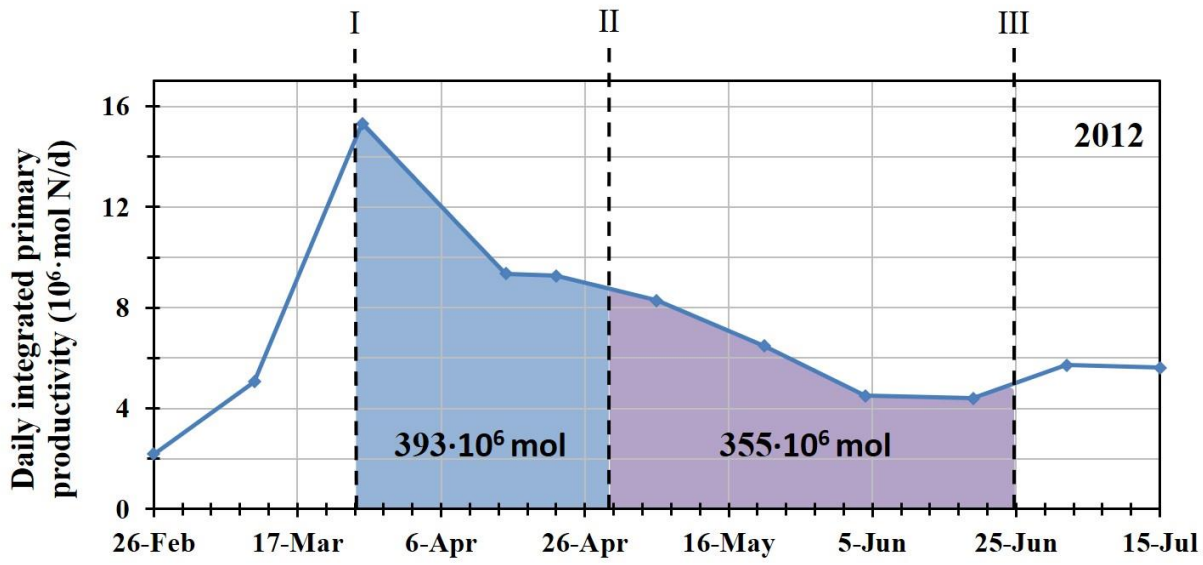


Fig. 4.10. The integrated water column primary productivity converted to nitrogen calculated from ^{14}C incubations of epilimnetic water column (depth range 0-15 m) during the year 2012 (see text for explanation). The vertical dashed lines mark the same time intervals as in Fig. 4.7.

4.5 Inter-annual variabilities in the mass-balance of nitrogen

Calculations similar to those described in detail for the year 2012 (sections 4.3 and 4.4) were conducted also for the years 2013 and 2014 and are summarized in Table 4.1. Three main conclusions are drawn from the results:

1. The annual variability in nitrogen removal from the lake as N_2 gas exchange with the atmosphere was rather small during these three years ($110 \cdot 10^6$, $147 \cdot 10^6$, $113 \cdot 10^6$ moles, respectively). Similarly, rather small variability was observed for the organic nitrogen consumed by denitrification (ΔNorg) in the hypolimnion ($55.4 \cdot 10^6$, $57.5 \cdot 10^6$, $58.9 \cdot 10^6$ moles, respectively). On the other hand, nitrogen inflow by runoff ($101 \cdot 10^6$, $113 \cdot 10^6$, $21 \cdot 10^6$ moles, respectively), and primary productivity ($493 \cdot 10^6$, $330 \cdot 10^6$, $191 \cdot 10^6$ moles, respectively) varied significantly during these years. This suggests that the overall rate limiting step in LK's nitrogen cycle is the ability of the hypolimnion to consume PNorg and convert it to dissolved N_2 and not the annual supply of nitrogen inflow to the lake. Apparently, the latter is important to LK's long-term nitrogen budget (being its major N-source), whereas the short-term amount of dissolved N_2 that is produced in the hypolimnion during the beginning of the stratified season (the primary N-sink) depends mainly on parameters such as the annual hypolimnetic DO inventory at the onset

of stratification and rate of PNorg mineralization.

2. Effects of primary productivity are inter-annual as demonstrated by the remarkably high productivity during the year 2012, and the high nitrogen removal in the following year 2013 (Table 4.1). Thus, the high PNorg produced by primary productivity sink down to the bottom of the lake, re-mineralized to ammonium during the stratified period, and nitrified to nitrate during the mixing season.

3. The differences between the amounts of nitrogen removed from the system by the "oxygenic denitrification" are lower than those removed by "regular" denitrification (Table 4.1, Fig. 4.8). This is because "oxygenic denitrification" depends on the DO hypolimnetic inventory (Fig. 4.8), which is more or less constant on a multi-annual time scale, due to its dependence on O_2 solubility in LK's water column. On the other hand, the "regular" denitrification processes depends on the NO_3^- inventory, which in turn depends on various processes such as annual nitrogen inflow to the lake, TNH_3 nitrification, and differences in primary productivity, which may vary quite significantly on an inter-annual time scale.

Table 4.1. Calculated values for nitrogen removal from the hypolimnion during the different stages of the stratification period for 2012-2014 (the values for the 2012 are presented in Figs. 4.8 and 4.9).

Year / Variable description	2012	2013	2014
	(Units of all numbers in the table are 10^6 mol)		
1. Inventories upon development of stratification			
Date	25-March	10-March	2-Feb
DO	478	496	508
NO_3^-	39.1	68.3	38
2. "Oxygenic denitrification" scenario			
Dates	25-March to 29-Apr	10-March to 28-Apr	2-Feb to March- 23
ΔDO	**-276** = -(478-202)	**-212** = -(496-284)	**-287** = -(508-221)
ΔNO_3^- , the expected increase	**32** = (-276) · (-0.116) [1]	**24.6** = (-212) · (-0.116)	**33.3** = (-221) · (-0.116)
ΔN_2, removed by 'oxygenic denitrification' scenario	**-18.7** = -32/1.71 [2]	**-14.4** = -24.6/1.71	**-19.5** = -33.3/1.71
3. Transition from mid-oxic to anoxic conditions			
Dates	29-Apr to 25-June	28-Apr to 30-June	March-23 to May-25
ΔDO	**-202**	**-284**	**-221**
ΔNO_3^-, Nitrification of organic N	**23.4** = (-202)·(-0.116)	**32.9** = (-284)·(-0.116)	**25.6** = (-221)·(-0.116)
ΔNO_3^- consumed by denitrification	**62.5** = 39.1+23.4	**101.2** = 68.3+32.9	**63.6** = 38+25.6
ΔN_2, removed by 'regular denitrification'	**-36.5** = -62.5/1.71	**-59.2** = -101.2/1.71	**-37.2** = -63.6/1.71
4. Total amount of N consumed in the hypolimnion between the onset of stratification and beginning of the anoxic period (dates specified in rows "Dates" of items #1 and #2)			
ΔPNorg total particulate N removed in the hypolimnion ΔNO_3^-, Nitrification of organic-N	**55.4** = 32 + 23.4	**57.5** = 24.6+32.9	**58.9** = 33.3+25.6
ΔNO_3^- total removed by the two denitrification processes	**94.5** = 55.4+39.1	**125.8** = 68.3+57.5	**96.9** = 38+58.9
N_2 escaped to the atmosphere by gas-exchange	**55** = 94.6/1.71	**73.6** = 125.8/1.71	**56.7** = 96.9/1.71
N Inflow by runoff (hydrological years, October-October)	**101.0**	**113.4**	**20.6**
5. Primary productivity during the time interval between the onset of stratification and beginning of the anoxic period (dates specified in rows "Dates" of items #1 and #2)			
PNorg produced by photosynthesis	**748** = 393+355	**501** = 234+267	**295** = 152+143

[1] According to Eq. 4.1, the ratio of $\Delta NO_3^-/\Delta DO$ is: 16/-138= -0.116

[2] According to Eq. 4.2, the ratio of $\Delta NO_3^-/\Delta N_2$ is: -16/9.355 = -1.71.

4.6 Hypolimnetic nitrogen inventories of nitrogen during anoxia

In the calculations presented above, the entire hypolimnetic NO_3^- inventory plus the organic nitrogen was assumed to have been mineralized to N_2 before all nitrate was consumed. However, as the hypolimnion becomes gradually reducing while DO and NO_3^- inventories decrease, TNH_3 starts accumulating (Fig. 4.3). This TNH_3 is the product of ammonification of PNorg that is not transformed to N_2. When the water becomes fully anaerobic (devoid of DO), TNH_3, N_2 and sulfide ($H_2S+HS^-+S^2$) form by oxidation of PNorg using first the little remaining NO_3^- as the oxidizing agent and then SO_4^{-2} (sulfate reduction, when NO_3^- is depleted) according to equations 4.6 and 4.7 (Froelich et al., 1979):

4.6 $$[(CH_2O)_{106}(NH_3)_{16}(H_3PO_4)] + 84.8HNO_3 \rightarrow 106CO_2 + 148.4H_2O + 42.4N_2 + 16NH_3 + H_3PO_4$$

4.7 $$[(CH_2O)_{106}(NH_3)_{16}(H_3PO_4)] + 53SO_4^{2-} \rightarrow 53CO_2 + 53HS^- + 53H_2O + 53HCO_3^- + 16NH_3 + H_3PO_4$$

According to eq. 4.6, 42.4 moles of N_2 are formed as 1 mole of organic matter is oxidized. This $\Delta N_2/\Delta$PNorg ratio is lower than the ratio of 55.2 during the denitrification process (Eq. 4.2). Thus, it appears that the actual amount of N_2 formed between stages I and III of Fig. 4.8 and later released to the atmosphere may be somewhat lower (up to ~15%) than the calculated values (average of ~$60\pm10\cdot10^6$ mol for the years 2012-2014; Table 4.1).

4.7 "Oxygenic denitrification and/or oxygenic anammox" - an overlooked pathway in the nitrogen cycle for LK

In this chapter I introduced the concept of "oxygenic denitrification/anammox", which adds a 'latent' pathway that transforms PNorg to dissolved N_2 (the vector from state 1 to state 2 in Fig. 4.8). This pathway was overlooked in earlier studies that estimated the magnitude of denitrification in LK using annual mass-balances (Smith et al., 1989; Nishri, 2014). The first comprehensive evaluation of the sources and sinks of nitrogen in LK for the years 1969-1984, estimated the annual mass of nitrogen that leaves the lake by denitrification to dissolved N_2 to be ~$80\pm70\cdot10^6$ mol or ~1120±1000 ton (Smith et al., 1989). This mass balance was based on the difference between the nitrogen inputs and

outputs, the latter being pumping and sedimentation. Similar estimate was provided by Nishri (2014), who suggested several nitrogen reducing steps, followed by N_2 escape to the atmosphere, as the major nitrogen removal pathway from the lake.

This study estimates the annual removal of nitrogen from LK (as N_2) to be within a rather narrow range of ~110 to $115 \cdot 10^6$ mol. This substantial increase in the estimate of nitrogen outflux is the result of adding the latent "oxygenic denitrification/anammox" to the denitrification process within the hypolimnion. The ability of this study to identify and quantify this process stems from calculations based on high temporal resolution in the variations of DO and nitrogen inventories. The study emphasizes that estimates based on annual resolution mass-balances, inherently miss short term processes.

4.8 Summary

LK's inventories of DO and nitrogen species conducted at high (weekly) temporal resolution, over several years, revealed that at the onset of stratification the hypolimnion loses substantial (about 50%) of its DO inventory with no significant change in the inventory of the nitrogen species. This phenomenon is in contrast to the expected increase in N-species that result from the negative correlation between oxygenic respiration (DO decrease) and remineralization of organic matter (e.g. increase in NO_3^-). The limnologic process suggested here to be responsible for this apparent enigma, is "oxygenic denitrification and/or anammox", which is the vectorial sum of a vector representing aerobic remineralization of PNorg to NO_3^- and the vector representing denitrification of this NO_3^- to N_2. This process however leaves an open question: why and how does denitrification, which uses the additional oxidized nitrogen, operate in an oxidizing hypolimnion?

I suggest to resolve this paradox by introducing the "oxygenic denitrification and/or anammox" processes which operate in low oxygen microenvironments provided by "***marine/lacustrine snow***" (organic matter particles) sinking through the water column down to the hypolimnion. According to this scenario, the aerobic remineralization of PNorg to NO_3^- occurs at the outer shell of the lacustrine snow particle, while denitrification and/or anammox, which produces dissolved N_2 occurs within the low DO (or anaerobic) inner part of the particle.

When water column DO decreases below ~150 μM, NO_3^- and DO start decreasing dramatically and TNH_3 increases due to sub-oxic remineralization and denitrification, reaching anoxic conditions and no NO_3^- in late spring.

The annual removal of nitrogen from LK (as N_2 degassing) estimated in this study (~110 to $115 \cdot 10^6$ mol) is ca. 27% higher than previous estimates, which did not consider "oxygenic denitrification/ anammox" in their nitrogen budgets of the lake. The higher estimate of nitrogen output through N_2 degassing in this study stems from calculations based on high temporal resolution in DO and nitrogen variation of inventories. This contrasts with previous estimates that were based on annual mass-balances, which inherently miss short term processes. This study emphasizes the importance of conducting lacustrine mass balances based on high temporal resolution which reveal processes otherwise overlooked.

Additional aspects of LK's nitrogen cycle are presented in the next chapter, which deals with the information provided by nitrogen isotopes.

5. The Nitrogen Cycle in Lake Kinneret – Evidence from Nitrogen Isotopes

5.1 Introduction

Nitrogen isotopic compositions ($\delta^{15}N$, see definition in Chapter 2) have been applied to identify nitrogen sources and processes in hundreds of studies over the past decades (e.g. Heaton, 1986). These studies have shown that the isotopic composition of nitrogen is also a powerful tool in evaluating biogeochemical pathways in the nitrogen cycle (e.g., Boettcher et al., 1990; Aravena et al., 1993; Wassenaar, 1995; Boehlke et al., 1997; Kendall, 1998; Kendall and Aravena, 2000; Schilman et al., 2004, 2007; Amberger and Schmidt, 1987; Fukada et al., 2003). In addition, the isotopic composition allows estimating the relative contribution of different sources of nitrogen to an ecosystem, provided these have distinct and different compositions. In many circumstances, isotopes offer a direct means of source identification because different sources of nitrogen often have distinct isotopic compositions. In addition, biological cycling of nitrogen often changes isotopic ratios in predictable and recognizable directions that can be reconstructed from the isotopic compositions (Kendal et al., 1998, 2007).

This study focuses on the nitrogen isotopic composition of the various N-species in LK. Oxygen isotopic composition, though measured in nitrates and nitrites (see Chapter 3), is not discussed in the present study.

5.1.1 Nitrogen isotope fractionation- Rules of the game

The nitrogen cycle is associated with significant isotopic fractionation. In accordance with the Rayleigh distillation process, in a closed system the $\delta^{15}N$ of the product depends on the fraction of the reactant reservoir already consumed, with bulk $\delta^{15}N_{product}$ approaching the initial $\delta^{15}N_{reactant}$ as all the reactant is consumed (Faure, 1986). Therefore, in N-limited systems, the fractionation between the initial nitrogen reservoir and the nitrogen product is minimal (Lehmann et al. 2004).

Each of the processes in the nitrogen cycle is characterized by typical isotopic fractionation:

Nitrification, is generally accompanied by significant negative nitrogen isotope fractionation, whereby the $\delta^{15}N$ values of the nitrate product is lower than the $\delta^{15}N$ of its "parent" NH_4^+ (Marioti et al., 1981), $\Delta^{15}N$ (the fractionation factor, $\Delta^{15}N_{nitrification} = \delta^{15}N_{nitrate} - \delta^{15}N_{TNH3}$) of this process ranges from -38 to -14‰ (Marioti et al. 1981; Casciotti et al. 2003; Kendal et al., 2007).

Assimilation is characterized by minor (negative) fractionation, i.e., the $\delta^{15}N$ value of the product is similar or somewhat lower than the source:

$\delta^{15}N_{POM} \leq \delta^{15}N_{NH4}^+$; $\delta^{15}N_{POM} \leq \delta^{15}N_{NO3}^-$.

Bacterial ***fixation*** of atmospheric N_2 commonly produces organic matter with $\delta^{15}N$ values usually in the range of -3 to +1‰, i.e., $\delta^{15}N_{POM} \approx \delta^{15}N_{N2}$ (Fogel and Cifuentes, 1993; Carpenter et al. 1997; Brandes and Devol 2002; Mahaffey et al. 2005).

Denitrification is characterized by negative isotopic fractionation (i.e. $\delta^{15}N_{N2} < \delta^{15}N_{NO3}^-$, causing the $\delta^{15}N$ of the residual nitrate to increase significantly as its concentrations decreases, with a large nitrogen isotope effect ranging from +15 to +30‰.

Ammonification usually involves only minor isotope fractionation (on the order of several permilles) between the organic matter and the NH_4^+ product (Kendal et al., 2007), i.e., $\delta^{15}N_{NH4}^+ \sim \delta^{15}N_{OM}$.

Dissimilatory nitrate reduction to ammonium (***DNRA)***, produces NH_4^+ (under anaerobic conditions), which has much lower $\delta^{15}N$ than its parent NO_3^- ($\delta^{15}N_{NH4}^+ << \delta^{15}N_{NO3}^-$), probably due to kinetic fractionation (McCready et al., 1983).

Ammonification, i.e., the mineralization of NH_4^+ bound to organic matter to inorganic NH_3/NH_4^+ is not accompanied by significant isotopic fractionation. However, NH_3 that volatilizes from animal waste and agricultural composting areas is isotopically depleted of ^{15}N, leaving the remaining $NH_3+NH_4^+$ (total ammonia, TNH_3) enriched with ^{15}N (Welman et al., 1968; Letole, 1980). Therefore, nitrate derived from livestock manure, manure and composted fertilizers or sewage have usually high $\delta^{15}N$, ranging between +7‰ and more than +20‰ (e.g., Gormly and Spalding, 1979; Kreitler, 1979; Kreitler and Browning, 1983; Aravena et al., 1993; Aravena and Robertson, 1998; Wassenaar, 1995; Kar et al., 2001; Rock and Mayer, 2004; Widory et al., 2004, 2013; Wassenaar et al., 2006; Mayer et al., 2013). The $\delta^{15}N$ of residual nitrogen following ammonia volatilization is generally higher than $\delta^{15}N$ of nitrate in atmospheric deposition (mainly dust, typically between -11‰ and +8‰), synthetic fertilizers (~0‰), and nitrate generated by nitrification processes in soils (~5 to 10‰; Kendal, 1998; Kendal et al.,

2007; Fig. 5.1). Hence, riverine $\delta^{15}N$ values in agricultural regions generally increase downstream, as a result of high $\delta^{15}N$ supply from tributaries containing drainage of irrigation waters.

Significant amounts of TNH_3 may enter riverine systems with wastewater effluents. Such wastewater is usually isotopically "heavy" (relatively high $\delta^{15}N$) and nitrification of its TNH_3 will first produce ^{15}N-depleted nitrate. However, as mentioned above, $\delta^{15}N_{NO3^-}$ values downstream of the effluents entrance point will progressively rise as more of the remaining ^{15}N-enriched TNH_3 will undergo nitrification (Feigin et al., 1974; Marioti et al., 1981; Cascioti et al., 2003). If some of the TNH_3 will undergo volatilization, which increases the residual $\delta^{15}N_{TNH3}$ ($\delta^{15}N$ of total ammonia), the final bulk nitrate product of the nitrification will end up with higher $\delta^{15}N_{NO3^-}$ than the $\delta^{15}N_{TNH3}$ of the original TNH_3 in the effluents.

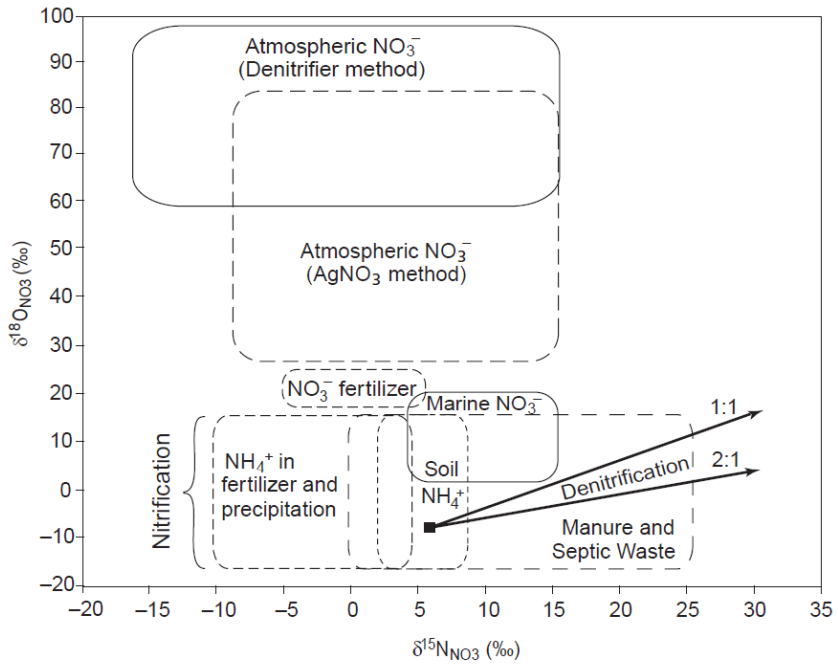


Fig. 5.1. Typical ranges for $\delta^{15}N$ and $\delta^{18}O$ values of nitrate from: atmospheric deposition, synthetic nitrate containing fertilizers, nitrification processes in soils, and sewage and manure. (from Kendal et al., 2007).

The following sections contain information on the isotopic composition of N-bearing species (i.e., NO_3^-, TNH_3 and PNorg) in LK inflows (section 5.2); the spatial and temporal distribution of the isotopic composition of N-bearing species with an attempt to identify the main paths in the N-cycle of the lake (section 5.3); and a description of an experiment designed to evaluate the isotopic fractionation of nitrogen isotopes during ammonification (section 5.4). The

results of this chapter demonstrate that the application of isotope techniques to the nitrogen system of the lake, provide information, which might otherwise be impossible or difficult to obtain.

5.2 The isotopic composition of nitrogen in inflows into Lake Kinneret

Water samples from eight locations in the watershed of LK (Fig. 5.2A) were collected between June 2013 and December 2014: The Banias and Dan Rivers are the main tributaries of the Jordan River which is the main water source to LK (Smith et al., 1989; Sites 1, 2 in Fig. 5.2A). The Jordan River was sampled at Bnot Yaacov Bridge, Pkak Bridge, Huri Bridge and Arik Bridge (Sites 3-6 in Fig. 5.2). Also sampled were Meshushim gorge (Site 7, Fig. 5.2A, representing the eastern drainage basin) and Fuliya spring (Site 8, Fig. 5.2A, one of the main springs discharging near LK) which drain directly to LK. Of these, Arik Bridge and Meshushim are the closest sites to the lake. All sites were visited and sampled several times over the study period. The samples collected were analyzed for their chemical and isotopic compositions of the N-species.

Fig. 5.2 plots $\delta^{15}N_{NO3^-}$ and $\delta^{15}N_{PNorg}$ against the NO_3^- and PNorg concentrations in the eight locations in the watershed of LK that were sampled routinely during the present study. NO_3^- is the main N-species in the various water sources, with a mean concentration of 113±21 μM while PON concentration is about one order of magnitude lower, 8 ± 4 μM. TNH_3 concentrations are negligible and in most samples were below the detection limit (see Supp. Table S7). Average $\delta^{15}N_{NO3^-}$ value is 6.7 ± 1.4 ‰. $\delta^{15}N_{NO3^-}$ values show a clear trend of increasing values from north to south along the Jordan River, varying from ~ 5‰ in the Dan and Banias Rivers (sites 1 and 2; Fig. 5.2), through ~6‰ in Bnot Yaacov Bridge and Pkak Bridge (sites 3 and 4; Fig. 5.2) to ~ 6-7‰ in Arik Bridge (site 6, Fig. 5.2). This trend is most probably due to limited contribution of ^{15}N-enriched nitrate into the Jordan River (e.g. drainage of oxidized ammonium from agricultural fertilizers; Fig. 5.1) along its flow path from north to south which nevertheless is not identified by an increase in NO_3^- concentration. This observation demonstrates the importance of N-isotopic composition in identifying nitrogen sources. Accordingly, the $\delta^{15}N_{NO3^-}$ value of the nitrate draining to LK from the Jordan River is taken in this study to be 6.0-6.5‰, which is the range measured at Pkak Bridge and

Arik Bridge (Fig. 5.2). This value is significantly lower than in Meshushim site (site 7 in Fig. 5.2) which is characterized by $\delta^{15}N_{NO3^-} \sim 9‰$. The ^{15}N-enriched isotope composition of the latter is probably derived from draining of the manure-products from the grazing fields of the cattle in the Golan Heights.

As opposed to the N-S trend observed for the $\delta^{15}N_{NO3^-}$, $\delta^{15}N_{PNorg}$ values do not show any geographic trend. Its average $\delta^{15}N$ value, 5.1±1.6‰, is lower by ~1‰ than the average $\delta^{15}N_{NO3^-}$ in the Jordan River. Seasonal variations in $\delta^{15}N_{PNorg}$ values are in the order of 1-2‰ (Supp. Table S7).

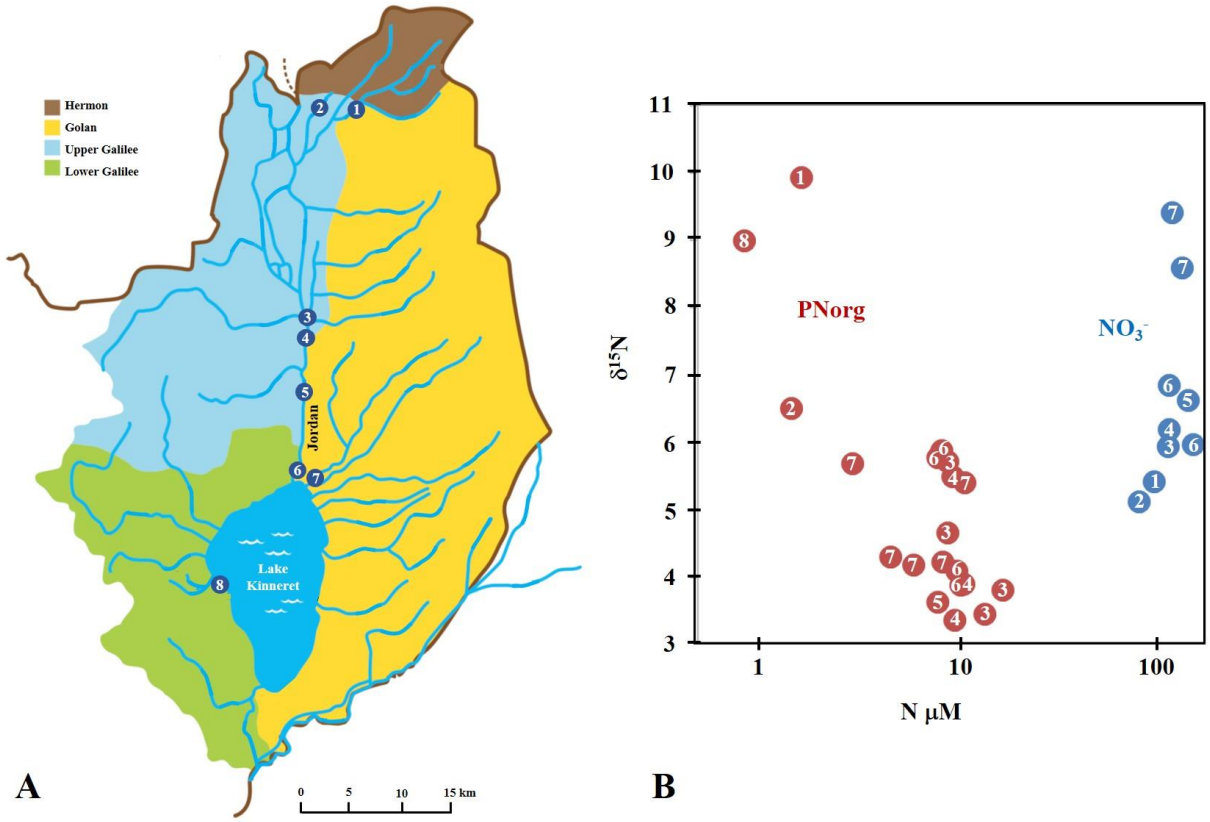


Fig. 5.2. A: Map of Lake Kinneret's watershed showing the location of the sampling sites. The numbers denote" 1-Banias, 2-Dan, 3-Bnot Yaacov Bridge, 4-Pkak Bridge, 5- Huri Bridge, 6- Arik Bridge, 7- Meshushim, 8- Fuliya. B. $\delta^{15}N_{NO3^-}$ and $\delta^{15}N_{PNorg}$ versus N concentrations in the water sources.

5.3 Temporal variations in $\delta^{15}N$ of TNH_3, PNorg, and NO_3^- in LK

Water samples were collected from LK at Site A at four depths (1m, 15m, 25m, 35m) representing the water column during four years (2011-2014). The temporal variations in $\delta^{15}N$ of

TNH_3, PNorg, and NO_3^- in the four selected water depths are shown in Fig. 5.3. All the isotopic data are given in Supplementary Table S7.

The increase in the concentration of NO_3^- in the water column during winter and early spring (Fig. 5.3A) is accompanied by an increase in $\delta^{15}N_{NO3^-}$ (Fig. 5.3B). $\delta^{15}N_{NO3^-}$ values continue to increase also when NO_3^- starts decreasing during the onset of the stratified season; $\delta^{15}N_{NO3^-}$ decreases only in the summer, when NO_3^- becomes very low, and concurrently with the increase in TNH_3 in the hypolimnion. The range of the annual change in $\delta^{15}N_{NO3^-}$ is ~6‰. The variations in $\delta^{15}N_{TNH3}$ and $\delta^{15}N_{PNorg}$ are considerably larger (Fig. 5.3C-F).

During winter, when the lake is fully mixed, its $\delta^{15}N_{NO3^-}$ value (~6 ‰) is very close to that of the Jordan River, which is the main source of nitrogen to the lake. Sometime after the onset of stratification, $\delta^{15}N_{NO3^-}$ values in the hypolimnion are for a short time higher than those of the epilimnion (best observed in years 2013 and 2014), before nitrate is fully removed (denitrified, see below) from the hypolimnion.

$\delta^{15}N_{TNH3}$ values are the highest of all measured N-species over the entire annual cycle. Hypolimnetic $\delta^{15}N_{TNH3}$ values are >25‰ when TNH_3 first begins to accumulate in the early summer and decrease (Fig. 5.3D) throughout the stratified season by ~10 ‰ to <15‰, while TNH_3 increases substantially (Fig. 5.3E). The most likely source for the increased TNH_3 is ammonification. However, one may expect that during such ammonification $\delta^{15}N_{TNH3}$ will be equal to the isotopic composition of the organic matter from which it is derived (i.e., $\delta^{15}N_{TNH3} \approx \delta^{15}N_{PNorg}$; e.g., Kendal et al., 2007; Bratkic et al., 2012). Yet, the observation shows that $\delta^{15}N_{TNH3} >> \delta^{15}N_{PNorg}$ (Fig. 5.3F). This issue will be addressed below.

The beginning of mixing (overturn of the water column) in late fall is characterized by substantial increase in $\delta^{15}N_{TNH3}$ in the deeper water (e.g., at 25m depth in Dec 2011; Figs. 5.3D, F). This isotopic enrichment is probably due to partial nitrification of hypolimnetic TNH_3 that was entrained within the deepening oxidized epilimnion. The increase in $\delta^{15}N_{TNH3}$ stems from isotopic fractionation during nitrification that produces NO_3^- which is lower than its parent TNH_3, and hence, the $\delta^{15}N_{TNH3}$ of the residual epilimnetic TNH_3 becomes high.

The annual variability in $\delta^{15}N_{PNorg}$ is the highest in the lake's nitrogen system (from ~ 0 to ~20‰; Fig. 5.3C) reaching maximum values in spring. Between 2011 and 2013, the maximum $\delta^{15}N_{PNorg}$

values increased consecutively from ~ 18‰ to ~ 21‰, whereas in 2014, maximum $\delta^{15}N_{PNorg}$ was lower, at ~ 16 ‰. $\delta^{15}N_{PNorg}$ minima appear in late winter, followed by a sharp increase to the spring maxima (Fig. 5.3C). Because assimilation is characterized by low fractionation of nitrogen isotopes, the $\delta^{15}N_{PNorg}$ reflects the isotopic composition of the assimilated N-species. Thus, the high $\delta^{15}N_{PNorg}$ recorded in spring indicate assimilation of the residual TNH_3 from nitrification with its high $\delta^{15}N_{TNH3}$ (e.g., as observed in early 2011; Figs. 5.3C, D). Assimilation of low $\delta^{15}N_{NO3^-}$ begins later, when TNH_3 is completely exhausted, as reflected by the gradual decrease of the $\delta^{15}N_{PNorg}$. $\delta^{15}N_{PNorg}$ may reach very low values in early winter, before inflow of NO_3^- with Jordan River water, most probably due to N_2 fixation, as would be expected when NO_3^- concentrations are still extremely low.

An interesting observation on the behavior of $\delta^{15}N_{PNorg}$ is that during summer-fall its values in the epilimnion are substantially higher than those in the hypolimnion (Figs. 5.3C). This enigma is further elaborated hereafter (section 5.3.1) and triggered an experimental study, described in Section 5.4.

5.3.1 Processes controlling the seasonal variations in lake's $\delta^{15}N$ values of the different nitrogen species

Mixing period: Winter $\delta^{15}N_{NO3^-}$ values in the lake are most likely derived from the nitrification of ammonium that follows the water column overturn and the external nitrate supply by the Jordan River. Nitrification is accompanied by a considerable isotopic fractionation (see explanation in section 5.1.1, above), whereby the $\delta^{15}N_{NO3^-}$ product is 5‰ to 35‰ lower ($\Delta_{nitrification}$) than the ammonium reactant (Mariotti et al. 1981; Casciotti et al. 2003; Kendal et al., 2007). Hence, as reaction progresses, the $\delta^{15}N_{TNH3}$ of the residual ammonium increases progressively (Rayleigh distillation) and so does $\delta^{15}N_{NO3^-}$, with a negative offset of ~15 ‰ (Figs. 5.3A, B). By late spring, as the surface waters heat up, stratification sets in and blooming begins, and nitrate concentration in the epilimnion starts decreasing due to assimilation. In the hypolimnion, denitrification of the trapped nitrate sets in some two months later. The two independent processes are accompanied by isotopic fractionations and both result in ^{15}N-enriched residual nitrate.

$\delta^{15}N_{PNorg}$ values during this homogeneous period are the highest in the annual cycle reflecting TNH_3 assimilation.

In summary, the main processes controlling the nitrogen cycle following overturn and during the period of homogeneous water column (mixing period) are nitrification of hypolimnetic-derived ammonium and phytoplankton photosynthesis (assimilation), and the external source.

Stratification period: Denitrification, the reduction of NO_3^- to N_2, starts only two months into stratification and only when oxygen levels in the hypolimnion have dropped below 150 μmole/L (depths 25m, 35m in Fig. 5.3A). The denitrification process is accompanied by a considerable isotopic fractionation ($\Delta_{denitrification}$) of -5 to -40‰ (Mariotti et al. 1981, 1982; Böttcher et al. 1990; Aravena & Robertson, 1998; Granger 2006); see explanation in section 5.1.1, above). Hence, as reaction progresses, the $\delta^{15}N_{NO3^-}$ of the residual nitrate increases progressively following Rayleigh distillation eq. (Figs. 5.3B). The contemporaneous hypolimnetic ammonium concentrations increase as a result of ammonification of organic matter. In the epilimnion, nitrate concentration continues to decrease due to primary production (assimilation) which results in increase in $\delta^{15}N_{NO3^-}$ of the residual nitrate (see explanation in section 5.1.1, above; (Cifuentes et al. 1989; Montoya et al. 1991; Kendal et al., 2007).

Ammonification continues in the hypolimnion also in fall, and ammonium continues to accumulate there. $\delta^{15}N_{TNH3}$ values decrease, following the observed trend of decrease in $\delta^{15}N_{PNorg}$ of the organic matter that sinks from above and undergoes mineralization (Figs. 5.3 C, D, F). It should be noted however, that throughout the year, $\delta^{15}N_{TNH3}$ values are significantly higher than $\delta^{15}N_{PNorg}$ values (Figs. 5.3 F). Since the ammonium in the hypolimnion is derived from the ammonification of the organic matter in the hypolimnion, it was expected that $\delta^{15}N_{TNH3}$ values will be similar or lower than $\delta^{15}N_{PNorg}$ (see section 5.1.1, above). Another interesting observation is that during stratification, $\delta^{15}N_{PNorg}$ in the hypolimnion is significantly lower than in the epilimnion (Fig. 5.3C), pointing to significant isotopic fractionation of the organic matter that precipitates from above and undergoes ammonification. This observation is also in contrast to the common view of no isotopic fractionation during ammonification (see section 5.1.1, above). These phenomena are further elaborated in the following section and investigated experimentally as detailed in the section 5.4, below.

In summary, the main processes controlling the nitrogen cycle during stratification are photosynthesis (assimilation), denitrification and ammonification.

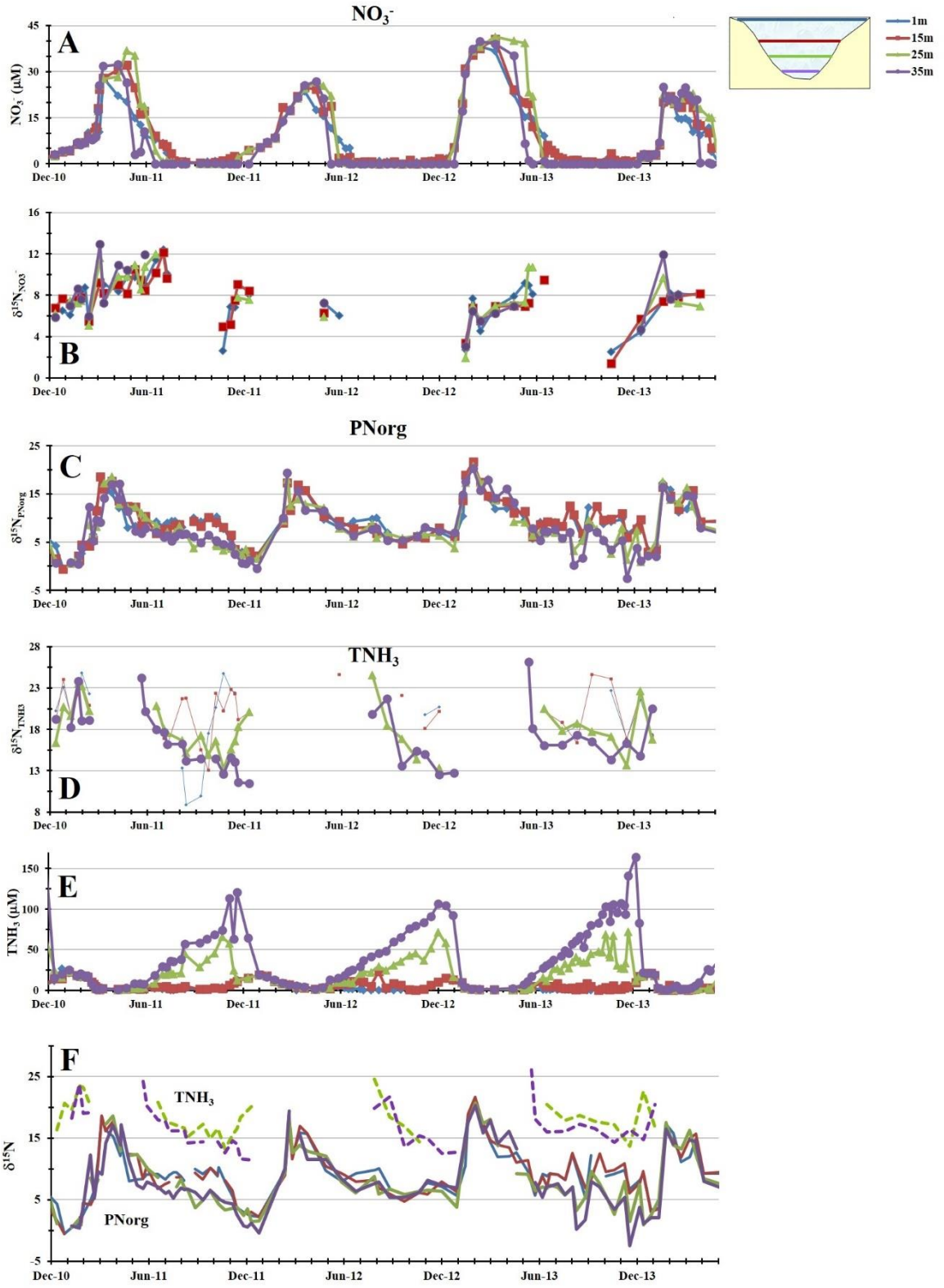


Fig.5.3. Variations in: (A) NO_3^- concentrations; (B) $\delta^{15}N_{NO3}^-$; (C) $\delta^{15}N_{PNorg}$; (D) $\delta^{15}N_{TNH3}$; (E) TNH_3 concentrations; and (F) $\delta^{15}N_{TNH3}$ (dashed lines) and $\delta^{15}N_{PNorg}$ (continuous lines), during December 2010 – June 2014 in 4 waters layers (1m, 15m, 25m, and 35m) of LK.

5.3.2. Field evidence for fractionation of nitrogen isotopes during ammonification

As shown in the previous section, during the entire study period, $\delta^{15}N_{TNH3}$ values were significantly higher than $\delta^{15}N_{PNorg}$ values (Figs. 5.3C, D, F). Since the ammonium in the hypolimnion is derived from the disintegrating organic matter in the hypolimnion, it was expected that its isotopic composition will be similar or lower than the PNorg ($\delta^{15}N_{TNH3} \leq \delta^{15}N_{PNorg}$). However, as shown in Fig. 5.3F, the isotopic relations are reversed, $\delta^{15}N_{TNH3} > \delta^{15}N_{PNorg}$. In addition, $\delta^{15}N_{PNorg}$ of the epilimnion are higher than those of the hypolimnion during the stratified period. During years 2011 and 2013, the $\delta^{15}N_{PNorg}$ value of the particulate organic matter formed in the epilimnion was ~10‰. This PNorg sank to the hypolimnion, disintegrated (ammonification), leaving a residual hypolimnetic PNorg, which is isotopically lower than the epilimnetic PNorg, while $\delta^{15}N_{TNH3}$ was higher. These observations suggest that the fractionation factor of nitrogen isotopes during ammonification is positive (Δ(ammonification) = $\delta^{15}N_{TNH3}$ - $\delta^{15}N_{PNorg} \approx$ 5 to 10‰, Fig. 5.3F), ***in contrast to the commonly accepted view that there is virtually no fractionation during ammonification*** (Kendal et al., 2007; Braktic et al., 2012). The difference between the $\delta^{15}N_{PNorg}$ values in the epilimnion and hypolimnion was not observed during the year 2012, which was the year with the highest TNH_3 inventories during the study period (Figs. 4.4, 4.5). The high TNH_3 resulted probably from very high primary productivity (PN_{org} production) that resulted in high PNorg downward flux. The high PNorg flux may have "pushed" the zone of excess ammonification that changes $\delta^{15}N_{PNorg}$ (and production of excess ^{15}N-enriched ammonia) downwards to the bottom, while in years of moderate productivity (e.g. 2011 and 2013) it occurs already in the hypolimnion. However, the overall large difference between $\delta^{15}N$ values of TNH_3 and PNorg ($\delta^{15}N_{TNH3}$ - $\delta^{15}N_{PNorg} >> 0$) remained throughout the 3 years of the study (Fig. 5.3F) indicating that Δ(ammonification) is large and positive.

To conclude, the field observations show clearly that ***the isotopic fractionation during ammonification is rather large and positive (Δ(ammonification)=$\delta^{15}N_{TNH3}$-$\delta^{15}N_{PNorg}$ is between 5 and 10‰), opposite to the common view of no fractionation***. The following section describes a laboratory experiment which was designed to verify this observation and to derive an estimate for the value of Δ(ammonification). Briefly, LK's suspended organic matter was incubated in lake's water and the isotopic composition of different nitrogen reservoirs was followed as a function of time.

5.4 Fractionation of nitrogen isotopes during ammonification - An experimental study

The incubation experiment described in this section was designed to study the isotopic fractionation of the deep hypolimnetic water of LK during the ammonification of POM the from the epilimnion.

5.4.1 Experimental setup

A large volume water sample was collected from the bottom (depth of 34.5 m) of the anoxic hypolimnion of LK using a 30 L Niskin bottle, during peak stratification (12/11/2015) and TNH_3 concentration (Fig. 4.2). The unfiltered water was divided into 20 experimental vessels of 132.5 ml that were purged with nitrogen (oxygen free) prior to filling. Suspended organic matter was collected from the surface water (around noon) using 20 μm plankton net towed by a boat at a depth of 1 m for ~ 20 min. The suspended organic matter was concentrated by centrifugation to a concentration of ~8 g/L (dry weight), and 1.5 ml was injected to each of the experimental vessels (Experiment E1-1). In a parallel experiment (Experiment E1-2), the procedure of experiment E1-1 was repeated with the addition of an oxidizing agent in the form of $NaSO_4$ (0.2 mL of 250 mM $NaSO_4$; 0.5 mM in the experiment vessel). Experimental vessels containing the hypolimnetic water without any treatment were used as a control (blank).

The experimental vessels were transferred to a shaking-incubator and kept for 7 weeks in darkness at 16^{o}C, to mimic the natural conditions in the hypolimnion. Initial measured or calculated relevant parameters in the experimental vessels were: 1. DO=0 mg/L; 2. TNH_3=65 μM; 3. POM=~90 mg/L; 4. $\delta^{15}N_{TNH3}$ =7.4‰; 5. $\delta^{15}N_{PNorg}$ =3‰.

During the 7 weeks of incubation, samples were collected 6 times. In each sampling, a bottle of water from each of the experiments (E1-1, E1-2 and blank) was removed from the incubator and filtered through a pre-weighted glass fiber filter (GF/F).

The amount and the isotopic composition of the (residual) particulate organic matter and the ammonia concentration were determined as a function of time. PNorg content was calculated by multiplying the POM (the dry weight of the sample accumulated on the filter, multiplied by the

volume of the filtered water), by the fraction of N measured (by EA) on the filters ($f(N_{POM})$). DON was calculated by multiplying the DOC by 9.5, the typical organic C/N ratio in LK (Goodwin, 2010).

The Dissolved Organic Carbon (DOC) was measured on the filtered samples by Shimadzu TOC Analyzer. The water samples were injected into a combustion tube containing platinum catalyst, in an oven at 680^{o}C with oxygen flowing through. The carbon dioxide generated by the combustion is detected by an infra-red gas detector and measured against a calibration curve that is based constructed on acid blank with sodium hydrogen phthalate standards at 1 ppm and 10 ppm.

5.4.2 Results

The nitrogen concentrations and the isotopic composition of the PNorg and the accumulating TNH_3 in the experiment vessels were determined as a function of time. The chemical and isotopic compositions during Experiment E1-1 are presented in Table 5.1 (the results of experiments E1-2 and blank are provided in Table S8). During both experiments (E1-1 and E1-2) PNorg concentration and its isotopic compositions decreased (Figs. 5.4A, B), TNH_3 increased and $\delta^{15}N_{TNH3}$ decreased (Figs. 5.4C, D), while the blanks showed no significant change. PNorg decreased significantly to about 25% of its original concentration (from ~370 to ~70 μM N; Fig. 5.4A). The TNH_3 values (after accounting for the initial TNH_3 concentration of 65 μM) increased by ~200 μM (Fig. 5.4C). The results of experiment E1-2, which contained excess $NaSO_4$ (see above), were similar to E1-1 (Fig. 5.4), indicating both the lack of significant influence of $NaSO_4$ on the process, and the quality of the results. The control (blank) experiment showed no significant variations throughout the incubation experiment (Figs 5.4A, C).

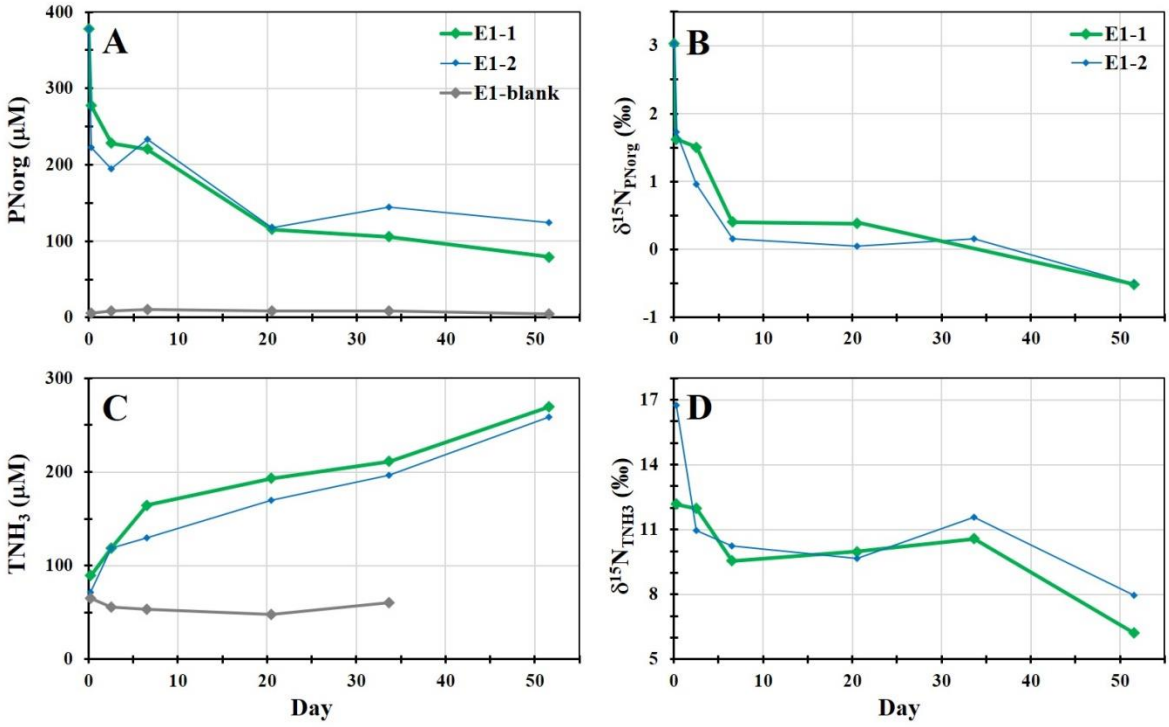


Fig 5.4. Chemical and isotopic compositions during experiments E1-1, E1-2 and blank A. PNorg; B. $\delta^{15}N_{PNorg}$; C. TNH_3; D. $\delta^{15}N_{TNH3}$. The details of the experiments are given in section 5.5.1.

Table 5.1. Chemical and isotopic compositions during Experiment E1-1.

Day from start / Variable	0	0.25	3	7	21	34	52
POM (mg/L)	97.4	89.8	79.2	58.9	34	34.7	29.4
$\delta^{15}N_{PNorg}$ (‰)	3.01	1.63	1.5	0.41	0.38	-	-0.52
[1] f(N_{POM})	0.054	0.044	0.041	0.053	0.048	-	0.038
[2] PNorg (µM)	378	278	228	221	115	106	79
TNH_3 (µM)	-	89	119	164	193	211	269
$\delta^{15}N_{TNH3}$ (‰)	-	12.2	12	9.6	10	10.6	6.2
DOC (ppm)	-	9.4	11.3	17.8	20.6	20.2	22.3
[3] DNorg (µM)	-	83	99	156	181	177	195
[4] TN (µM)	-	450	446	541	489	494	544
[5] SO_4 (mg/L)	-	47	48	-	-	57	30
[5] NO_3 (mg/L)	-	2.6	-	1.7	1.7	-	9.4
[6] Mg (mg/L)	-	34	34	33	-	31	32
[6] Ca (mg/L)	-	60	61	61	-	58	59
[6] Na (mg/L)	-	133	138	132	-	126	133
[6] K (mg/L)	-	8.2	8.3	7.8	-	7	8

The initial value of PNorg (day 0) is the calculated total suspended organic matter before its injection into the reaction vessels

[1] Weight fraction of N in the POM

[2] PNorg (µM) = POM (mg/L) ·f(N_{POM})

[3] DNorg =DOC/9.5

[4] TN = PNorg+DNorg +TNH_3

[5] SO_4 and NO_3 were measured with Ion-Chromatograph.

[6]Ca, Mg, Na, K were measured by ICP-OES.

5.4.3. Variations in nitrogen species concentrations

The results of the plankton incubation experiment as calculated after subtracting initial values (Fig. 5.5A) show that whereas the PNorg decreased by ~300 μM, the calculated TNH_3 increased just by < 200μM. This indicates that besides TNH_3, dissolved organic nitrogen (DNorg) is also produced during POM decomposition (Fig. 5.5B), which is estimated here using the measured DOC values (see above). It is reassuring that the total N (TN) calculated as the sum of PNorg + DNorg + TNH_3, almost did not vary and stayed ~400 μM throughout the experiment (Fig. 5.5B). This indicates that the variations measured during the experiment on the 3 N-species mentioned above, are reliable representative of the behavior of the nitrogen system during ammonification.

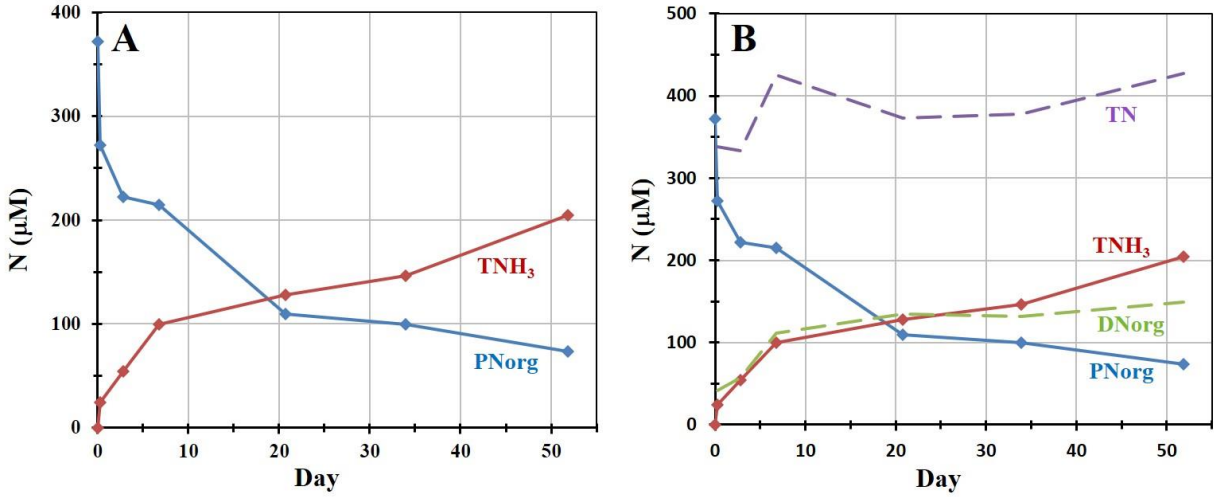


Fig 5.5. Chemical variations in the N-system during the plankton incubation experiment E1-1. **A -** Variations of PNorg and TNH_3; PNorg; **B -** Variations of DNorg, PNorg, TNH_3 and TN. See text for explanation of variables.

5.4.4. Evolution of nitrogen isotope compositions during the incubation experiment

$\delta^{15}N$ values of the TNH_3 formed during the experiment ($\delta^{15}N_{TNH3}$) were calculated by accounting for the initial concentration and isotopic composition of the TNH_3 (65mM; 7.4‰). Plotting the isotopic composition of TNH3 and PNorg against the fraction of the residual N (PNorg) in the POM (f(PNorg)=(measured PNorg)/(initial PNorg); Fig. 5.6), reveals that the very

high initial $\delta^{15}N_{TNH3}$ values decrease significantly during the course of the experiment whereas $\delta^{15}N_{PNorg}$ values decrease only moderately. This suggests that POM decomposed to ^{15}N-enriched ammonium (high $\delta^{15}N_{TNH3}$), leaving behind low residual $\delta^{15}N_{PNorg}$.

Thus, the experiment corroborates the field observations that decomposition of POM (ammonification) leads to production of significantly isotopic ^{15}N-enriched ammonium, as observed in LK in the hypolimnion during the lake's stratification (e.g. Fig. 5.3F).

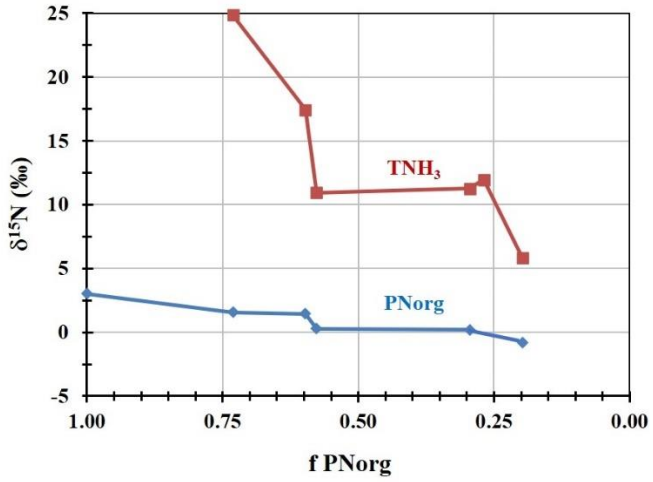


Fig 5.6. $\delta^{15}N_{PNorg}$ and calculated $\delta^{15}N_{TNH3}$ of the minerallized PNorg plotted against the fraction of residual N in POM ($f(N_{POM})$).

5.4.5. Fractionation factor of stable nitrogen isotopes (α) during ammonification

To calculate the fractionation factor for ammonification, I applied the Rayleigh distillation Equation using the measured $\delta^{15}N_{PNorg}$ values:

5.1 $$ln(\delta + 1000) = ln(\delta_0 + 1000) + (\alpha - 1) \cdot ln(f)$$

Where f is the fraction of the residual PNorg left in the experiment; δ is the measured $\delta^{15}N_{PNorg}$ for each f; δ_0 is the initial $\delta^{15}N_{PNorg}$ value (3.0‰); α is the fractionation factor of nitrogen during the disintegration of the POM.

The equation components are plotted against each other in Fig. 5.7A. The slope yields a fractionation factor of 0.0021 (i.e. instantaneous $\Delta_{product\text{-}PNorg}$ of 2.1‰), and the calculated initial $\delta^{15}N$ (δo) is 2.7‰, very close to the measured initial value (3.0‰).

The isotopic composition of the produced ammonium **does not** follow the Rayleigh distillation curve expected from the derived fractionation coefficient (Fig 5.7B – the cumulative product). Thus, it is concluded that the product of the disintegration of the POM includes also another product that would incorporate the isotopes that are lighter than the original PNorg. It is assumed here that this component is newly formed DNorg. Based on mass-balance calculations between the measured $\delta^{15}N_{TNH3}$ and the expected $\delta^{15}N$ of the product, I calculated the $\delta^{15}N$ value of this DNorg (~ +1 to -7‰; Fig. 5.7B; green triangles).

The $\delta^{15}N$ values of all the components are plotted against f PNorg in Fig. 5.7B. $\delta^{15}N_{TNH3}$ values, spread far above (up to +20‰) from the calculated line.

To conclude, the results of the incubation experiment prove that decomposition of PNorg matter leads to significantly isotopically ^{15}N-enriched ammonium product, as observed in LK during stratification period.

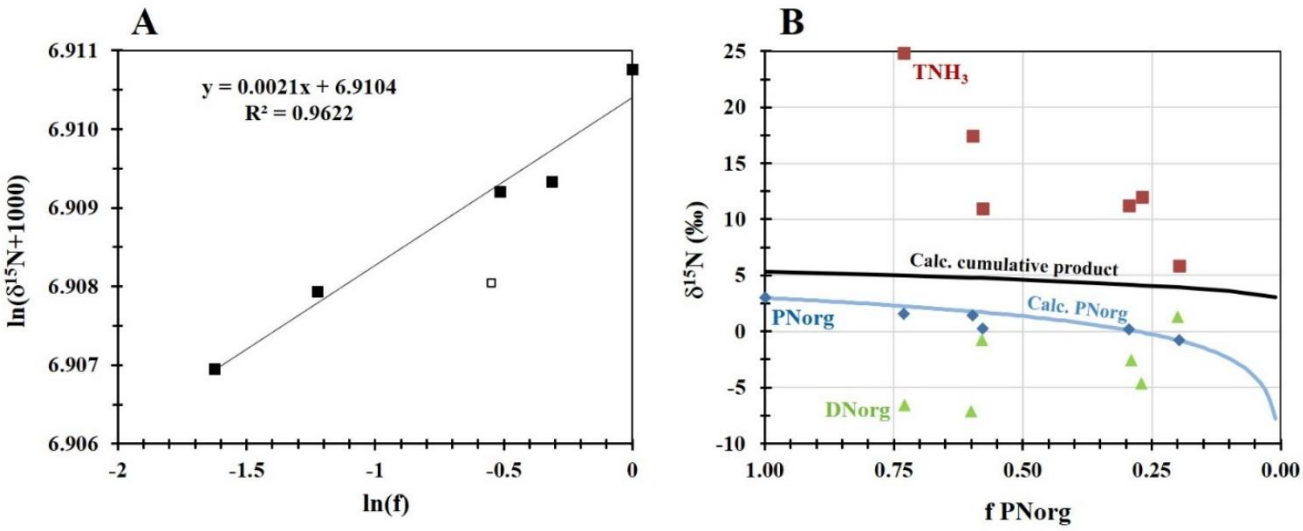


Fig. 5.7. A. ln ($\delta^{15}N$+1000) plotted against ln (f PNorg) of the PNorg during the incubation experiment. The plotted data are derived from the Rayleigh distillation Equation (eq. 5.1)); B. $\delta^{15}N$ values of the N-species in the incubation experiment, plotted against f (PNorg). Blue diamonds are the measured $\delta^{15}N_{PNorg}$ values; Red squares are the calculated $\delta^{15}N_{TNH3}$ values derived from isotopic measurements and corrected for initial ammonium in the sample,; The blue line is the calculated PNorg trend; Black line is the calculated cumulative product; Green triangles are the calculated DNorg values. The open square in A, is an outlier sample.

5.5 Conclusions

Careful examination of seasonal variations in the distribution of the N-species in the water column, together with their isotopic composition which vary considerably along the annual cycle, enables better understanding of the nitrogen cycle in LK.

The main processes controlling the nitrogen cycle during the mixing period are nitrification of hypolimnetic-derived ammonium, assimilation of nitrate and ammonium during phytoplankton photosynthesis, and the external supply of nitrate by the Jordan River. Nitrification is accompanied by a considerable isotopic fractionation, whereby the NO_3^- product is isotopically lower than the ammonium reactant. Hence, as reaction progresses, the $\delta^{15}N_{TNH3}$ of the residual ammonium increases progressively (Rayleigh distillation).

The main processes controlling the nitrogen cycle during stratification period are photosynthesis (assimilation) in the epilimnion and denitrification and ammonification in the hypolimnion. Denitrification process is accompanied by a considerable isotopic fractionation. Hence, as reaction progresses, the $\delta^{15}N_{NO3^-}$ of the residual nitrate increases progressively. In the epilimnion, nitrate concentration continues to decrease due to primary production (assimilation) which also results in increase in $\delta^{15}N_{NO3^-}$ of the residual nitrate.

The annual variability in $\delta^{15}N_{PNorg}$ is the highest in the lake's nitrogen system, reflecting the isotopic composition of the assimilated N-species. The high $\delta^{15}N_{PNorg}$ is recorded in the spring, indicating assimilation of the high residual $\delta^{15}N_{TNH3}$ from the nitrification. Assimilation of ^{15}N-depleted NO_3^- begins later, when TNH_3 is completely exhausted, as reflected by the gradual decrease of the $\delta^{15}N_{PNorg}$. $\delta^{15}N_{PNorg}$ may reach very low values in early winter, before onset of massive inflow of NO_3^- with Jordan River water, most probably due to N_2 fixation.

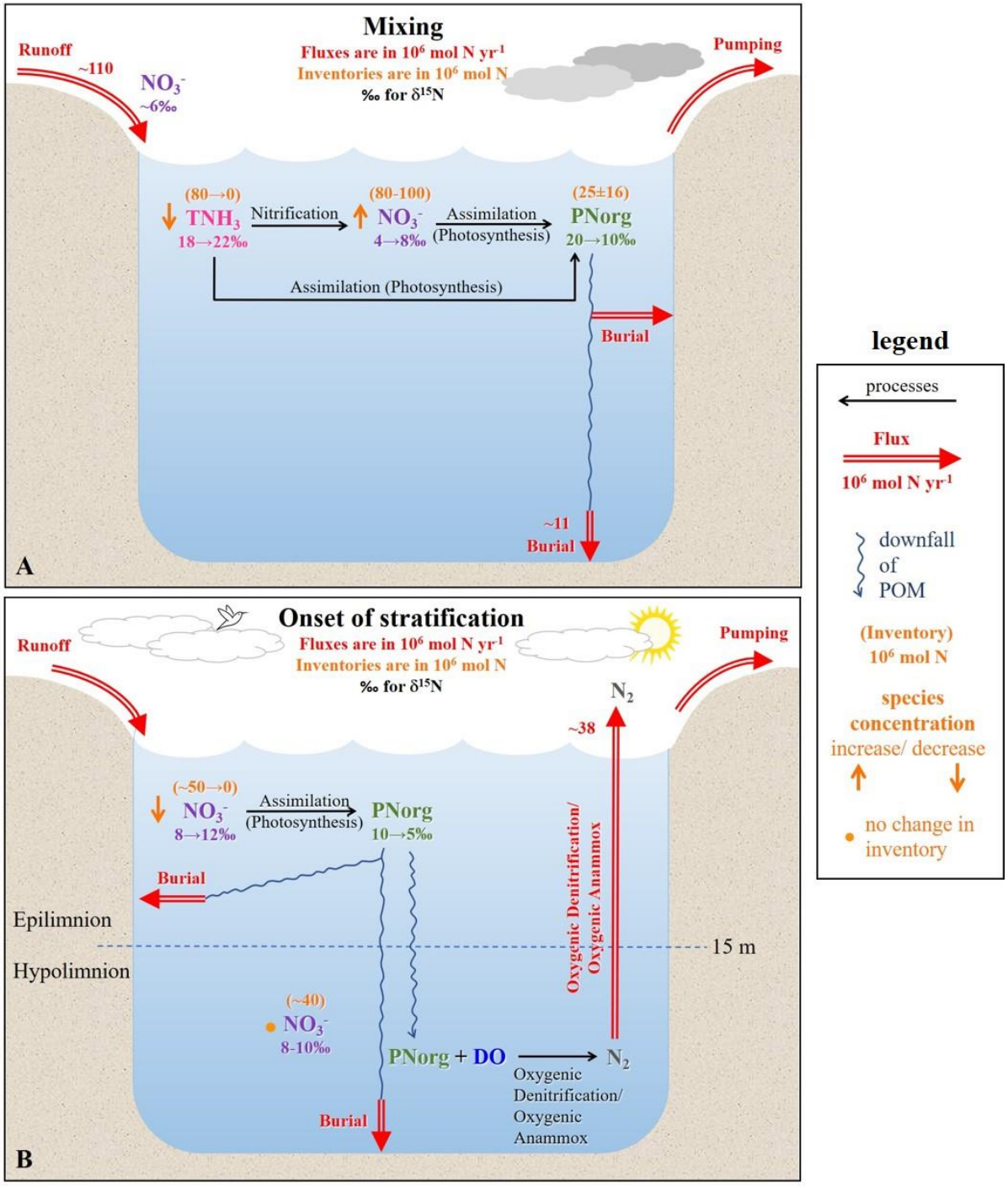
Ammonification of PNorg in the hypolimnion of the lake produces ^{15}N-enriched ammonium relative to PNorg, suggesting that the fractionation factor of nitrogen isotopes during ammonification is rather large and positive, in contrast to the commonly accepted view that there is virtually no fractionation during ammonification. To study this issue, an incubation experiment was performed. The results of the incubation experiment prove that decomposition of POM leads to significantly isotopically ^{15}N-enriched ammonium product, as observed in LK during stratification period. Mass- and isotopic-balances of PNorg and TNH_3 indicate that ammonium is not the sole product of the decomposition. I suggest that isotopically low DNorg is also formed.

6. Summary and Conclusions

6.1 Synthesis – The nitrogen cycle during different seasons

This study describes patterns of the annual dynamics in Lake Kinneret's nitrogen reservoirs of nitrate (NO_3^-), nitrite (NO_2^-), ammonium (TNH_3), and POM (PNorg) and its water sources and their isotopic compositions. The data collected was used to construct nitrogen (and dissolved oxygen) and isotopic ($\delta^{15}N$) mass-balances, which were used to identify and quantify the various governing biogeochemical processes in the lake.

The research comprises four consecutive layers: 1. Methodology development (Chapter 3), which enabled a reliable determination of the isotopic compositions of a single nitrogen species in the presence of others; 2. High temporal resolution of lake's water column chemical and isotopic composition of various nitrogen species (Chapters 4 and 5); 3. Incubation experiments (Section 5.4); and 4. Nitrogen mass-balance calculations (Chapters 4 and 5). The insights provided by careful evaluation of these four layers are summarized in 4 cartoons below, presenting my view of the main processes controlling the nitrogen cycle in the lake in three distinctive limnologic periods (Fig. 6.1), depicting, mixing (Fig. 6.1A), onset of stratification (Fig. 6.1B), stratification (Fig. 6.1C), and a general annual cycle (Fig. 6.1D). The cartoons show also the two main discoveries of this research: 1. ***"Oxygenic denitrification" and/or "oxygenic anammox"***, an overlooked significant pathway in the overall nitrogen budget of the lake; and 2. Large and positive fractionation of nitrogen isotopes during ammonification producing ***^{15}N-enriched ammonia relative to PNorg*** ($\delta^{15}N(TNH_3)$-$\delta^{15}N$(PNorg)≈10-15 ‰), which is in ***contrast*** to the commonly accepted view of ***virtually no fractionation during ammonification***.


Mixing
Fluxes are in 10⁶ mol N yr⁻¹
Inventories are in 10⁶ mol N
‰ for δ¹⁵N
Runoff
~110
NO3-
~6‰
Pumping
(80→0)
TNH3
18→22‰
Nitrification
(80-100)
NO3-
4→8‰
Assimilation
(Photosynthesis)
(25±16)
PNorg
20→10‰
Assimilation (Photosynthesis)
Burial
~11
Burial
A
Onset of stratification
Fluxes are in 10⁶ mol N yr⁻¹
Inventories are in 10⁶ mol N
‰ for δ¹⁵N
Runoff
Pumping
N2
~38
(~50→0)
NO3-
8→12‰
Assimilation
(Photosynthesis)
PNorg
10→5‰
Burial
Epilimnion
Hypolimnion
15 m
Oxygenic Denitrification/
Oxygenic Anammox
(~40)
NO3-
8-10‰
PNorg + DO
N2
Oxygenic
Denitrification/
Oxygenic
Anammox
Burial
B
legend
processes
Flux
10⁶ mol N yr⁻¹
downfall
of
POM
(Inventory)
10⁶ mol N
species
concentration
increase/ decrease
no change in
inventory

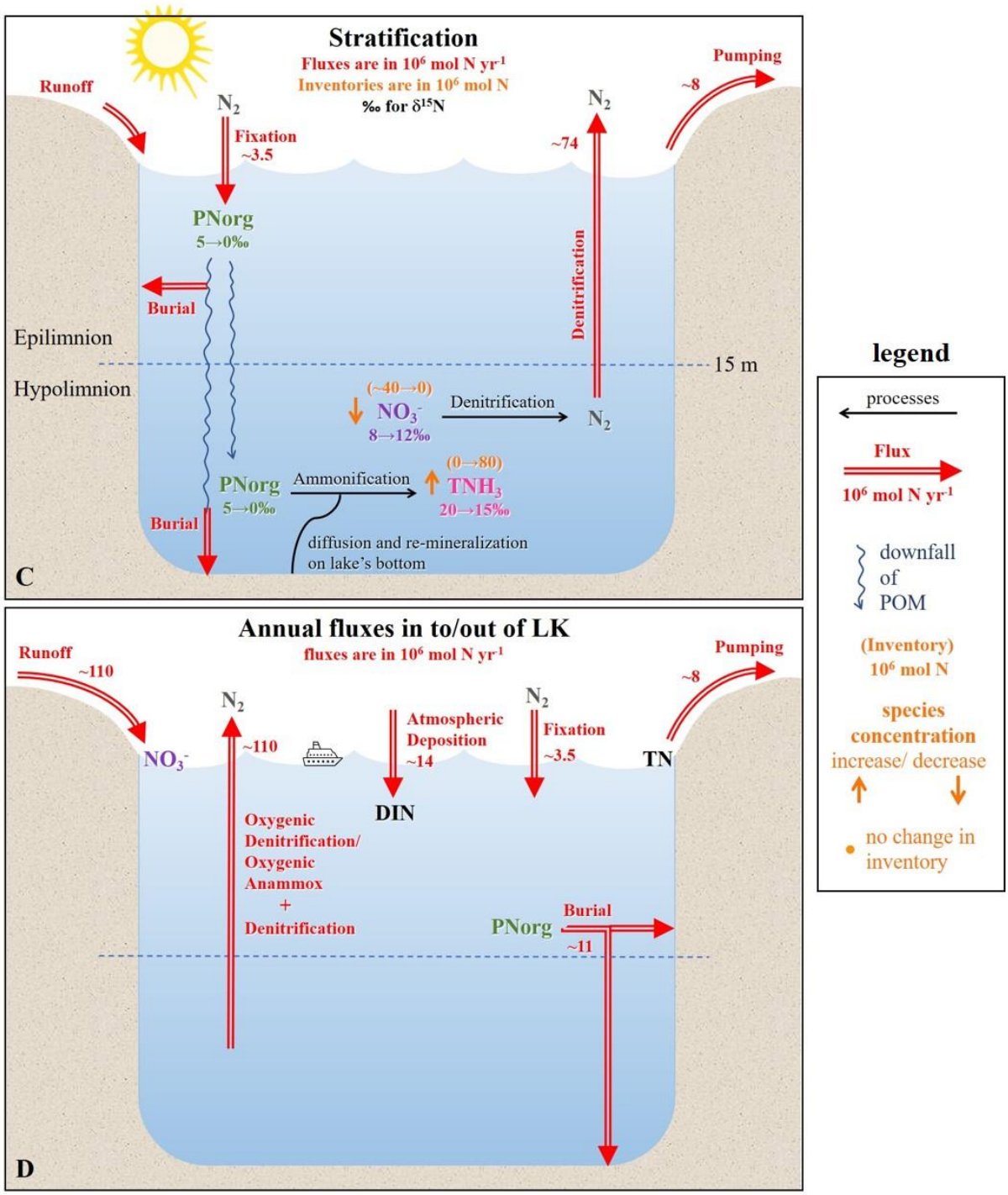


Fig. 6.1. Conceptual cartoon of the nitrogen cycle in LK depicting the main nitrogen input and output fluxes, processes and inventories in different limnologic statuses. A-Mixing; B - Onset of stratification; C- Stratification; and D- Annual input and output fluxes. The different markers are explained in the legends of the cartoons. Fluxes of sedimentation, atmospheric deposition and nitrogen fixation are from Nishri (2014), other fluxes are estimated for the study period. The main fluxes for each lake status are given in Figs. A, B and C and the annual fluxes are given in Fig. D. Note that the fluxes during the statuses represented in A, B and C do not balance because the lake is obviously not at steady-state over such short periods. The difference between the annual fluxes as presented in D shows a small, ~10% excess of outputs from the lake. This imbalance implies either that, on average, the lake was not in steady state during the study period or it reflects the rather large uncertainties in the fluxes not estimated in this research (see Nishri, 2014).

6.2 Conclusions

The synthesis above (Section 6.1, Fig. 6.1) contains a cartoon type description of the processes (pathways in the limnologic nitrogen cycle) controlling the nitrogen reservoirs and their isotopic compositions during different lake's statuses. Below I itemize the main achievements of the research which are not included in the synthesis:

1. I developed methodologies to determine the isotopic composition of different nitrogen species in the presence of other potentially interfering nitrogen species. These methodologies were tested in different mixtures of ammonia, nitrite and nitrate and the procedures were used to measure the nitrogen isotopic composition of these species in LK. Briefly, prior to IRMS analysis, every dissolved nitrogen species to be measured was transformed to $N_2O(g)$ and introduced to the mass-spectrometer by a Gas-Bench. Nitrite (if present) should be removed using the SA prior to the determination of the isotopic composition of nitrate or ammonium. Ammonia (if present) should be removed using a Cd-column prior to the determination of the isotopic composition of nitrate or nitrite.
2. At the onset of stratification, LK's hypolimnion loses about ***half of its DO inventory with no reciprocal change in the inventories of nitrogen species***. This obvious paradox lead me to the idea of "oxygenic denitrification and/or oxygenic anammox", which is a macro scale (limnologic scale) phenomenon of a microscale process operating in low oxygen POM microenvironments. These microenvironments comprise micro particles of "***marine/lacustrine snow***" (organic matter particles), which sink through the water column down to the hypolimnion.
3. The annual removal of nitrogen from LK, as N_2 escape, is estimated in this study to be ~$110 \cdot 10^6$ mol, Fig. 6.1D). This estimate is ca. 30% higher than previous estimates, which did not know about "oxygenic denitrification/anammox" and hence, did not consider it in their nitrogen budgets. It should be noted that "oxygenic denitrification/anammox" was discovered here by analyzing the DO and nitrogen profiles at high temporal resolution (weekly) of the database collected during this work.
4. Ammonification of PNorg in the hypolimnion of the lake produces ammonium which is enriched with ^{15}N relative to its parent PNorg. This indicates that the ***fractionation factor of***

nitrogen isotopes during ammonification is rather large and positive, in contrast to the common view that ammonification proceeds with virtually no fractionation of nitrogen isotopes. An incubation experiment performed to study this issue corroborated the field observation and model fitted to the data estimates a fractionation factor $\Delta_{product\text{-}PNorg}$ of +2.13‰. Elemental and isotopic balances of PNorg and TNH_3 indicate that ammonium is not the sole product of the POM decomposition and it most likely involves also production of ^{15}N-depleted DN_{org} (relative to PNorg).

This study demonstrates the importance of high temporal resolution of limnologic water column profiles of N-species and their isotopic composition, as determined simultaneously on several individual N-species. Such lacustrine mass balances provided new insights on biogeochemical processes otherwise overlooked, and on processes controlling the nitrogen cycle in lakes.

7. Bibliography

Alldredge, A.L., and Cohen Y. (1987). Can microscale chemical patches persist in the sea? microelectrode study of marine snow, fecal pellets. *Science* **235**, 689-691

Altabet, M.A., Pilskaln, C., Thunell, R.C., et al. (1999). The nitrogen isotope biogeochemistry of sinking particles from the margin of the Eastern North Pacifi c. *Deep Sea Research, Part I* **46**, 655–679.

Amberger, A., and Schmidt, H.L. (1987). Natuerliche isotopengehalte von nitrat als indikatoren fuer dessen herkunft. Translated Title: Natural isotope contents of nitrate as indicators of its origin. *Geochimica et Cosmochimica Acta* **51**, 2699-2705.

American Public Health Association (1992). Standard methods for examination of water and waste water, 18th ed., APHA.

Aravena , R., and Robertson, W.D. (1998). Use of multiple isotope tracers to evaluate denitrification in ground water: study of nitrate from a large-flux septic system plume, *Ground Water* **36,** 975–982.

Aravena, R., Evans, M.L., and Cherry, J.A. (1993). Stable isotopes of oxygen and nitrogen in source identification of nitrate from septic systems. *Ground Water* **31**, 180-186.

Arrigo, K.R. (2005). Marine microorganisms and global nutrient cycles. *Nature* **473**, 349-355.

Avery, A.A. (1999). Infantile methemoglobinemia: reexamining the role of drinking water nitrates. *Environmental Health Perspectives* **107**(7):583–586.

Berman, T. (1973). Modification of filtration methods for the measurement of inorganic 14C uptake by photosynthesizing algae. *Journal of Phycology* **9** 327-330.

Berman T., and Holenberg M. (2005). Don't fall foul of biofilm through high TEP levels. *Filtration & Separation* **42**, 30-32. https://doi.org/10.1016/S0015-1882(05)70517-6.

Berman T., Yacobi, Y. Z., and Pollingher, U. (1992). Lake Kinneret phytoplankton: stability and variability during twenty years (1970-1989). *Aquatic Sciences* **54,** 104-127.

Berman-Frank, I., Erez, J., and Kaplan, A. (1998). Changes in inorganic carbon uptake during the progression of a dinoflagellate bloom in a lake ecosystem. Canadian Journal of Botany-Revue *Canadienne De Botanique* **76,** 1043-1051.

Boettcher, J., Strebel, O., Voerkelius, S., and Schmidt, H.L. (1990). Using isotope fractionation of nitrate-nitrogen and nitrate-oxygen for evaluation of microbial denitrification in a sandy aquifer. *Journal of Hydrology* **114**, 413-424.

Bohlke, J.K., and Coplen, T. (1995). Reference and intercomparison materials for stable isotopes of light elements. Intern. Atomic Energy Agency, Vienna, IAEA TECDOC **825**, 51-66.

Bohlke, J.K., Ericksen, G.E., and Revesz, K. (1997). Stable isotope evidence for an atmospheric origin of desert nitrate deposits in northern Chile and southern California, U.S.A. *Chemical Geology Isotope Geoscience* **136**, 135-152.

Bohlke, J.K., Smith, R.L., and Hannon, J.E., (2007). Isotopic Analysis of N and O in Nitrite and Nitrate by Sequential Selective Bacterial Reduction to N_2O. *Analytical Chemistry* **79**, 5888-5895.

Brandes, J. A., and Devol, A. H., (2002). A global marine-fixed nitrogen isotopic budget: Implications for Holocene nitrogen cycling. *Global Biochemical Cycles* **16**, 1120, doi: 10.1029/2001GB001856

Bratkiˇc, A., ˇSturm, M., Faganeli, J., and Ogrinc, N., (2012). Semi-annual carbon and nitrogen isotope variations in the watercolumn of Lake Bled, NW Slovenia. *Biogeosciences*, **9**, 1-11.

Brewer, P.G., and Riley, J.P. (1965). The automatic determination of nitrate in seawater. *Deep-Sea Research* **12**, 765-772.

Brooks, P.D., Stark, J.M., McInteer, B.B., and Preston, T., (1989). Diffusion method to prepare soil extracts for automated nitrogen–15 analysis. *Soil Science Society of America Journal*, **53,** 1707–1711.

Bunton, C.A., and Masui, M., (1960). Oxygen exchange between nitrous acid and water. Part II. exchange in acetate buffers. *Journal of Chemical Society* 304-308.

Bunton, C.A., and Stedman, G., (1959). Mechanism of the azide-nitrite reaction. Part III. Reaction in ^{18}O water. *Journal of Chemical Society*, 3466-3474.

Bunton, C.A., Halevi, E.A., and Llewellyn, D.R., (1953). Oxygen exchange between nitric acid and water. Part III. Catalysis by nitrous acid. *Journal of Chemical Society*., 2653-2657.

Bunton, C.A., Halevi, E.A., and Llewellyn, D.R., (1958). Oxygen exchange between nitric acid and water. Part IV. The nitration of 2-mesitylethanesulphonic acid. *Journal of Chemical Society*, 2420-2421.

Bunton, C.A., Llewellyn, D.R., and Stedman, G., (1959). Oxygen exchange between nitrous acid and water. *Journal of Chemical Society*, 568-573.

Carpenter E. J., Capone, D. G., Fry, B., and Harvey, H. R., (1997). Biogeochemical tracers of the marine cyanobacterium, *Trichodesmium* spp. *Deep Sea Research.* **44**, 27-38.

Casciotti, K.L., Sigman, D.M., Galanter Hastings, M., Boehlke, J.K., and Hilkert, A., (2002). Measurement of the oxygen isotopic composition of nitrate in seawater and freshwater using the denitrifier method. *Analytical Chemistry* **74**, 4905-4912.

Cascioti, K.L., Sigman, D.M., Ward, B.B., (2003). Linking diversity and stable isotope fractionation in ammonia-oxidizing bacteria, *Geomicrobiol Journal* **20**, 335–353.

Cavari B.Z. and Phelps, G., (1977). Denitrification in Lake Kinneret in the presence of oxygen. *Freshw Biology **7**, 385–391.*

Cleveland, C.C., Townsend, A.R., Schimel, D.S., et al. (1999). Global patterns of terrestrial biological nitrogen (N2) fixation in natural systems. *Global Biogeochemical Cycles*, **13**, 623–646.

Cline, J.D., and Kaplan, I.R., (1975). Isotopic fractionation of dissolved nitrate during denitrification in the eastern tropical north pacific ocean, *Marine Chemistry* **3,** 271–299.

Cifuentes, L.A., Fogel, M.F., Pennock, J.R., and Sharp, J.H., (1989). Biogeochemical factors that influence the stable nitrogen isotope ratio of dissolved ammonium in the Delaware Estuary. Geochimica et Cosmochimica Acta **53**, 2713–2721.

Cuello, C., Correa, P., Haenszel, W., Gordillo, G., Brown, Ch., Archer, M., and Tannenbaum, S., (1976). Gastric cancer in Colombia. I. Cancer risk and suspect environmental agents. *Journal of the National Cancer Institute* **57**, 1015-1020.

Dubowski, Y., Erez, J., and Stiller, M., (2003). Isotopic paleolimnology of Lake Kinneret. *Limnology and Oceanography* **48**, 68-78.

Edwards, A.P., (1973). Isotopic tracer techniques for identification of sources of nitrate pollution, *Journal of Environmental Quality* **2,** 382.

FAO/WHO (1996). Toxicological evaluation of certain food additives and contaminants. Geneva, World Health Organization, Joint FAO/WHO Expert Committee on Food Additives (WHO Food Additives Series No. 35).

Faure, G., (1986). Principles of Isotope Geology, 2nd edition. John Wiley & Sons, New York, 589 pp.

Feigin, A., Shearer, G., Kohl, D.H., and Comoner, B., (1974). The amount and nitrogen–15 content of nitrate in soil profiles from two central Illinois fields in a cornsoybean rotation, Soil Science Society of America Proceedings **38**, 465–471.

Flinn, N.A.P., (2012). The use of stable nitrogen and carbon isotopes to examine the sources, sinks and cycling of nitrogen in a small, artifincially neutrophic Boreal lake. MSc Thesis, Waterloo University, Canada.

Fogel, M.L., and Cifuentes, L.A., (1993). Isotope fractionation during primary production. In: *Organic Geochemistry* (Eds M.H. Engel & S.A. Macko), pp. 73–98. Plenum Press, New York.

Francis, C.A., Berman, J.M., and Kuypers, M.M.M., (2007). New processes and players in the nitrogen cycle: the microbial ecology of anaerobic and archaeal ammonia oxidation. The ISME Journal **1**, 19–27.

Froelich, P.N., Klinkhammer, G.P., Bender, M.L., Luedtke, N.A., Heath, G.R., Cullen, D., and Dauphin, P., (1979). Early oxidation of organic matter in pelagic sediments of the eastern equatorial Atlantic: suhoxic diagenesis. Geochimica et Cosmochimica Acta **43**, 1075-1090.

Fukada , T., Hiscock , K.M., Dennis , P.F., and Grischek , T., (2003). A dual isotope approach to identify denitrification in groundwater at a river-bank infiltration site, *Water Research* **37,** 3070–3078.

Galloway, J.N., Schlesinger, W.H., Levy, H. II, Michaels, A., and Schnoor, J.L,. (1995) Nitrogen fixation: anthropogenic enhancement–environmental response. *Global Biogeochemistry Cycles*, **9**, 235–252.

Galloway, J.N., Dentener, F.J., Capone, D.G., Boyer, E.W. et al. (2004). Nitrogen cycles: past, present, and future. *Biogeochemistry*, **70**, 153–226.

Gonfiantini, R., Stichler, W., and Rozanski, K., (1995). Standards and intercomparison materials distributed by the IAEA for stable isotope measurements. Internatinal Atomic Energy Agency, Vienna, 1-18.

Goodwin, A., (2010). Stable carbon and nitrogen isotopes in Lake Kinneret food web 2008. M.S.c Thesis, The Hebrew University of Jerusalem.

Gophen M., Smith, V.H., Nishri, A., and Threlkeld, S.T., (1999). Nitrogen deficiency and invasion of Lake Kinneret, Israel, by the N2-fixing cyanobacterium *Aphanizomenon ovalisporum*. *Aquatic Science* **61**, 293–306

Gormly, J.R., and Spalding, R.F., (1979). Sources and concentrations of nitrate-nitrogen in ground water of the Central Platte Region, Nebraska, Ground Water **17**, 291–301.

Granger, J. (2006). Coupled nitrogen and oxygen isotope of nitrate imparted during its assimilation and dissimilarity reduction by unicellular plankton. Unpublished PhD dissertation, University of British Columbia.

Granger J., Sigman D.M., Needoba J.A., and Harrison P.J., (2004). Coupled nitrogen and oxygen isotope fractionation of nitrate during assimilation by cultures of marine phytoplankton. *Limnology and Oceanography* **49**(5), 1763–1773.

Hadas, O., Altabet, M.A., and Agnihotri, R., (2009). Seasonally varying nitrogen isotope biogeochemistry of particulate organic matter in Lake Kinneret, Israel. *Limnology and Oceanography*. **54,** 75-85.

Hambright, K. D., Parparov, A., and Berman, T., (2000). Indices for water quality for sustainable management and conservation of an arid region lake, Lake Kinneret (Sea of Galilee), Israel. *Aquatic Conservation marine and Freshwater Ecosystems* **10,** 393-406.

Hambright, K. D., Zohary, T., Eckert, W., Schwartz, S.S., Schelske, C.L., Laird, K.R., and Leavitt, R.R., (2008). Exploitation and destabilization of a warm, freshwater ecosystem through engineered and hydrological change. Ecology Application **18** (7), 1591-603.

Heaton, T.H.E., (1986). Isotopic studies of nitrogen pollution in the hydrosphere and atmosphere: a review, *Chemical Geology* **59,** 87–102.

Hill, M.J., Hawksworth, G., and Tattersall, G., (1973). Bacteria, nitrosamines and cancer of the stomach. *British Journal of Cancer* **28**, 562–567.

Hoch M.P., Fogel M.F., and Kirchman, D.L. (1992). Isotope fractionation associated with ammonium uptake by a marine bacterium. *Limnology and Oceanography*, **37**(7), 1447–1459.

Hoering , T., (1955). Variations of nitrogen–15 in abundance in naturally occurring substances, *Science* **122,** 1233–1234.

Hoering , T., (1957). The isotopic composition of the ammonia and the nitrate ion in rain, *Geochimica et Cosmochiica. Acta* **12,** 97–102.

Huang, J.Y.C., and Wozniak, D.J., (1981). Nitrogen Transformations in Streams. *Journal of Environmental Science* **24**, 41-45.

Kar, J.D., Showers, W.J., Giliam, J.W., and Andres, A.S., (2001). Tracing nitrate transport and environmental impact for intensive swine farming using delta nitrogen–15, *Journal of Environmental Quality*. **30**, 1163–1175.

Kellogg, R.L., Maizel, M.S., and Goss, D.W., (1992). Agricultural Chemical Use and Ground Water Quality: Where are the Potential Problem Areas?. US Dep. Agriculture, Grant No. 91-38813-6966.

Kendall, C., (1998). Tracing nitrogen sources and cycling in catchments. In Isotope-tracers in catchment hydrology. Edited by C. Kendall and J.J. McDonnel. Elsevier, Amsterdam, The Netherlands, pp. 534–569.

Kendall, C., and Aravena, R., (2000). Nitrate isotopes in groundwater systems. In Environmental tracers in subsurface hydrology. Edited by P. Cook and A.L. Herczeg. Dordrecht: Kluwer Academic Publishers, pp. 261–297.

Kendall, C., Elliott, E.M., and Wankel, S.D., (2007). Tracing anthropogenic inputs of nitrogen to ecosystems", Stable Isotopes in Ecology and Environmental Science (Michener, R.H., Lajtha, K., Eds), Blackwell Publishing, Oxford, 375–449.

Kohl, D.H., Shearer, G.B., and Commoner, B., (1971). Fertilizer nitrogen: contribution to nitrate in surface water in a corn belt watershed, *Science* **174,** 1331–1334.

Kornexl, B.E., Werner, R.A., and Gehre, M., (1999). Standardization for oxygen isotope ratio measurement - Still an unsolved problem. Rap. Commun Mass Spectrometry **13**, 1248-1251.

Kreitler, C.W., (1979). Nitrogen-isotope ratio studies of soils and groundwater nitrate from alluvial fan aquifers in Texas, *Journal of Hydrology* **42,** 147–170.

Kreitler, C.W., and Browning, L.A., (1983). Nitrogen-isotope analysis of groundwater nitrate in carbonate aquifers: natural sources versus human pollution, *Journal of Hydrology* **61,** 285–301.

Kreitler, C.W., and Jones, D.C., (1975). Natural soil nitrate: the cause of the nitrate contamination of ground water in Runnels County, Texas, *Ground Water* **13,** 53–61.

Lam, P., and Kuypers, M.M.M., (2011). "Microbial Nitrogen Processes in Oxygen Minimum Zones". *Annual Review of Marine Science* **3**, 317–345.

Lehmann, M.F., Sigman, D.M. and Berelson, W.M., (2004). Coupling the 15N/14N and 18O/16O of nitrate as a constraint on benthic nitrogen cycling. *Marine Chemistry* **88**, 1–20.

Letole, R., (1980). "Nitrogen–15 in the natural environment", Handbook of Environmental Isotope Geochemistry: The Terrestrial Environment (Fritz, P., Fontes, J.C., Eds), Elsevier, Amsterdam, 407–433.

Mahaffey, C., Michaels, A. F., and Capone, D. G., (2005). The conundrum of marine N2 fixation. *American Journal of Science* **305,** 546-595.

Marchant, H. K., Lavik, G., Holtappels, M., and Kuypers, M. M. M., (2014). "The Fate of Nitrate in Intertidal Permeable Sediments". PLoS ONE. **9** (8): e104517.

Mariotti , A., (1984). Utilisation des variations naturelles d'abondance isotopique en 15N pour tracer l'origine des pollutions des aquifers par les nitrates", *Isotope Hydrology*, IAEA.

Mariotti, A., Germon, J.C., Hubert, P., Kaiser, P., Letolle, R., Tardieux, A., and Tardieux, P., (1981). Experimental determination of nitrogen kinetic isotope fractionation: some principles; illustration for the denitrification and nitrification processes, *Plant and Soil* **62,** 413–430.

Mariotti, A., Germon, J.C. and Leclerc, A., (1982). Nitrogen isotope fractionation associated with the $NO2^{-} \rightarrow N2O$ step of denitrifi cation in soils. *Canadian Journal of Soil Science*, **62**, 227–241.

Mayer, B., Sebilo, M., and Wassenaar, L.I., (2013). Isotopic assessment of nitrogen cycling in river basins: potential and limitations for nutrient management purposes, Application of Isotope Techniques for Assessing Nutrient Dynamics in River Basins, IAEA-TECDOC-1695, IAEA, Vienna, 15–34.

McCready R.G.L., Gould W.D. and Barendregt R.W., (1983). Nitrogen isotope fractionation during the reduction of NO_3^- to NH_4^+ by Desulfovibrio sp. *Canadian Journal of Microbiology*, **29(2**), 231-234.

McIlvin , M.R., and Altabet, M.A.,(2005). Chemical Conversion of Nitrate and Nitrite to Nitrous Oxide for Nitrogen and Oxygen Isotopic Analysis in Freshwater and Seawater, *Analytical Chemistry* **77** 17, 5589–5595.

Mekorot, Israel National Water Co., Home page - https://www.mekorot-int.com.

Montoya, J.P., Korrigan, S.G. and McCarthy J.J., (1991). Rapid, storm-induced changes in the natural abundance of 15N in a planktonic ecosystem, Chesepeake Bay, USA. *Geochimica et Cosmochimica Acta*, **55**(12), 3627–3638.

Morris, A.W., and Riley, J.P., (1963). Determination of nitrate in sea water. Analytica Chimica Acta **29**, 272-279.

NATIONAL RESEARCH COUNCIL, COMMITTEE ON TOXICOLOGY, 1995. Nitrate and Nitrite in Drinking Water, National Academies Press, Washington, D.C.

Nishri, A., (2014). Quantitative Aspects of the Nitrogen Cycle. In: T. Zohary et al. (eds.), *Lake Kinneret*, Aquatic Ecology Series 6, DOI 10.1007/978-94-017-8944-8_21, © Springer Science+Business Media Dordrecht 2014.

Nishri, A., Rimmer, A., Wagner, U., Rosentraub, Z. and Yeats, P., (2011). Physical controls on the spatial variability in decomposition of organic matter in Lake Kinneret. *Aquatic Geochemistry* **17**, 195–207.

Nolan, B.T., Hitt, K.J., and Ruddy, B.C., (2002). Probability of nitrate contamination of recently recharged ground waters in the conterminous United States, *Environmental Science and Technology* **36** 10, 2138–45

Norwitz, G. and Keleher, P.N., (1984). Spectrophotometric determination of nitrite with composite reagents containing sulphanilamide, sulphanilic acid or 4-nitroaniline as the diazotisable aromatic amine and N-(1-naphthyl) ethylenediamine as the coupling agent. *Analyst* **109**, 1281-1284.

Ohte, N., Nagata, T., Tayasu, I., Kyozu, A., Yoshimizu, C., and Osaka, K., (2013). Simultaneous measurement of nitrogen and oxygen isotopes of nitrate to evaluate nitrate sources and processes in catchments. Application of Isotope Techniques for Assessing Nutrient Dynamics in River Basins, IAEA-TECDOC-1695, IAEA, Vienna, 49-67.

Ostrovsky, I., Wynne, D., Bergstein-Ben Dan, T., Nishri, A., Yacobi. Y.Z., Koren, N., and Parparova, R., (1997). Spatial distributions of biogeochemical parameters in Lake Kinneret bed sediments. *Water Air Soil Pollut* **62**, 497–505.

Pennock, J., Velinsky, D., Ludlam, J., et al. (1996). Isotopic fractionation of ammonium and nitrate during uptake by *Skeletonema costatum*: Implications for δ15N dynamics under bloom conditions. *Limnology and Oceanography*, **41**(3), 451–459.

Peterson, B.J., Wollheim, W.M., Mulholland, P.J., Webster, J.R., Meyer, J.L., Tank, J.L., Marti, E., Bowden, W.B., Valett, H.M., Hershey, A.E., McDowell, W.H., Dodds, W.K., Hamilton, S.K., Gregory, S., and Morrall, D.D., (2001). Control of nitrogen export from watersheds by headwater streams. *Science* **292**, 86-90.

Rajagopal, R., and Tobin, G., (1989). Expert opinion and ground-water quality protection: the case of nitrate in drinking water. *Ground Water* **27**, 835-847.

Redfield, A.C., Ketchum, B.H., and Richards, F.A., (1963). The influence of organisms on the composition of sea-water. Hill, M.N. (Ed.), The Sea: Vol 2: Composition of Seawater Comparative and Descriptive Oceanography, Interscience, London, 26-77

Revesz, K., Boehlke, J.K., and Yoshinari, T., (1997). Determination of δ15N and δ18O in nitrate. *Analytical Chemistry* **69**, 4375-4380.

Rock, L., and Mayer, B., (2004). Isotopic Assessment of Sources of Surface Water Nitrate within the Oldman River Basin, Southern Alberta, Canada, *Water Air Soil Poll.: Focus* **4**, 545–562.

Schilman, B., and Teplyakov, N., (2005). Development of a reduction method for the δ15N and δ18O analyses of nitrate: proxies for the identification of potential contamination sources of nitrates in groundwater. Geological Survey of Israel Report, TR-GSI/13/2005, 6 pp.

Schilman, B., and Teplyakov, N., (2006). A modified chemical technique for nitrate reduction to nitrous oxide for δ15N and δ18O analysis in fresh and marine waters. Geological Survey of Israel Report, TR-GSI/02/2006, 13 pp.

Schilman, B. and Teplyakov, N., (2007). Detailed Protocol for Nitrate Chemical Reduction to Nitrous Oxide for $\delta^{15}N$ and $\delta^{18}O$ Analysis of Nitrate in Fresh and Marine Waters. Geological Survey of Israel Report GSI/15/2007.

Schilman, B., Teplyakov, N., and Gavrieli, I., (2004). Identification of nitrate contamination sources in ground water in Israel using the nitrogen and oxygen isotopic composition: Wadi Kelt-Jericho area as a case study. Geological Survey of Israel Report GSI/25/2004, 12 pp.

Schilman, B., Teplyakov, N., Gavrieli, I., and Guttman, Y., (2007). Identification of the sources of nitrate contamination in the Western Galilee aquifers, north Israel, using a multi-proxy stable isotope and chemical approach. Geological Survey of Israel Report, GSI/17/2007, 44 pp.

Seitzinger, S.P., Styles, R.V., Boyer, E., Alexander, R.B., Billen, G., Howarth, R., Mayer, B., and Van Breemen, N., (2002). Nitrogen retention in rivers: model development and application to water-sheds in the eastern US. *Biogeochemistry* **57/58**, 199–237.

Serruya, C., (1971). Lake Kinneret: the nutrient chemistry of the sediments. *Limnology and Oceanography* **16** (3), 510-521.

Serruya, C., (1978). The chemical environment. In C. Serruya [ed.] Lake Kinneret, p. 184-204. W. Junk, The Hague.

Serruya, C., Gophen, M., and Pollingher, U., (1980). Lake Kinneret: Carbon flow patternsand ecosystem management. *Archiv Fur Hydrobiologie* **88,** 265-302.

Sigman, D.M., Altabet, M.A., Michener, R., McCorkle, D.C., Fry, B., and Holmes, R.M., (1997). Natural abundance level measurement of the nitrogen isotopic composition of oceanic nitrate: an adaptation of the ammonia diffusion method. *Analytical Chemistry* **57**, 227-242.

Sigman, D.M., Casciotti, K.L., Andreani, M., Galanter, M., and Boehlke, J.K., (2001). A bacterial method for the nitrogen isotopic analysis of nitrate in seawater and freshwater. *Analytical Chemistry* **73**, 4145-4153.

Silva, S.R., Kendall, C., Wilkison, D.H., Ziegler, A.C., Chang, C.C.Y., and Avanzino, R.J., (2000). A new method for collection of nitrate from fresh water and the analysis of nitrogen and oxygen isotope ratios. *Journal of Hydrology* **228**, 22-36.

Smith, S.V., Serruya, S., Geifman, J., and Berman,T., (1989). Annual mass balance of P,N,Ca and Cl in Lake Kinneret, Israel. *Limnology and Oceanography* **34,** 1202-1213.

Stedman, G., (1952). Oxygen exchange between nitric acid and water. *Journal of Chemical Society* 4913-4916.

Stedman, G., (1959a). Mechanism of the azide-nitrite reaction. Part I. *Journal of Chemical Society*, 2943-2949.

Stedman, G., (1959b). Mechanism of the azide-nitrite reaction. Part II. *Journal of Chemical Society*, 2949-2954.

Thamdrup, B. & Dalsgaard, T. (2002). Production of N2 through anaerobic ammonium oxidation coupled to nitrate reduction in marine sediments. *Appl. Environ. Microbiol.* **68**, 1312–1318.

Vitousek, P.M., Aber, J.D., Howarth, R.W., Likens, G.E., Matson, P.A., Schindler, D.W., Schlesinger, W.H., and Tilman, D.G., (1997). Human alteration of the global nitrogen cycle: Sources and consequences, *Ecological Applications* **7**, 737–750.

Waser, N.A.D., Harrison, P.J., Nielsen, B., and Calvert, H.E., (1998). Nitrogen isotope fractionation during the uptake and assimilation of nitrate, nitrite, ammonium and urea by a marine diatom. *Limnology and Oceanography*, **43**(2), 215–224.

Wassenaar, L.I., (1995). Evaluation of the origin and fate of nitrate in the Abbotsford Aquifer using the isotopes of 15N and 18O in NO_3^-. *Applied Geochemistry* **10**, 391–405.

Wassenaar, L.I., Hendry, M.J., and Harrington, N., (2006). Decadal geochemical and isotopic trends for nitrate in a transboundary aquifer and implications for agricultural beneficial management practices, *Environmental Science Technology* **40,** 4626–4632.

Welman, R.P., Cook, F.D., and Krouse, H.R., (1968). Nitrogen–15: Microbiological alteration of abundance, *Science* **161,** 269–270.

Weyer, P.J., Cerhan, J.R., Kross, B.C., Hallberg, G.R., Kantamneni, J., Breuer, G., Jones, M.P., Zheng, W., and Lynch, C.F., (2001). Municipal drinking water nitrate level and cancer risk in older women: the Iowa Women's Health Study. *Epidemiology* **11**, 327-338.

WHO (World Health Organization) 1986. Ammonia: Environmental Health Criteria 54, Geneva.

Widory, D., (2013). The benefit of using isotopes in the NO_3 water quality management. Application of Isotope Techniques for Assessing Nutrient Dynamics in River Basins, IAEA-TECDOC-1695, IAEA, Vienna, 35-48.

Widory, D., Kloppmann, W., Chery, L., Bonnin, J., Rochdi, H., and Guinamat, J-L., (2004). Nitrates in groundwater: an isotopic multi-tracer approach, *Journal Contaminant Hydrology.* **72,** 165–188.

Wood, E.O., Armstrong, F.A.J., and Richards, F.A., (1967). Determination of nitrate in seawater by cadmium-copper reduction to nitrite. *Journal Marine Biology Association*U.K. **47**, 23-31.

Yakushiji, H., and Kanda, J. J., (1998). Determination of Experimentally Enriched 15N in Nitrate Nitrogen Based on an Improved Method of Azo Dye Formatio Determination of Experimentally Enriched 15N in Nitrate Nitrogen Based on an Improved Method of Azo Dye Formationn. *Oceanogr*aphy **54**, 337-342.

Zeng, H. and Wu, J., (2015). Tracing the Nitrate Sources of the Yili River in the Taihu Lake Watershed: A Dual Isotope Approach. *Water* **2015**, *7*, 188-201.

Zhang, L., Altabet, M. A., Wu, T. and Hadas, O., (2007). Sensitive Measurement of NH_4^+ $^{15}N/^{14}N$ ($\delta^{15}NH_4^+$) at Natural Abundance Levels in Fresh and Saltwaters. *Analytical Chemistry* **79**, 5297-5303.

Zohary, T., (2004). Changes to the phytoplankton assemblage of Lake Kinneret after decades of a predictable, repetitive pattern. *Freshwater Biology* **49,** 1355-1371.

Zohary, T., Erez, J., Gophen, M., Berman-Frank, I., and Stiller, M., (1994). Seasonality of stable carbon isotopes within the pelagic food web of Lake Kinneret. *Limnology and Oceanography* **39**, 1030-1043.

Zohary, T., Sukenik, A., and Berman, T., (2014). Peridinium gatunense. In: Zohary, T., Sukenik, A., Berman, T.,Nishri, A. (eds), Lake Kinneret: Ecology and Management, Chap. 11, 191-212.

מחקר זה מראה כי בדיקה מדוקדקת של השינויים העונתיים הגדולים בתפוצת צורוני החנקן וההרכבים האיזוטופיים שלהם בעמודת המים, ברזולוצית זמן גבוהה ולאורך מספר מחזורים שנתיים, יכולים להוביל לתובנות חדשות על מחזור החנקן באגמים בכלל ובאגם הכנרת בפרט. תהליכים כ-"דניטריפיקציה חמצנית" ו/או "אנמוקס חמצני" אובחנו במחקר זה, בזכות ניתוח מעמיק של מסד הנתונים הרחב שנבנה. תהליכים אלו שהוערכו כחשובים מאוד במחזור החנקן באגם לא נלקחו כלל בחשבון במחקרים קודמים. האמור לעיל מצביע שלתובנות מחקר זה השלכות חדשות להבנת התהלכים העיקריים השולטים במחזור החנקן של אגמים.

בעזרת מאזני מסה נמצא כי "דניטריפיקציה חמצנית" ו/או "אנמוקס חמצני" ודניטריפיקציה ישירה, אחראים ביחד לצריכה של כ- $110 \cdot 10^6$ מול חנקן ליצירה של חנקן גזי מומס, שנפלט במשך השנה לאטמוספירה. מכאן שכמות החנקן המסולקת מהאגם אינה תלויה אך ורק בשטף הכניסה של חנקן, אלא גם ביעילות שבה פועלים תהליכים אלו. משתנים אחרים, אשר אינם קשורים ישירות למאגר החנקן, כמו ריכוז החמצן המומס, קצב פרוק החומר האורגני החלקיקי ושקיעתו לתחתית האגם, משפיעים גם הם על סילוק חנקן מאגם.

התהליכים העיקריים השולטים במחזור החנקן בתקופת הערבוב הם ניטריפיקציה של אמוניום מההיפולימניון, אסימילציה (פוטוסינטיזה של פיטופלנקטון) באפילימניון, ואספקה חיצונית, בעיקר מנהר הירדן. הניטריפיקציה מלווה בפרקציונציה איזוטופית משמעותית, שבה התוצר, NO_3^-, מדולדל באיזוטופ ^{15}N יחסית לאמוניום שממנו הוא נוצר. לכן, עם התקדמות הניטריפיקציה, וככל שריכוז האמוניום השאריתי יורד, $\delta^{15}N_{TNH3}$ עולה (זיקוק ריילי).

התהליכים העיקריים השולטים במחזור החנקן בתקופת השיכוב הם אסימילציה, דניטריפיקציה ואמוניפיקציה. הפרקציונה של איזוטופי החנקן בתהליכי האסימילציה של ניטראט באפילימניון ודניטריפיקציה בהיפולימניון גורמת לכך שבסוף עונת האביב ה- $\delta^{15}N_{NO3^-}$ של הניטראט השאריתי עולה משמעותית כתוצאה מזיקוק ריילי. כמו כן, נמצא שערך ה-$\delta^{15}N_{TNH3}$ של האמוניום הנוצר בתהליך האמוניפיקציה של חומר אורגני חלקיקי בהיפולימניון גבוה מערך ה-$\delta^{15}N_{PNorg}$. תצפית זו מצביעה על כך שמקדם הפרקציונציה של איזוטופי החנקן בתהליך האמוניפיקציה הוא גבוה וחיובי, זאת בניגוד לדעה המקובלת שתהליך האמוניפיקציה אינו מלווה בפרקציונציה איזוטופית. ניסוי אינקובציה של חומר אורגני חלקיקי שנעשה במסגרת העבודה אימת מסקנות אלו, כפי שמתואר מטה.

השינויים העונתיים בערכי $\delta^{15}N_{PNorg}$ הם הגבוהים ביותר במערכת החנקן באגם, ומשקפים את ההרכב האיזוטופי של צורוני החנקן העוברים אסימילציה. ערך ה-$\delta^{15}N_{PNorg}$ הגבוה שנצפה באביב, מציין אסימילציה של אמוניום שאריתי שהועשר קודם לכן באיזוטופ ^{15}N בתהליך הניטריפיקציה. אסימילציה של ניטראט עם ערך $\delta^{15}N_{NO3-}$ נמוך, מתחילה מאוחר יותר, כאשר האמוניום נצרך לחלוטין, כפי שבא לידי ביטוי בירידה ההדרגתית של ערכי $\delta^{15}N_{PNorg}$ שקובע באסימילציה של הניטראט באפילימניון. ערכי $\delta^{15}N_{PNorg}$ הנמוכים מאד בתחילת החורף נובעים כנראה מקיבוע של חנקן (N_2) מומס.

ערכו של מקדם הפרקציונציה האיזוטופית של חנקן בתהליך האמוניפיקציה הוערך בניסוי אינקובציה של חומר אורגני חלקיק שנאספף בעמודת המים של הכינרת בעזרת רשת פלנקטון. תוצאות הניסוי מוכיחות שפרוק של חומר אורגני חלקיקי מוביל לעליה משמעותית בערכי $\delta^{15}N_{TNH3}$ (תוצר האמוניפיקציה), ומאששות את המסקנות אליהן הגעתי מתוך המדידות שנעשו בעמודת המים של אגם הכנרת בתקופת השיכוב (ראו למעלה). מאזן מסה והרכבים איזוטופיים של החומר האורגני החלקיקי ואמוניום בניסוי, מצביעים על כך שאמוניום אינו תוצר הפרוק היחידי, והאמוניפיקציה מלווה ביצירת חומר אורגני מומס בעל הרכב איזוטופי קל.

האגם מובילים לתנודות בולטות במצבי החימצון/חיזור של עמודת המים, מהיפולינמיון מחוזר במהלך השיכוב לתנאים מחמצנים לחלוטין בכל עמודת המים במשך תקופת הערבוב. השינויים במחזור החנקן באגם, הנשלטים על ידי דינמיקה זו, נחקרו באמצעות מדידות שבועיות של ריכוזי צורוני החנקן שבוצעו במעבדת הכנרת בפרופילים אנכיים של עמודת המים במרווחים של 5 מ' במשך כ- 6 שנים. דוגמאות נבחרות המייצגות עומקי מים אופייניים ואת עונות השנה השונות עברו אנליזה איזוטופית של צורני החנקן הראשיים. מאזני-מסה של ריכוזי צורוני החנקן והרכבם האיזוטופי שנבנו על בסיס פרופילים אלה, שימשו לאפיון וכימות התהליכים העיקריים השולטים במערכת החנקן באגם. נמצא שמאגרי הניטראט והאמוניום הם דומים בגודלם, אך מתחלפים (כאשר האחד עולה, השני יורד) במהלך השנה ולהם נפיצות שונה בעמודת המים, בהתאמה לדינמיקה הפיסיקו-כימית של האגם. שינויים עונתיים במאגר צורוני החנקן והחמצן המומס בהיפולימניון (מ-15 מ' ומטה) שימשו לכימות ולהגדרת התהליכים והשטפים החלים במחזור השנתי של מערכת החנקן באגם.

בחודשים מרץ-אפריל, בתחילת עונת השיכוב שבה עמודת המים של ההיפולימניון עוברת מתנאים מחמצנים לתנאים תת-מחמצנים, ריכוז החמצן המומס יורד בצורה ניכרת, אך ללא שינוי ניכר בנפיצות צורוני החנקן במים. תצפית זו עומדת בניגוד לקורלציה השלילית הצפויה בין ירידה בחמצן ועליה בצורוני חנקן הנובעת מחימצון של חומר אורגני חלקיקי בעזרת חמצן מומס, לפי סטוכיומטריית Redfield. *אני מציעה שתופעה זו נובעת מתהליכים שאני מכנה כ-"דניטריפיקציה חמצנית" (”oxygenic denitrification“) ו/או "אנמוקס חמצני" (”oxygenic anammox“)*. לפי המוצע כאן, תהליכים אלו חלים כאשר בתנאי סביבה מחמצנים, ניטראט או ניטריט הנוצרים על ידי חימצון של חומר אורגני חלקיקי בעזרת חמצן מומס, יצרכו בו-זמנית בתהליכים תת-מחמצנים או אנארוביים (דניטריפיקציה או אנמוקס, בתלות בצורון החנקן מקבל האלקטרונים, ניטראט או ניטריט, בהתאמה), כך שבתהליך נטו, נוצר חנקן (N_2) מומס. זהו לכאורה פרדוקס, שלפיו, בקנה-מידה של האגם, תהליכים בקטריאליים אנארוביים (מחזרים) מתרחשים בתנאי סביבה ארוביים (מחמצנים). שמות התהליכים שנבחרו מתארים תהליך פרדוקסלי זה.

בתזה זו מוצע פתרון פשוט לתצפית פרדוקסאלית זו: *התהליכים מתרחשים על-פני ובתוך מיקרו-סביבה מוצקה הבנויה מחומר אורגני חלקיקי השוקע דרך עמודת המים, מה שמכונה* ***"שלג ימי (אגמי), Marine (lacustrine) snow".*** תהליכי נשימה *ארוביים* צורכים חמצן במעטפת החיצונית של "השלג האגמי", והניטראט/הניטריט הנוצר נצרך בתוך המעטפת הפנימית המחזרת של החלקיקים, בתהליכי דניטריפיקציה/אנמוקס בהם נוצר חנקן גזי מומס. זה האחרון עובר בדפוזיה דרך פני שטח החלקיק לעמודת המים ומהווה מבלע של חנקן המשתחרר בסופו של התהליך לאטמוספירה.

כאשר ריכוז החמצן המומס בעמודת המים יורד מתחת לכ - $150\ \mu mol \cdot L^{-1}$, ריכוז הניטראט מתחיל לרדת במקביל לירידה חדה בריכוז החמצן המומס בעוד ריכוז האמוניום עולה. התהליכים הדומיננטים הפועלים בשלב זה הם דניטריפיקציה (חיזור ניטראט) ואמוניפיקציה של חנקן אורגני. עד סוף הסתיו ההיפולימיון מאבד את כל החמצן המומס, מתפתחים בו תנאים אנוקסיים, והאמוניפיקציה נמשכת דרך חיזור סולפאט.

תקציר

המטרה העיקרית של עבודה זו היא לאפיין ולכמת את מחזור החנקן באגם הכנרת באמצעות מאזני-מסה של צורוני החנקן והרכבם האיזוטופי ($\delta^{15}N$).

המחקר מתואר ב- 4 פרקים עיקריים הדנים בנושאים הבאים:

1. פרק 3 הכולל פיתוח ואימות שיטות למדידת ההרכבים האיזוטופיים של צורוני חנקן מומסים במים ויישום שיטות אלה למים שפירים בכלל ולאגם הכנרת בפרט (שינויים קלים לשיטות המדידה המקובלות תוארו בפרק שיטות העבודה, פרק 2). הפרק בוחן ומצביע על ההפרעות במדידה של ההרכב האיזוטופי של צורוני חנקן בנוכחות צורוני חנקן אחרים. בהמשך מתוארת שיטה משופרת ופרוטוקולים שפותחו, המאפשרים מדידת ערכי $\delta^{15}N$ ו - $\delta^{18}O$ של כל אחד משלושת צורוני החנקן האי-אורגניים העיקריים המומסים במים, ניטראט (NO_3^-), ניטריט (NO_2^-) ואמוניה (TNH_3) בנוכחות צורון חנקן נוסף היכול פוטנציאלית להפריע בתהליך המדידה האיזוטופית. השיטה המתוארת בפרק 3 שימשה במחקר זה למדידת דוגמאות מים מאגם הכנרת שעליהן מתבססות התובנות הביו-גיאוכימיות/לימנולוגיות של התיזה.
2. פרק 4 הכולל תיאור של שינויים עונתיים בנפיצות צורוני חנקן וחמצן מומס בעמודת המים של האגם, בהתבסס על פרופילי עומק שבועיים שנדגמו במרכז האגם במהלך 2010-2016. פרופילים אלה שמשו לבניית מאזן מסה של החנקן ולכימות התהליכים המבקרים את מחזור החנקן בכנרת.
3. פרק 5 הכולל תיאור של הדינמיקה העונתית של ההרכבים האיזוטופיים של 3 צורוני החנקן המפורטים בסעיף 1 ושל חומר אורגני חלקיקי (PNorg) בפרופילי עומק באגם במשך מספר שנים. נתונים אלה מוצגים יחד עם תכולת החנקן וההרכב האיזוטופי של מקורות החנקן העיקריים לאגם (לדוגמא נהר הירדן, נחל משושים). מדידות ההרכבים האיזוטופיים של חנקן באגם ובמקורותיו הוכחו כחיוניות לזיהוי ולהבנה של התהליכים השולטים במערכת החנקן באגם. פרק זה כולל גם ניסוי אינקובציה אשר בוצע במטרה לעקוב אחר תהליכי פרוק החומר האורגני החלקיקי בעמודת המים של האגם ולאפיין את הפרקציונציה האיזוטופית של החנקן בתהליך האמוניפיקציה של החומר האורגני.
4. פרק 6 הוא סיכום של ממצאי העבודה. פרק זה מכיל סינתזה (סעיף 6.1) בה מובאים 4 איורים המסכמים את התובנות של התיזה (המתבססות על הנתונים המוצגים בפרקים 4 ו – 5) על אופן פעולתו של מחזור החנקן באגם הכנרת במהלך שלוש עונות לימנולוגיות חשובות: ערבוב, מעבר לשיכוב, ושיכוב.

סיכום קצר של תוצאות המחקר מובא להלן:

אגם הכנרת הוא אגם מונומיקטי (עמודת המים מתערבבת אחת לשנה) המפתח תנאים מחזרים בהיפולימניון במשך תקופת השיכוב באביב/קיץ ועובר היפוך וערבוב מלא של עמודת המים בתחילת החורף. מאפיינים פיסיקליים אלה של

המכון הגיאולוגי
משרד האנרגיה

מחזור החנקן בכנרת
מבט גיאוכימי ואיזוטופי

תמי זילברמן

חיבור לשם קבלת התואר "דוקטור לפילוסופיה"

הוגש לסנט האוניברסיטה העברית בירושלים.

העבודה נעשתה בהדרכתם של:

ד"ר איתי גבריאלי, המכון הגיאולוגי לישראל
פרופ' בעז לזר, האוניברסיטה העברית בירושלים
ד"ר עמי נשרי, חקר ימים ואגמים לישראל המעבדה לחקר הכינרת

דוח מס' GSI/03/2021 פברואר 2021

